VŠB – Technical University of Ostrava
Faculty of Electrical Engineering and Computer Science
Department of Telecommunications

Studium vláknově optických zesilovačů EDFA pro pasivní optické sítě

Study of Fiber Optical Amplifiers EDFA for Passive Optical Network

2013 **Bc. Radek Pobořil**

VŠB - Technical University of Ostrava
Faculty of Electrical Engineering and Computer Science
Department of Telecommunications

Diploma Thesis Assignment

Student: **Bc. Radek Pobořil**

Study Programme: N2647 Information and Communication Technology

Study Branch: 2601T013 Telecommunication Technology

Title: Studium vláknově optických zesilovačů EDFA pro pasivní optické sítě
Study of Fiber Optical Amplifier EDFA for Passive Optical Network

Description:

The task of the student will be the study of problematic of EDFA amplifiers for optical networks and their current developments. The work is of a scientific nature and the student will have to demonstrate a lot of skills from physics to optoelectronics field during realization. And also solve the nonlinear phenomena, optimization of amplifiers noise, suppression of unwanted phenomena associated with the application of the amplifier into the optical line.

1. Study the characteristics of EDFA fiber optic amplifiers.
2. Find the optimal length of the amplifying fiber for different working conditions of the fiber amplifier.
3. Measure the sensitivity of the fiber amplifier parameters on the changes in the spectral characteristics of the pumping laser.
4. Assemble the experimental workplace with the application of EDFA amplifier in to the optical network.

References:

[1] Premaratne, M., Agrawal, G., P. *Light Propagation in Gain Media: Optical Amplifiers*, Cambridge: Cambridge University Press, 2011. 284 p. ISBN 978-0521493482.
[2] Bjarklev, A. *Optical Fiber Amplifiers: Design and System Applications (The Artech House Optoelectronics Library)*, Vydání 1. Artech Print on Demand, 1993. 408 p. ISBN 978-0890066591.
[3] Shimada, S., Ishio, H. *Optical Amplifiers and their Applications*, Vydání 1. John Wiley & Sons, 1994. 288 p. ISBN 978-0471940050.
[4] Lee, T. P. *Current Trends in Optical Amplifiers and Their Applications (Selected Topics in Electronics and Systems)*. World Scientific Pub Co Inc, 1996. 222 p. ISBN 978-9810226954.
[5] Desurvire, E. *Erbium-Doped Fiber Amplifiers: Principles and Applications (Wiley Series in Telecommunications and Signal Processing)*. Wiley-Interscience, 1994. 800 p. ISBN 978-0471589778.
[6] Nemova, G. *Optical Amplifiers (Physics Research and Technology)*. Nova Biomedical Books, 2011. 337 p. ISBN 978-1612098357.
[7] Desurvire, E., Bayart, D., Desthieux, B., Bigo, S. *Erbium-Doped Fiber Amplifiers, Device and System Developments*. Wiley-Interscience, 2002. 763 p. ISBN 978-0471419037.

Extent and terms of a thesis are specified in directions for its elaboration that are opened to the public on the web sites of the faculty.

Supervisor: **Ing. Jan Látal**

Date of issue: 16.11.2012

Date of submission: 07.05.2013

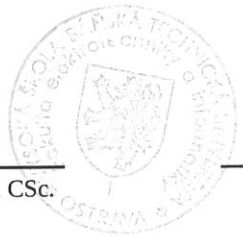

prof. RNDr. Vladimír Vašinek, CSc.
Head of Department

prof. RNDr. Václav Snášel, CSc.
Dean of Faculty

Declaration Made by the Student

I hereby declare that this master's thesis was written by myself. I have quoted all the references I have drawn upon.

On *1.5.2013*

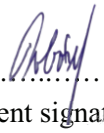

……
Student signature

Acknowledgements

First and foremost, I would like to thank my supervisor, Ing. Jan Látal, whose methodical guidance and valuable advice have been indispensable throughout the whole process of writing this thesis. I must also express my gratitude to prof. RNDr. Vladimír Vašinek, CSc. and Ing. Martin Smrž, Ph.D. from Institute of Physics of the Academy of Sciences of the Czech Republic for their willingness to advise and to lend me all the necessary facilities. And last but not least, my special thanks go to Bc. Nela Stebnická, Ing. Petr Šiška Ph.D., Owen Perring from company FiberCore, and Jan Dořičák from company Safibra s.r.o.

Abstrakt

Cílem této práce je přiblížit čtenáři problematiku týkající se optických vláknových zesilovačů používaných v optických sítích, především pak erbiem dopovaných vláknových zesilovačů, které jsou hlavním zájmem této práce. Práce je rozdělena do dvou základních částí, z nichž první se zabývá teoretickými základy pro pochopení tematiky zesilovačů a druhá je zaměřena na stavbu zesilovače a jeho následné testování. Celá práce tedy vychází z bodů zadání diplomové práce.

V kapitolách 2, 3 a 4 byly postupně vysvětleny základní fyzikální jevy, popsány nežádoucí jevy ovlivňující vlastnosti zesilovačů a představeny ostatní typy zesilovačů. V kapitole 5 je záměrem podrobný rozbor zesilovačů typu EDFA s důrazem na základní funkce, stavbu a parametry jeho jednotlivých komponent. V dalších kapitolách je také podrobně rozebráno samotné dopované vlákno a pumpovací lasery.

Druhá část práce, začínající kapitolou 6, obsahuje popis návrhu zesilovače spolu s měřením jeho vlastností. Byla ověřena stabilita laseru použitého pro pumpování, dále pak vliv teplotních změn působících na dopované vlákno a jejich vliv na parametry zesilovače. Dalším bodem práce bylo otestování vlivu teplotních změn pumpy na parametry zesilovače.

V poslední části práce byl zkonstruovaný zesilovač připojen do reálné topologie a byly otestovány jeho vlastnosti.

Klíčová slova

EDFA zesilovač, optické zesilovače, erbium, vzácné zeminy, pumpovací laser, teplotní namáhání, PON, WDM, komponenty v optické síti, SOA, dopované vlákno.

Abstract

The aim of this thesis is to explain the issues relating to amplifiers used in optical networks, and especially to erbium-doped fiber amplifiers, which represent the main subject of this work. The thesis is divided into two parts, the first one of which deals with a theoretical basis necessary for understanding the issues of amplifiers, and the second one is focused on constructing the amplifier and on its subsequent testing. The whole work therefore follows the points given in the assignment.

In Chapters 2, 3 and 4 we have gradually explained basic physical phenomena, described undesirable effects influencing the characteristics of amplifiers, and presented other types of amplifiers. In Chapter 5 we have focused on a detailed analysis of EDFA amplifiers, and pointed out basic functions, structure and parameters of their individual components. We have also discussed in detail pumping lasers and the doped fiber itself.

The second part of the work, initiated by Chapter 6, describes a proposal of the amplifier along with measurements of its properties. We have verified stability of the laser used for pumping, as well as the influence of temperature changes on the doped fiber and also their influence on parameters of the amplifier. Another point of the work consisted in testing the effect of temperature changes of the pump on the parameters of the amplifier.

The final part of this thesis resided in connecting the designed amplifier to a real topology and in its subsequent testing.

Key Words

EDFA amplifier, optical amplifiers, erbium, rare earths, pumping laser, thermal stress, PON, WDM, optical network components, SOA, doped fiber.

Contents

1 Introduction

The crucial matter in optical telecommunication systems is the need to span long distances between the endpoints of a topology. The optical signal from a transmitter must pass through an optical fiber and then must be decoded by a receiver. However, we can come across certain problems, the biggest one of which is the loss of signal in the form of attenuation.

The cause of these losses may reside in optical fibers or other optical components such as couplers, splitters, AWGs, etc. After these losses the signal can be very weak for its detection, that is why, the main objective in the optics in the last decade has consisted in finding a method to regenerate the signal so it can be easily detectable. Devices performing such regeneration are the so-called regenerators, and also optical amplifiers.

As far as the former are concerned, they only receive the optical signal, convert it to the electric one, fix it (i.e. amplify it) and then convert it back. As for the latter, i.e. the amplifiers, they do the same, plus their main advantage, compared to receivers, is their versatility. Let us illustrate it with an example: if there is a change in bit-rate or in wavelength, we have to replace all the regenerators because they are designed only for certain network settings. Optical amplifiers, on the other hand, are adaptable and thus do not have to be replaced and the systems which are using them can be easily upgraded.

The following Chapters 2, 3 and 4 gradually get from the basics to more complex mechanisms appearing in optical amplifiers. The main part of the work, Chapter 5, will be focused on erbium-doped fiber amplifiers. In the last chapter, Chapter 6, we will focus on building an amplifier for the C-band and on its testing. The actual amplifier will be tested mainly at various temperature conditions, and the results of these measurements will be documented in the last chapter, Chapter 7. All results are included in the appendix section.

2 Optical amplifiers

Before we get to the main part of the work dealing with optical amplifiers, it is necessary to understand the basics of the issue.

In this chapter, we will focus on some basic principles, on stimulated and spontaneous emission, on placing the amplifiers in a topology and on their classification.

2.1 Stimulated emission

Stimulated emission represents the basic principle in the process of light amplification. It is generally known that electrons are located in energy levels of an atom, and the farther they are from the core of the atom, the higher their energy is. For a better understanding of the issue, we are going to use a two-level system only. Multi-level systems will be explained in other chapters.

The basic level is called E_1 and the higher one E_2, so the relation between them is $E_2>E_1$. The electromagnetic field meeting the f_c frequency requirement defined by the relation $hf_c=E_2–E_1$ allows us to perform two basic types of transition. Firstly, the absorption, i.e. transition of the electrons from E_1 to E_2, and secondly, the emission, i.e. their transition from E_2 to E_1; where h stands for the Planck constant ($6{,}33\times10^{-24}J$). A level higher than the ground state is called excited. The stimulated emission lies in the fact that the incident radiation makes the electrons descent from the excited to the ground level, during which a photon is emitted. This photon is of the same wavelength, polarization and phase as the photon that has caused the stimulated emission. In this case, it is a coherent radiation. Another way an electron can descent to the lower level is the spontaneous emission on which we are going to focus in Chapter 2.2.

The process of amplification means that transitions from E_2 to E_1 dominate over the ones from E_1 to E_2. Otherwise, we talk about the process of attenuation. If we take into consideration principles of quantum mechanics, the speed of the E_1 to E_2 transition equals to the speed of the E_2 to E_1 transition, thanks to which we can define the common speed v.

Population of E_1 and E_2 energy levels can be designated as N_1 and N_2. The net energy increase for a unit of time is then represented by the formula $(N_2–N_1)vhf_c$. Thus, if we want to amplify the incoming radiation, it is necessary that $N_2>N_1$. This phenomenon is called the population inversion. Because of the thermal equilibrium in the atom, there are less electrons in higher levels than in lower ones. Therefore, what holds true is that $N_1>N_2$.

What predominates in these systems is the absorption which causes the signal amplification rather than its attenuation. That is why we need to create the population inversion which can be achieved by the energy supply by means of pumps, making thus the electrons move from lower levels to higher ones. The energy supplied by the pumps can be both of electric as well as of light character [1], [2].

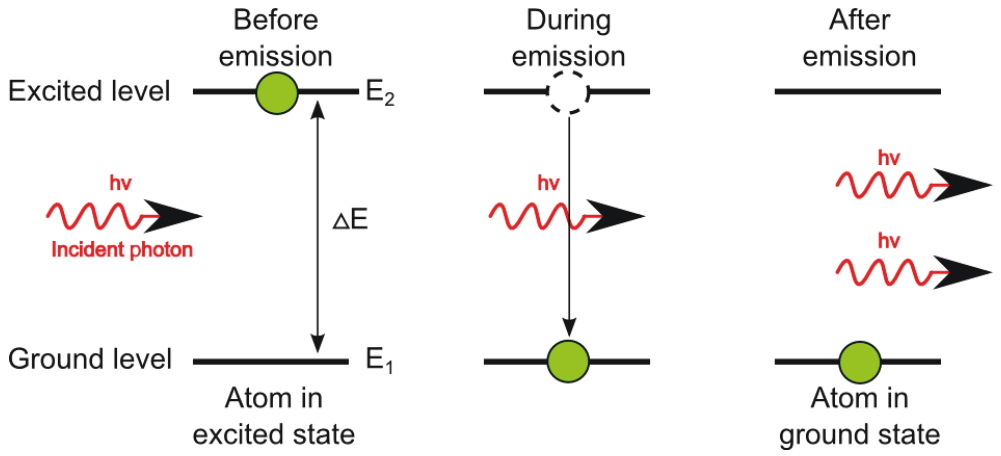

Figure 2.1: Stimulated emission [1]

2.2 Spontaneous emission

In Chapter 1.1 we focused on the stimulated emission. However, what is important for the complete view of the issue of amplifying is the understanding of the spontaneous emission. Again, we can illustrate this process with the two-level system. As in the previous case, it is a transition from E_2 to E_1.

An electron descends to the lower energy level during the radiant or the non-radiant transition. As for the former, i.e. the radiant transition, a photon with a random polarization, phase and wavelength arises. In this case, it is an incoherent radiation. As for the latter, the non-radiant transition, no photon is created and the excess energy is absorbed by the crystal lattice of a material and converted to heat. Probability of the radiant transition rises with the size of the band gap. It is given by the formula $P=A_{21}\times N_2$, where A_{21} is the Einstein's coefficient of spontaneous emission, and N_2 is a number of excited electrons.

Spontaneous emission rate for an atom is marked τ_{21} and is called the spontaneous emission lifetime. This implies that if there is N_2 atoms in the E_2 level, the spontaneous emission rate is N_2/τ_{21} and the spontaneous emission of energy is hf_cN_2/τ_{21}.

As far as optical amplifiers are concerned, the spontaneous emission represents an undesirable phenomenon because while amplifying the original signal, the spontaneous emission is amplified as well, creating thus an undesirable noise. The amplified spontaneous emission is called ASE [1], [2].

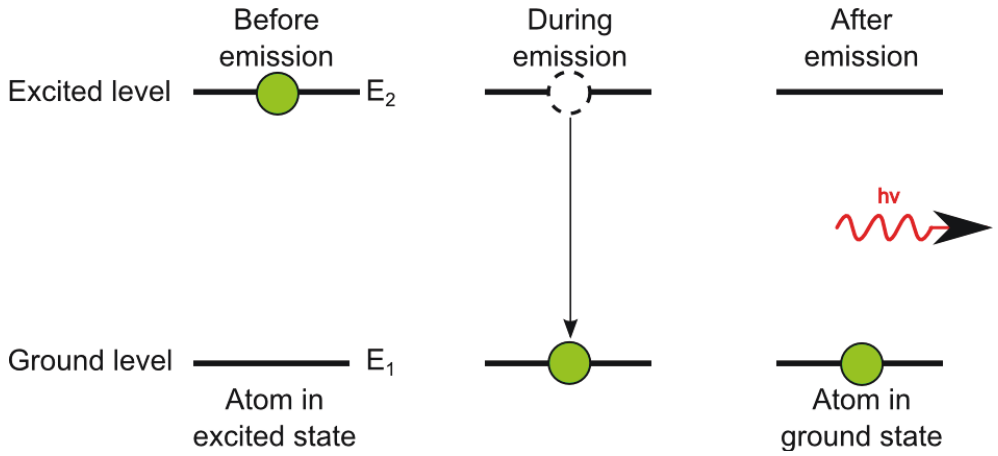

Figure 2.2: Spontaneous emission [1]

2.3 Placing of optical amplifiers

An optical amplifier belongs among the most important components in optical paths as well as in the optics generally. In the previous chapters we got acquainted with the basic principle of amplification represented by the stimulated emission. Now we need to look at the amplifiers from the topological point of view. The optical amplifier as such can be connected in three different ways, performing so three different functions: as a preamplifier, an in-line amplifier and a power amplifier.

As for the preamplifier, is connected at the end of the path in front of the detector in order to increase its sensitivity. Great emphasis is put on its lowest possible noise.

Regarding the power amplifier, it is connected at the beginning of the path. It is used in order to achieve the highest possible intensity of the input signal. The input signal level can be dependent e.g. on the possibility to couple energy into the fiber.

As far as the power amplifier is concerned, it is usually inserted in the middle of the path or into any other part of it – it always depends on the topology – and its main purpose is to compensate the attenuation of the very path. The power amplifiers combine qualities of the preamplifiers and boosters [3].

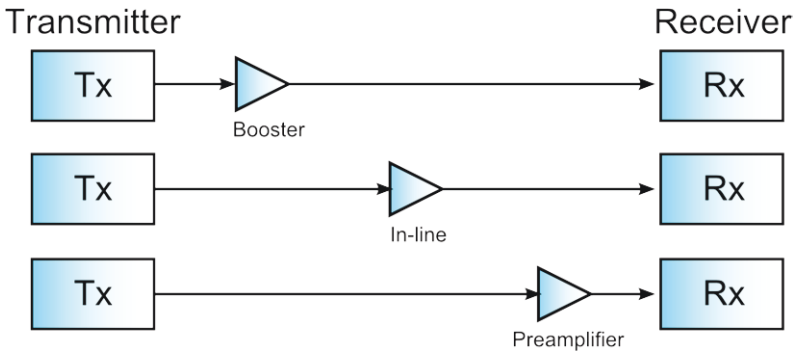

Figure 2.3: Placing of optical amplifiers [3]

2.4 Types of reconstruction signal

After we have gone through the division of amplifiers according to their position and function, it is now important to mention their classification according to the type of operation they do to the signal. This classification is very simple. The amplifiers are divided into these three categories – 1R, 2R, 3R – according to the type of signal regeneration they perform. In the following subchapters we will explain basic properties of each type of amplifiers, or more precisely regenerators [3].

2.4.1 1R regenerators

This category includes regenerators that cause ordinary signal amplification. Although this type of signal regeneration is only elementary, its applicability is very wide. The category is represented by optical amplifiers, which implies its principal advantage. There is no conversion of the optical signal to the electrical one and back, that is why the amplifier is independent of the type of signal coding or other signal properties [3].

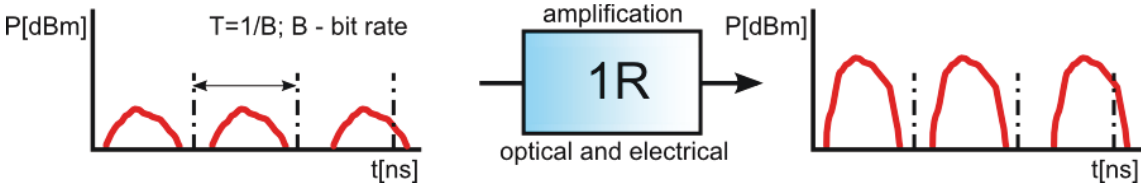

Figure 2.4: Principle of 1R regenerators [3]

2.4.2 2R regenerators

The second category includes regenerators that restore not only low intensity of the signal but also its shape. This regenerator type converts the optical signal to the electrical one and regenerates it to the closest possible form to the original transmitted signal. The regenerated signal is then converted back to the optical signal and, using the radiation source, it is transmitted back to the topology. A big disadvantage of this type of regenerators is their little flexibility [3].

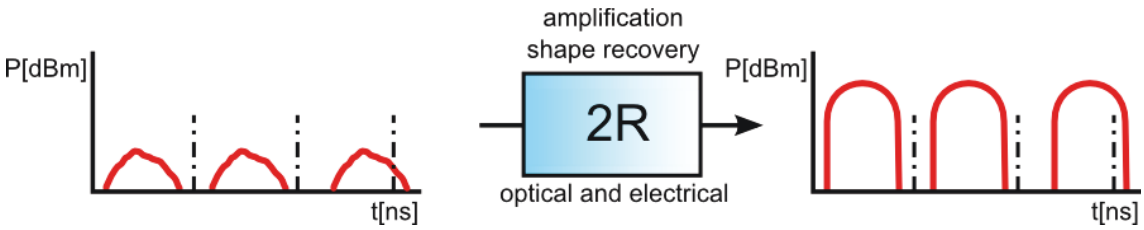

Figure 2.5: Principle of 2R regenerators [3]

2.4.3 **3R regenerators**

The last category comprises regenerators that cause complete signal regeneration. These regenerators restore not only the intensity or shape of the signal but also the timing of particular impulses. This type of regeneration can be seen in Fig. 2.6 [3].

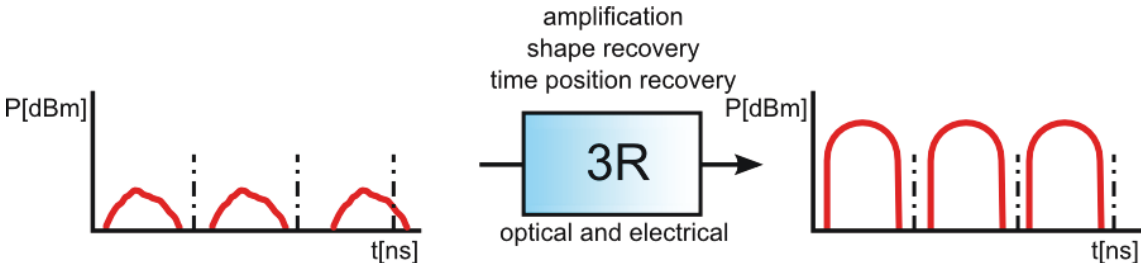

Figure 2.6: Principle of 3R regenerators [3]

In both categories (2R and 3R), the shape of the signal and its timing deteriorate due to fiber dispersion used for transmission in the optical path, which is an undesirable phenomenon. These will be described in detail in the next chapter [3].

3 Undesirable effects

Optical fiber technology has replaced the old copper lines in almost all cases. While in the early days the optical fibers were spread only primarily in backbone networks, in recent years they are accessible to all end users. The optical fiber, unlike the metallic one, allows us to achieve higher bit rate and to span much greater distances. However, since the optical transmission is much faster than the traditional metallic connection, there are some undesirable effects to be found which are based on physical limitations and characteristics of the actual optical fiber transmission medium.

This chapter is focused on these undesirable effects occurring during the transmissions with the optical fiber. At first, we are going to familiarize ourselves with the phenomenon of attenuation, and in other chapters we will inspect dispersions and nonlinear effects such as Brillouin and Raman scattering or the Kerr effect.

We will also examine phenomena occurring in all the components – the noises. We will describe them in detail, covering general properties and types, including, of course, the most important one, the ASE noise, as well.

3.1 Attenuation

The attenuation is one of the primary problems in optical transmission paths. After passing the path, the optical signal loses its intensity. This decline is represented by the very attenuation whose unit is measured in decibels and whose value can be calculated from the following formula [4]:

$$\alpha = 10 \log_{10} \frac{P_1}{P_2} [dB], \tag{3.1}$$

where P_1 is input power, P_2 is output power, and α is attenuation (in dB).

There are two main causes of attenuation in fibers – material absorption and Rayleigh scattering. As for the former, it involves absorption of silicon dioxide as well as of impurities present in the fiber itself. The impurities get to the fiber during the process of their production. We can disregard material dispersion of SiO_2 at wavelengths from 0.8 to 1.6 μm – these are used primarily in optical communications – as it can be seen in Fig. 3.1. Regarding ordinary fibers, the main absorption centres are OH ions. These so-called Water Peaks represent a very problematic issue in the optical fiber manufacturing. They are located at wavelengths of 950 nm, 1244 nm and 1383 nm. However, these optical difficulties can now be suppressed using properly designed optical fibers. That is why, we can now come across e.g. optical fibers with water peak suppression, accomplished during their production [4],[5].

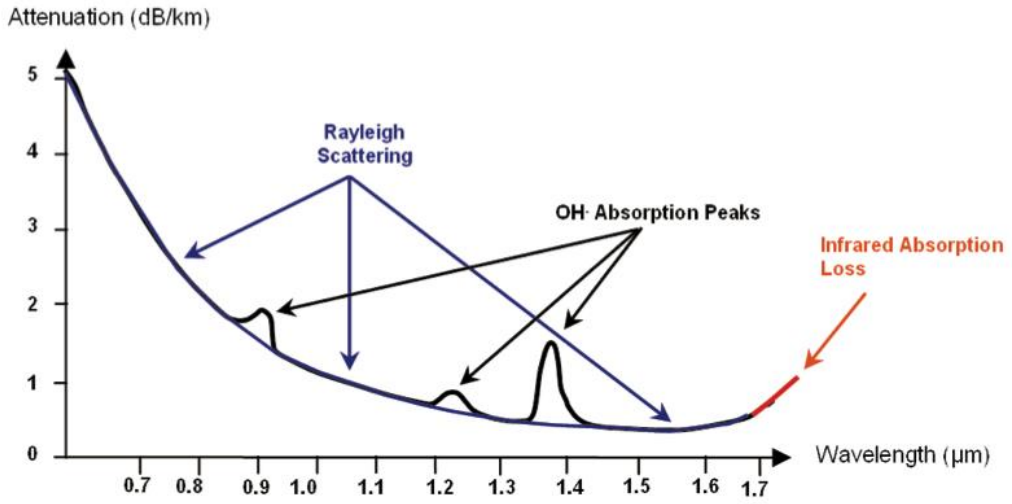

Figure 3.1: Spectral attenuation review for typical single mode fiber [5]

Assuming we use the fibers ITU-T G.653 with suppressed water peaks, what is the main limiting factor now is the Rayleigh scattering. It arises in the fiber on particles smaller than a wavelength, e.g. metal oxides. Thus, we can claim that Rayleigh scattering decreases with increasing wavelength. The loss coefficient α_R can be calculated from the following formula: [5]

$$\alpha_R = \frac{A}{\lambda^4}\left[dB \cdot \mathrm{km}^{-1}\right], \tag{3.2}$$

where A is the Rayleigh scattering coefficient and λ is a wavelength.

On the basis of this assertion it would seem that Rayleigh scattering could be solved with the use of longer wavelengths. However, this solution is not ideal. Regarding longer wavelengths, the attenuation curve gains other undesirable factor – the absorption of infrared area. This problem can be solved using chalcogenide and zirconium fluoride glasses. However, a disadvantage of these fibers lies is their high cost and the need of high-quality radiation sources and detectors. That is why, the optical communications focus on the area from 0.8 to 1.625 um where conditions for transmission are very favourable (see Fig. 3.2) [5], [6].

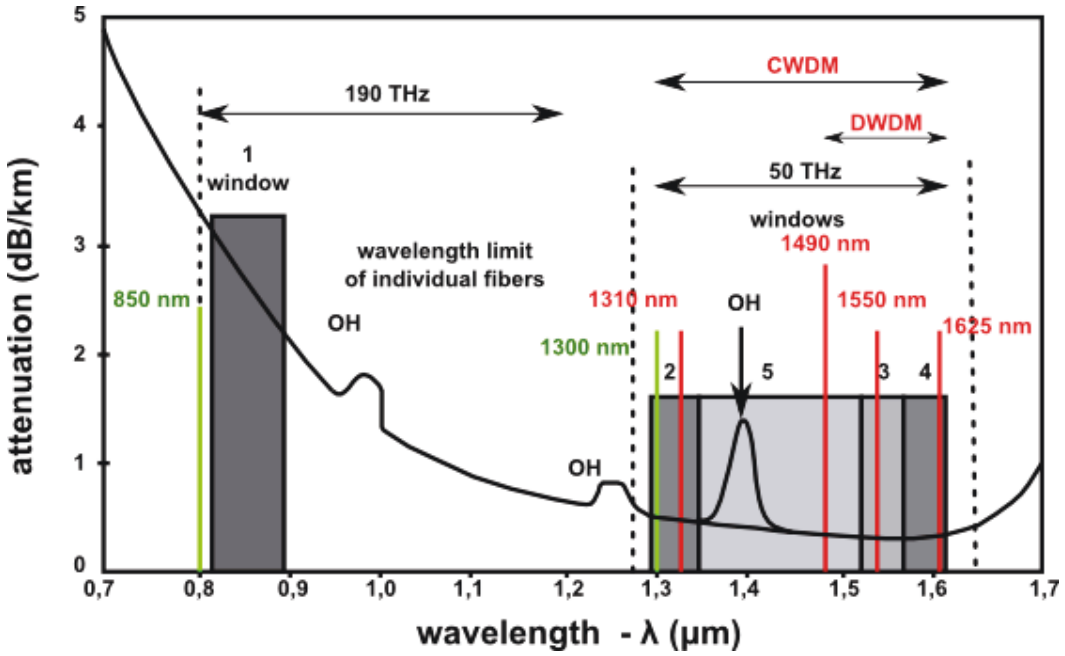

Figure 3.2: Transmission windows for optical telecommunications [5]

3.2 Dispersion

Dispersion is a phenomenon during which the signal transmission quality deteriorates due to undesirable characteristics of a fibre. Individual pulses are separated by interval gaps in order to be read. However, while a light beam passes through the optical system, the pulses stretch until they may eventually merge. Let us illustrate it with an example – while an original signal is represented by the sequence 0101, the resulting signal, after being degraded by dispersion, will be represented by the value 0111, which would lead to an increase in BER parameter outside the permitted values. In the following subchapters we will look at individual types of dispersion, describing their basic characteristics.

3.2.1 Mode dispersion

Mode dispersion is one of the basic dispersions which are being produced only in multi-mode fibers. Since the signal transmission uses several modes, not only one (as is the case with single-mode fibers), the pulses are stretched in time. It occurs because of the fact that each mode in the fibre takes different path, thus they reach the end of the path with different time delays. To some extent, this phenomenon can be suppressed using the narrowest possible spectral line width, gradient refractive index fibers or single-mode fibers, where this phenomenon cannot occur because they have just one mode. What is being used in practice, regarding multi-mode fibers, are the fibers with gradient refractive index profile which is defined by the following formula [7].

$$n^2(r) = n_1^2 \times \left[1 - 2\Delta \times \left(\frac{r}{a}\right)^g\right][-], \tag{3.3}$$

where *n(r)* is the refractive index profile of the core of a fiber, *Δ* is the relative difference of refractive indices of the core n_1 and of the cladding n_2, given by the formula [7]:

$$\Delta = \frac{\left(n_1^2 - n_2^2\right)}{2n_1^2}[-], \tag{3.4}$$

otherwise, there is the *a* standing for the radius of the core of the particular type of fiber, *g* which is power profile parameter, and *r*, representing distance of a given point from the axis of the fiber [7].

3.2.2 **Profile dispersion**

Another type of dispersion emerging in multi-mode fibers is the so-called profile dispersion. This phenomenon is related to the fact that the optimum refractive index of a fiber is dependent on a wavelength. Assuming that dispersive properties of dopants differ from SiO_2 which is the basic material, or among themselves, for each wavelength there will be different conditions for spreading and thus different optimum refractive index of the core. It follows that with an increasing wavelength, the gradient profile parameter g will decrease [7].

Profile dispersion is usually marked with the variable *P* which can be calculated from the formula [7]:

$$P = \frac{\lambda}{\Delta} \times \frac{d\Delta}{d\lambda}[-], \tag{3.5}$$

expressing different dispersive properties of SiO_2 and dopants in the fiber.

3.2.3 **Material dispersion**

Another type of dispersion occurring in optical transmissions is material dispersion. It is caused by dependence of the refractive index of the material used in optical fibre production at the wavelength of radiation sources. This dependence relation can be described using the Sellmeier equation [7]:

$$n^2 = 1 + \sum_{j=1}^{M} \frac{A_j}{\left(\omega_j^2 - \omega^2\right)} = 1 + \sum_{j=1}^{M} B_j \lambda^2 \times \left(\lambda^2 - \lambda_j^2\right)[-], \tag{3.6}$$

$$A_j = \frac{Nq^2}{\varepsilon_0 m}, B_j = \frac{A_j \lambda_j}{\left(2\pi c\right)^2}[-], \tag{3.7}$$

where q is the electron charge and ε_0 is the vacuum permittivity. Because of this dependence, each spectral part of the transmitted signal travels with different group velocity.

An electromagnetic plane wave propagates in the environment according to the formula:

$$\tau = \tau_g \times L = \left(\frac{d\beta}{d\lambda}\right) \times \left(\frac{d\lambda}{d\omega}\right) \times L = \left(\frac{L}{c}\right) \times \left(n - \lambda \times \frac{dn}{d\lambda}\right)[-], \tag{3.8}$$

where τ_g is group delay of a wave, β is the phase constant of the propagation of this wave defined by the formula [7]:

$$\beta = n \times \left(\frac{2\pi}{\lambda}\right)[-], \tag{3.9}$$

otherwise, there is the L which is the length of the path of a given environment, n that stands for the refractive index, and λ representing the wavelength.

If we take the Sellmeier equation into consideration, i.e. that $n=n(\lambda)$ and $dn/d\lambda \neq 0$, the time delay τ_g for every spectral component of light travelling through the optical fiber will be different. Therefore, if we use a signal source with spectral half-width $\Delta\lambda$, the transmitted optical pulses will be supplemented with [7]:

$$\Delta\tau = \Delta\lambda \times L \times \left(\frac{d\tau_g}{d\lambda}\right)[-], \tag{3.10}$$

3.2.4 **Waveguide dispersion**

Another type of dispersion is represented by waveguide dispersion. Its influence on the optical signal resides in its dependence on geometrical dimensions of the fiber. Supposing, theoretically, that the material dispersion is zero, the propagation constant and the group delay of each mode become functions of a wavelength. This very phenomenon is referred to as the waveguide dispersion, due to which (as is the case of other dispersions as well) the signal suffers distortion.

Waveguide dispersion along with material dispersion form the so-called chromatic dispersion [7].

3.2.5 Polarization mode dispersion

The last type of dispersion that causes signal distortion during the transmission through the optical fiber is polarization mode dispersion (PMD). This type of dispersion is not the main limiting factor, the most undesirable one is still chromatic dispersion. However, the latter can be effectively suppressed using e.g. fibers for dispersion suppression, Bragg grating or sources with narrow spectral line width, e.g. DFB. Assuming we manage to suppress chromatic dispersion, PMD dispersion represents another undesirable phenomenon. Its principle is relatively simple. What can happen during the propagation of the mode which consists of two components, an electric and magnetic one – perpendicular to each other – is that one of the components starts to lag. As a result, the transmitted pulse is propagated [7].

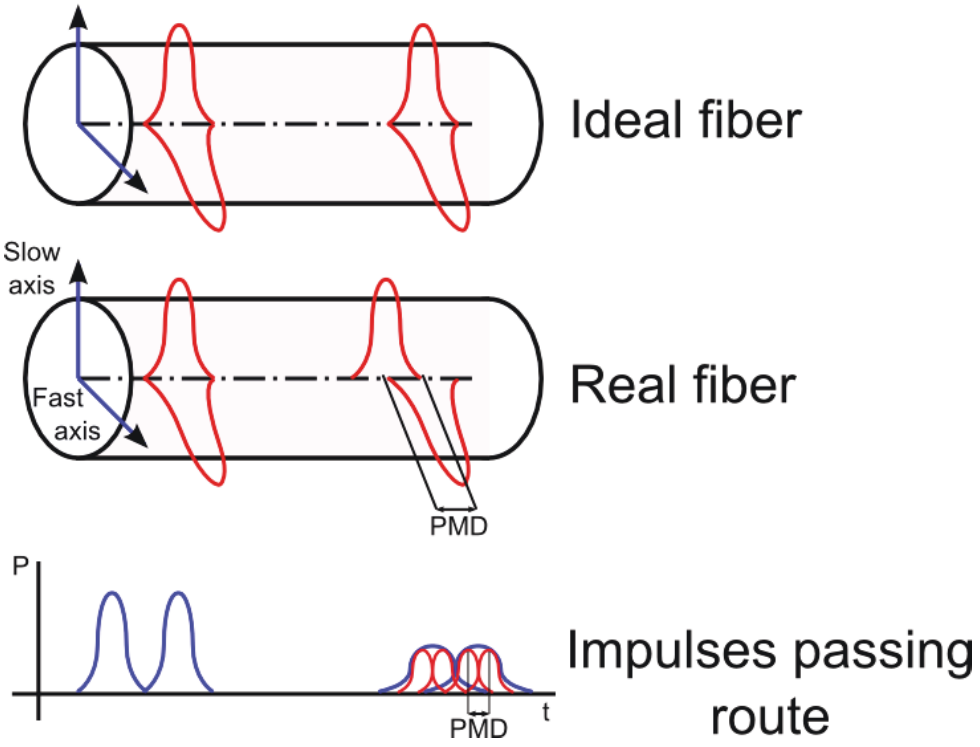

Figure 3.3: Polarization mode dispersion [7]

3.3 Nonlinear effects

Other factors influencing the passage of light through the optical fiber are nonlinear effects. These phenomena occur only when using more powerful radiation sources to span

longer distances, and at higher data rates. Since most of the optical paths use DWDM systems which due to their efficiency gradually displace old TDM systems, the nonlinear effects should be discussed and taken into account when designing a topology. Assuming lower data rates up to 2.5 Gb×s^{-1} used by the older systems, the effects can be overlooked. However, when using e.g. 10 Gb×s^{-1} speed or when we need to span longer distances using more powerful lasers, the effects start to emerge and have a significant influence on communication.

Nonlinear effects can be divided into two basic groups. The first one concerns interaction of light waves with photons (molecular vibrations) in a silicon medium, and comprises effects such as the stimulated Brillouin and Raman scattering on which we will focus in this chapter.

The second group is represented by effects that are caused by dependence of the refractive index on the intensity of an applied electric field. This category includes primarily self-phase modulation (SPM) and four-wave mixing (FWM). Moreover, we will also focus on cross phase modulation (XPM, or CPM) and the Kerr effect.

3.3.1 **Brillouin scattering**

Brillouin scattering belongs among nonlinear effects. It is one of the so-called nonlinear attenuation mechanisms that arise in fibers when using high powers e.g. in DWDM systems. It is a transmission of the optical signal among individual modes, and the signal is propagated in the same or the opposite direction and at different frequency [8].

The light (electromagnetic wave) passing through solid or liquid substances can react to the presence of other waves. Thermal vibrations of molecules in optical fibers are the cause of the formation of acoustic waves whose presence in the optical fiber causes elastic deformation of space in time, and thus the local change in refractive index. This scattering of electromagnetic waves on the acoustic wave is called Brillouin scattering. Particles representing the acoustic wave are called phonons.

Brillouin scattering can be expressed using the quantum mechanical interaction of acoustic and optical waves. The light passing through light tubes can be thought of as a set of phonons, i.e. particles with the energy of a photon [8]:

$$E_F = \hbar\omega_F , \tag{3.11}$$

where ω_F stands for the angular velocity of the light wave, and $\hbar$ for the reduced Planck constant. Similarly, we can imagine the acoustic wave as a set of phonons with the energy of a photon [8]:

$$E_A = \hbar\omega_A . \tag{3.12}$$

The following figure describes the appearance and disappearance of a phonon, and photon energy transfer. Because of the fact that the law of conservation of energy must be valid, the sum of the energy of the photon and all the arisen phonons must equal the energy of the newly arisen particle called the "scattered photon".

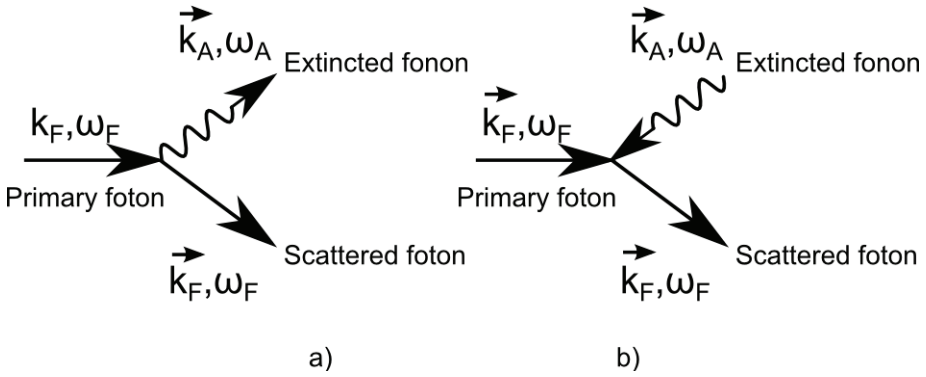

Figure 3.4: (a) Creating and (b) absorbing a phonon by a photon [8]

Frequency of the acoustic wave is given by the formula [8]:

$$\omega_A = 2\omega_F n(\omega_F)\frac{v_F}{c}\sin\left(\frac{\Theta}{2}\right), \tag{3.13}$$

and the wavelength of the propagated wave can be found out from the relation [8]:

$$\omega'_F = \omega_F \pm \omega_A . \tag{3.14}$$

Formula 3.14 indicates that Brillouin scattering generates two side components of the original spectrum which are called Stokes and anti-Stokes components.

Therefore, the main parameter for Brillouin scattering is the optical power which we try to couple into the core of the optical fiber. This power is given by the formula [8]:

$$P_B = 4{,}4\times10^{-3} d^2\lambda^2\alpha_{dB}\delta\lambda \ \text{(W)}, \tag{3.15}$$

where d is the core diameter, α_{dB} is the attenuation (in dB.km^{-1}), and $\delta\lambda$ is the spectral width of the light source (in GHz). The usual value in single-mode fibers is about 80 mW [8]:

3.3.2 **Raman scattering**

Another nonlinear effect is Raman scattering which is characterized by transmission of energy from the mode with the shorter wavelength to the mode with the longer wavelength. This phenomena is illustrated in Fig. 3.5 [1], [9].

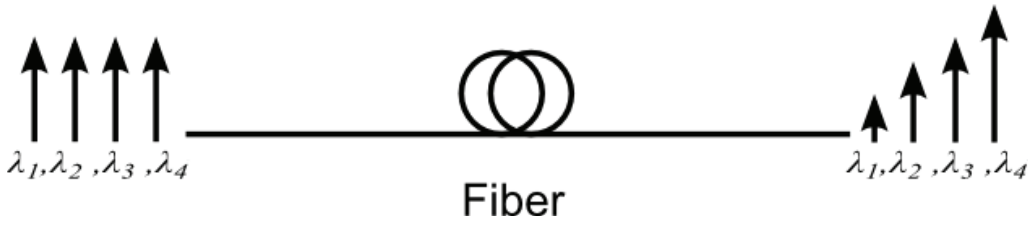

Figure 3.5: The effect of stimulated Raman scattering [1]

Energy of the photon is given by the formula [1]:

$$E = \frac{hc}{\lambda}[J], \tag{3.16}$$

where h stands for the Planck constant (6.63×10^{-34} J×s), λ for the wavelength and c for the speed of light. It clearly follows that photons of the shorter wavelength should have higher potential of energy. This phenomena is one of the basic effects used in optical amplification and lasers.

The transfer of energy from the photons of the shorter wavelength to the signal of longer wavelength is associated with emission of the photon of the shorter wavelength that is caused by photons with higher potential of energy. If there are elastic collisions of the photon with molecules in the material through which the light passes, we talk about the already mentioned Rayleigh scattering. On the other hand, if there is an inelastic collision, the incident photon gives a part of its energy to the molecule or receives certain quantity from it. The resulting radiation has different frequency from the original radiation. This phenomenon is called Raman scattering. The frequency shift between the source and the scattered radiation is called the Raman shift.

In inelastic collisions of the photon that excites the radiation with a molecule, there can be a decrease or an increase of energy of the photon. This phenomenon is described by the formulas 3.17 – 19 [9].

Let us now focus on the first case, on the energy decrease. After the collision, the photon has lower energy and thus also lower frequency. The area to which it moves is called the Stokes area. These energy relations are described by the following formulas: [9]

$$E_0 = h \times \nu_0 , \tag{3.17}$$

$$E_1 = h \times \nu_1 , \tag{3.18}$$

$$\Delta E = h \times (\nu_0 - \nu_1) = h \times \Delta \nu , \tag{3.19}$$

where E_0 stands for the energy of the photon before the collision; E_1 for the energy of the photon after the collision; ν_0 represents the frequency of the photon before the collision; ν_1 represents the frequency of the photon after the collision; ΔE is the energy decrease of the photon caused by the collision; $\Delta \nu$ is the frequency of the Raman shift (band frequency in Raman spectrum); and h is the Planck constant [9].

During the collision of the photon with the molecule, the latter gets to the virtual vibrational state and then drops to the lowest vibrational level with higher potential than in the basic level (see Fig. 3.6).

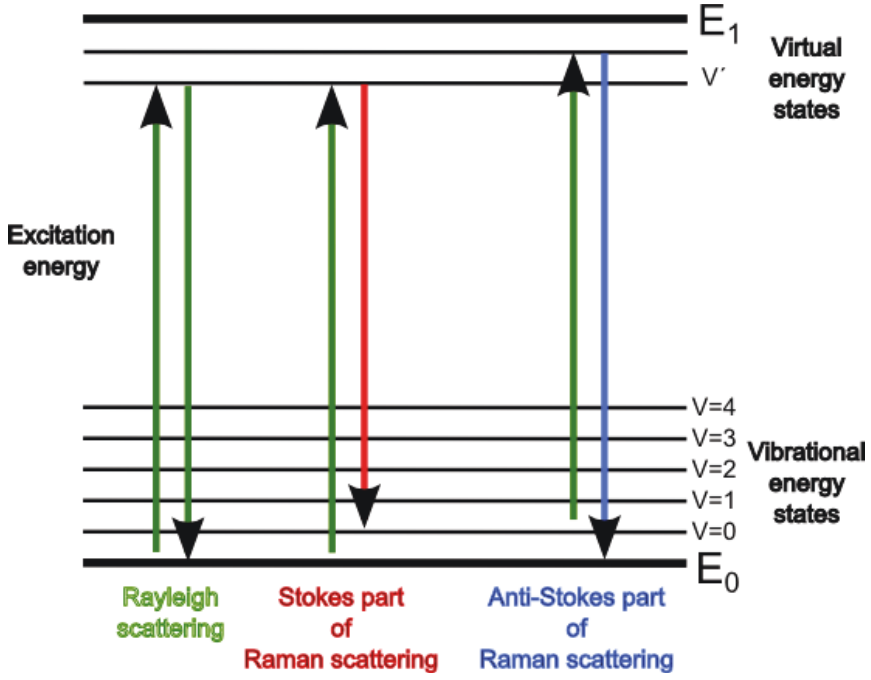

Figure 3.6: Raman effect [9]

On the other hand, let us now illustrate the energy increase. If the photon increases its energy, it also increases its frequency. This energy comes from the molecule which, after the collision, remains in the excited state. The relations are described by the following formulas [9]:

$$E_0 = h \times \nu_0 , \tag{3.20}$$

$$E_2 = h \times \nu_2 , \tag{3.21}$$

$$\Delta E = h \times (\nu_0 + \nu_2) = h \times \Delta \nu, \tag{3.22}$$

where E_0 stands for the energy of the photon before the collision; E_2 for the energy of the photon after the collision; v_0 represents the frequency of the photon before the collision; v_2 represents the frequency of the photon after the collision; ΔE is the energy increase of the photon caused by the collision; Δv is the frequency of the Raman shift; and h is the Planck constant. Fig. 3.7 shows Stokes and anti-Stokes areas.

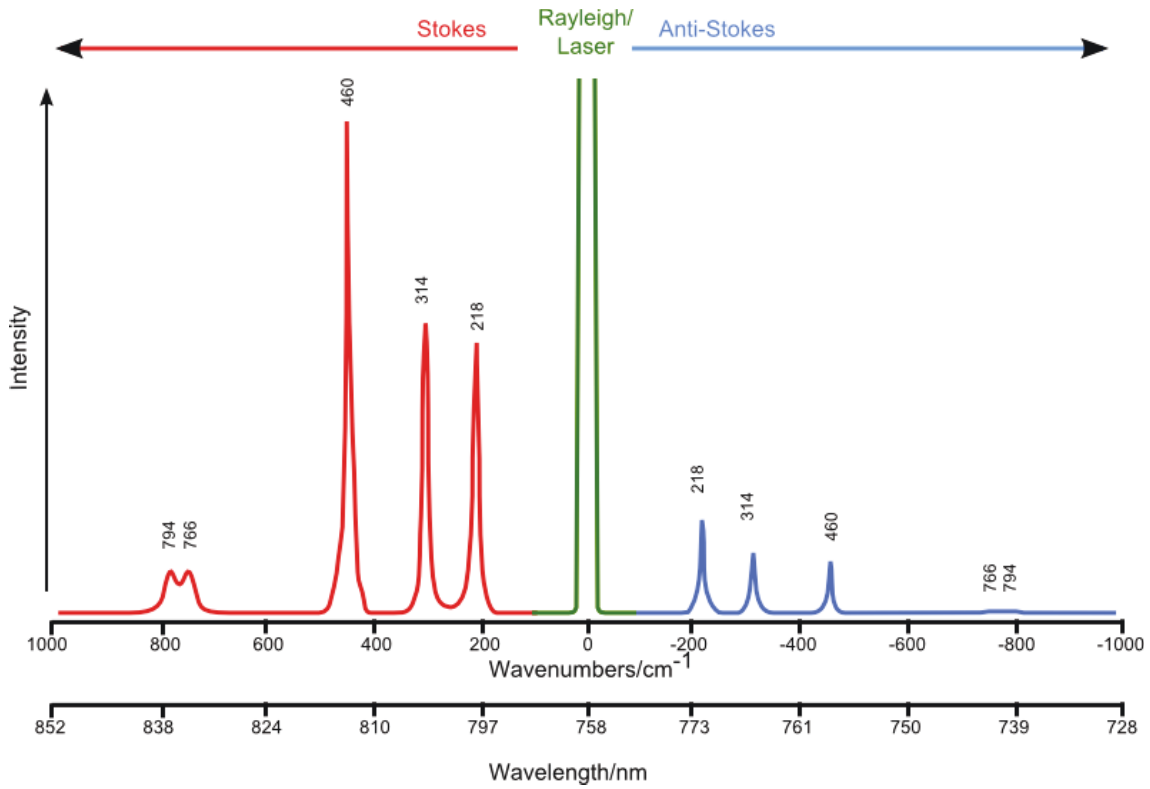

Figure 3.7: Comparison of Raman scatter, Rayleigh scatter and fluorescence intensities [10]

3.3.3 **Four-wave mixing**

Four-wave mixing resides in the following principle: if there are three signals with frequencies ω_i, ω_j, ω_k in the nonlinear medium, due to their reciprocal interaction there emerge signals with frequencies $\pm \omega_i \pm \omega_j \pm \omega_k$. The most affected signal is characterized by the formula [11]:

$$\omega_{ijk} = \omega_i + \omega_j - \omega_k, i \neq k, j \neq k, . \tag{3.23}$$

Thus the newly created frequency channels are very close to the original channels of the original signal. Because of this, there can be crosstalks among the individual channels. When using the three original channels, twelve new channels are created, four of which are based on the original frequencies. In systems with higher number of channels W, the total number of channels W_n will be created according to the following formula [11]:

$$W_n = \left[W(W-1)^2\right][-], \tag{3.24}$$

Fig. 3.8 describes the case of two signals and the multiplying effect of FWM.

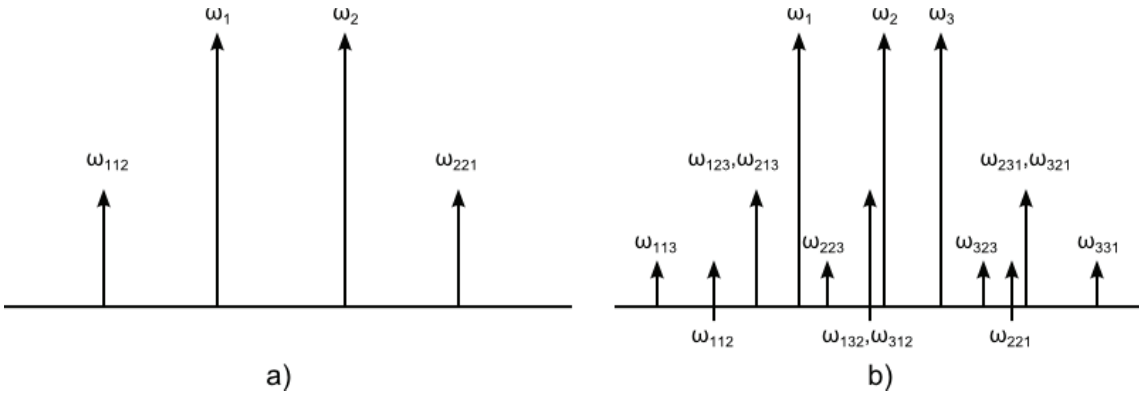

Figure 3.8: Additional frequencies through FWM in the partially degenerate (a) and non-degenerate (b) case [11]

3.3.4 **Kerr effect**

The Kerr effect is a basic nonlinear effect which was discovered in the 19th century by the Scottish physicist John Kerr. This phenomenon can be briefly characterized as a local change in refractive index due to high intensity of the electromagnetic field, i.e. the light in the optical fiber. The Kerr effect is very important for our measurement and the theoretical background of this work because other nonlinear effects, which will be described in the following chapters, are based on it. The local change in refractive index is characterized by the formula [12], [13]:

$$n\left(\lambda,|\mathrm{E}|^2\right) = n_0(\lambda) + n_2|E|^2, \tag{3.25}$$

where $n(\lambda,|E|^2)$ is the effective refractive index; $n_0(\lambda)$ is the refractive index of linear waves; and $n_2|E|^2$ is the refractive index of waves of higher intensity. The formula shows that if we describe electromagnetic waves within the electric field, the adaptation of effective refractive index to linear refractive index will be in proportion to the square of the amplitude of

the electromagnetic field. The refractive index n_2 is different for each dielectric material. In the case of silicon dioxide, the following formula applies [12]:

$$n_2 = (2.2 - 3.4) \times 10^{-29}, \left(m^2 / W\right). \tag{3.26}$$

3.3.5 Self-phase modulation

SPM is a nonlinear effect in which a phase of a signal is modulated by the signal itself. The signal is influenced mainly by nonlinearities of the medium in the form of local changes in refractive index, because of which the original signal propagation is disrupted. This dependence is given by the formula: [14]

$$\Delta\varphi = 2\pi \times n \times \frac{L}{\lambda_0 A} \times P, \tag{3.27}$$

where n stands for the refractive index, L represents the path length, A is the cross-section of the optical medium, P is the input power, and λ_0 is the wavelength.

By changing the refractive index the phase modulation occurs. The rising edge of the pulse causes that the wavelength shifts to longer wavelengths (red shift), while the falling edge causes its shift to shorter wavelengths (blue shift) – see Fig. 3.9 [15].

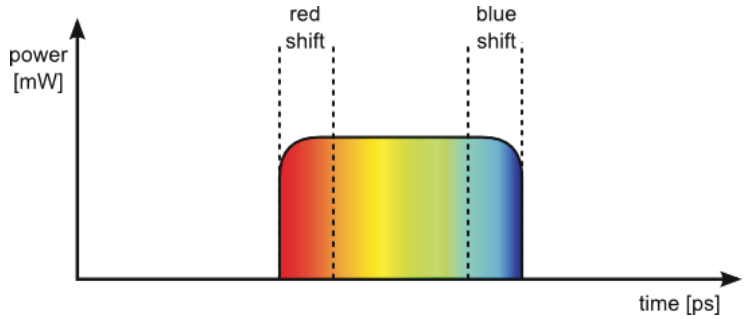

Figure 3.9: Red and blue shift of the wavelength

3.3.6 Cross-phase modulation

XPM is another nonlinear effect that adversely affects the quality of the transmitted signal in an optical fiber. Again, it is dependent on the intensity of the optical signal linked to the fiber. If we link many beams to the fiber, as e.g. in WDM network, despite their initial low intensity the group intensity is the sum of all intensities. Due to such increased intensity nonlinear effects may occur.

This intensity-dependent phase shift and related chirping, created using SMP, is then powered by surrounding channels. This very effect is the so-called cross-phase modulation.

In practice, this problem can be suppressed by larger separation of channels. XMP represents a serious problem in WDM systems with higher bit rate (10 Gb×s^{-1} and more) when using dispersion shifted fibers [1], [15].

3.4 Noises

Noises represent a significant problem in optoelectronics because they distort the original signal in a relatively high degree, which has an impact on its overall quality. In this chapter, we will focus on different types of noises that occur when using optical fibers. The first two subchapters are rather informative and we will describe there the issue of shot noise and thermal noise that occur in optical receivers and transceivers. In the next subchapter, we will focus on the noise that arises as a result of amplification of spontaneous emission, i.e. on the ASE noise. The last-mentioned is the most important one of the three because it represents an acute problem of fiber optical amplifiers.

3.4.1 Shot noise

Shot noise is caused by a deviation of the current number of electrons from the average amount. The very number of detected electrons is what this phenomenon is dependent on. The exact number of photons cannot be determined with accuracy because the detector monitors only quanta. That is why, the overall number of created electrons in the structure of the photodetector is unknown as well.

For the above reasons, when describing the shot noise, we use the Poisson distribution:

$$P(n) = \frac{e^{-n^*} \times (n^*)^2}{n!}, \tag{3.28}$$

where n^* is the mean value of the number of electrons [16]. Shot noise can also be expressed by the formula for the shot noise current I_{shot}:

$$\left(I_{shot}^2\right) = 2qI_P B_W M^2 F(M), \tag{3.29}$$

where I_p is the average photocurrent, M is the multiplication factor of the APD (in case of the PIN, it is 1), and $F(M)$ is the APD noise figure [17].

3.4.2 Thermal noise

Thermal noise, sometimes called Johnson or Nyquist noise, is an electric noise. It is a result of the random motion of carriers in resistive materials at finite temperatures. This

movement results in the random current I. We can also say that it is a change in the number of electrons compared to mean values. This noise has a Gaussian distribution and it can be expressed by the following formula [17]:

$$\sigma^2_{i_{th}(t)} = \frac{4k_B T}{R}\Delta\nu[-], \tag{3.30}$$

where $\sigma^2_{i_{th}(t)}$ is the standard deviation of current source (i_{th} is in parallel with R); k_B stands for the Boltzmann constant (in J×K^{-1}); T is the resistor's absolute temperature (in K); and $\Delta\nu \simeq 1/2\tau$ is the bandwidth of the detector.

3.4.3 Amplified spontaneous emission noise

The last of the noises mentioned in this chapter is the ASE noise which is caused by the amplified spontaneous emission. In high-power lasers, amplification of luminescence caused by the spontaneous emission can achieve very critical values. However, thus amplified luminescence can be used in many applications where there are no demands on the time coherence, but only on the spatial one. Despite the fact the luminescence as such is multidirectional, the ASE noise is only unidirectional.

When using high-performance fiber lasers or fiber amplifiers, the ASE noise represents highly undesirable phenomenon due to which performances are limited to 40-50 dB. For higher performance it is necessary to connect the amplifiers to cascades that are separated by filters. There are several ways to suppress the ASE noise, e.g. using different lengths of fiber, various levels of fiber doping or different types of fibers (photonic crystal fibers). Fig. 3.10 clearly shows that the ASE noise intensity may vary depending on the direction of rare-earth doped fiber pumping [18].

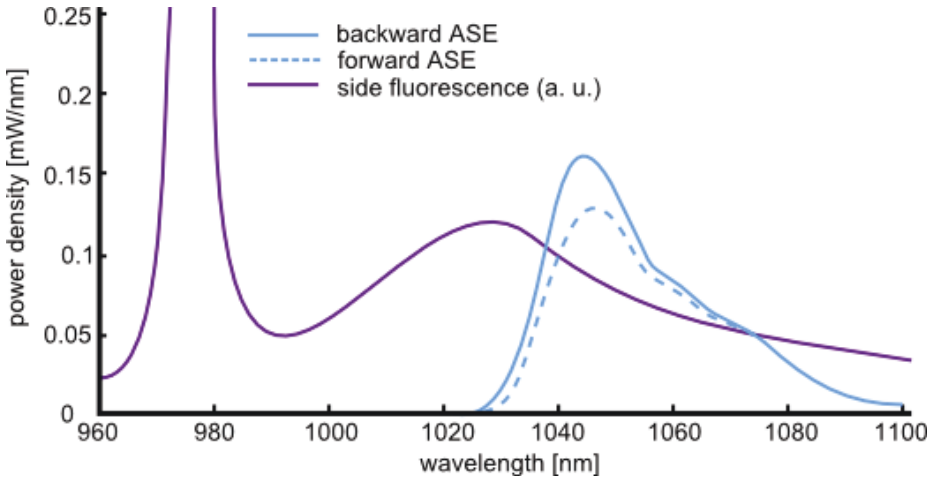

Figure 3.10: Spectrum of forward and backward ASE in ytterbium-doped fiber amplifier [18]

An important finding is the influence of the pump laser level on the ASE noise. Another interesting fact is that the ASE noise intensity is not dependent on the properties of the single-mode fiber (such as the core size or numerical aperture) but on the number of modes.

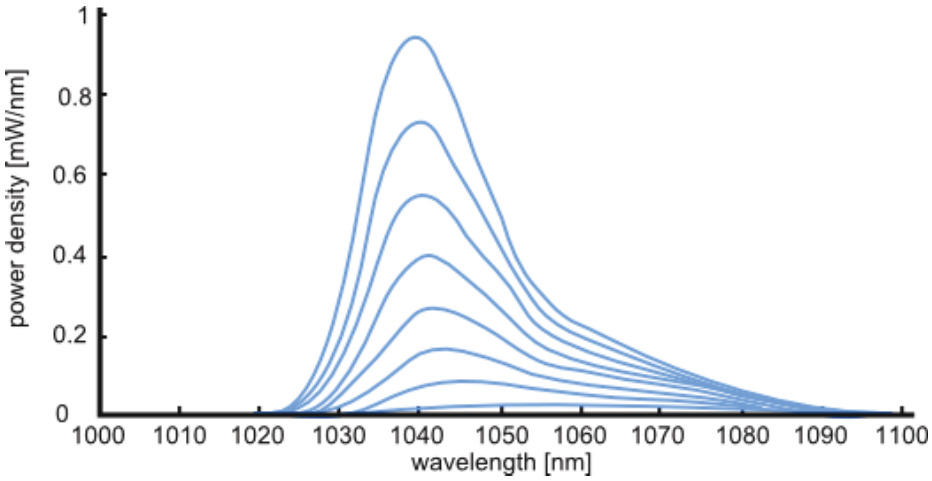

Figure 3.11: Spectrum of backward ASE in different pump power levels [18]

The ASE noise is sometimes referred to as superluminescence and it is used in broadband sources such as e.g. white light sources. The noise in EDFA amplifiers is given by the formula [19]:

$$P_{ASE}^{out} \cong 2n_{sp}h\nu(G-1)\Delta B[W], \tag{3.31}$$

where n_{sp} is the spontaneous emission factor that equals the relation $N_2/(N_2–N_1)$; h is the Planck constant ($m^2 \times kg \times s^{-1}$); v is the optical carrier frequency (in Hz); G is amplification by EDFA; and ΔB is the width of the optical band where the noise is propagated (in Hz).

The EDFA noise figure is defined as $F \approx 2n_{sp}$ and the lowest theoretical value is 2 dB. Typically, the value of the noise is from 4 to 5 dB [3].

4 Another types of optical amplifiers

In this chapter, we will focus on basic types of amplifiers which are used in optical communications. The main advantage of optical amplifiers, compared to the conventional ones, is that they do not need to convert the optical signal to the electrical one and back. Because of this, it is of no importance what polarization, coding or bit rate the amplified signal has. Therefore, the optical amplifiers are highly versatile.

It is obvious that this area undergoes rapid evolution. The original SOA amplifiers have been replaced by amplifiers that use the stimulated Raman or Brillouin scattering, or by amplifiers with rare-earth doped fibers (EDFA).

The following three subchapters deal with the first three types of the mentioned amplifiers in detail. We will describe their basic principles, and highlight their advantages and disadvantages. The last-mentioned type of amplifier, i.e. the EDFA, will be discussed separately in the next chapter because EDFA is what the work is primarily focused on.

4.1 Semiconductor optical amplifier

The SOA is a type of amplifier based on a semiconductor material, or more precisely, on a p-n junction. Its structure is similar to that of a common laser with Fabry-perot cavity. However, there are some key differences. As for this amplifier, great emphasis is put on the fact that it is not a laser. That is why, in contrast to lasers which have semi-permeable mirrors, these amplifiers have anti-reflective surface. And in order to suppress the front-end reflection even more, it uses e.g. tilted waveguide and window regions [1].

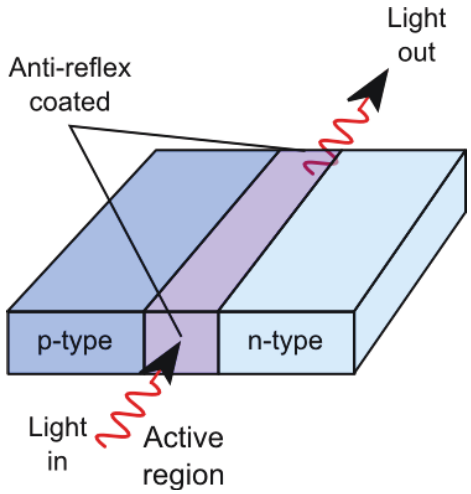

Figure 4.1: Block diagram of a semiconductor optical amplifier [1]

In comparison to other types of amplifiers, SOA differs in the way to achieve a population inversion. It is also important to take into account the fact that energy carriers are not

represented only by electrons in various energy levels, but also by electrons and holes in semiconductor materials. The holes can be energy carriers as well as electrons with the only difference being that the holes have the positive charge. In semiconductors, the carriers can be placed in two levels: in a low-mobility level, the so-called valence band, or in a high-mobility level, the so-called conduction band. Between these two bands, there is the so-called bandgap that has no energy levels. We can use a p-type semiconductor material as an example. In thermal equilibrium, there are only few electrons in the conduction band. However, if a population inversion occurs, the concentration of electrons in the conduction band will be much higher (see Fig. 4.2).

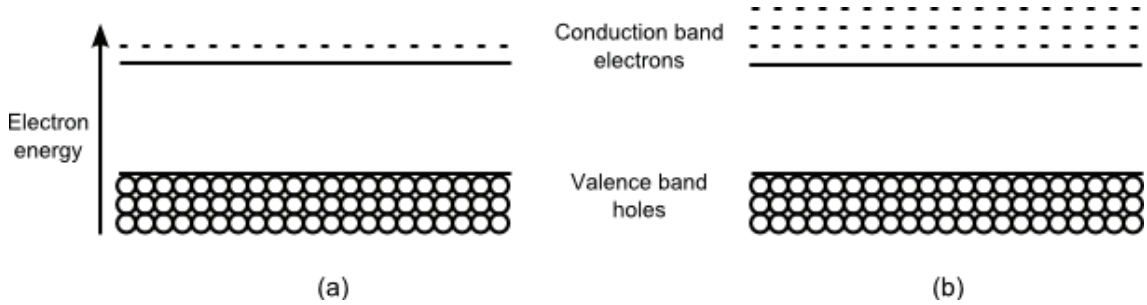

Figure 4.2: The energy band in a p-type semiconductor and the electron concentration in (a) thermal equilibrium and (b) population inversion [1]

When optical signal is present, the increased concentration behaves like stimulated emission in the transition from the conduction band to the valence band, and like absorption in the transition from the valence band to the conjunction band. The population inversion in the SOA is achieved using forward-biasing and p-n junction. The p-n junction is composed of two semiconductors, one of which is of p-type and contains excess holes, and the other one is of n-type and contains excess electrons. When we combine these two semiconductors together, the electrons will diffuse into the p-type semiconductor and the holes into the n-type semiconductor (see Fig. 4.3.a). This fusion gives rise to a negatively charged area in the p-type semiconductor, and a positively charged area in the n-type semiconductor (see Fig. 4.3.b). If there is no bias applied to the interface, the concentration of minority carriers remains in thermal equilibrium. If we apply bias to the crossover in the conducting state, positive bias to the p-type semiconductor and negative bias to the n-type semiconductor (see Fig. 4.3.c), depending on the voltage (bias), the electrons begin to move from the n-type semiconductor to the p-type semiconductor and vice versa. If the voltage (bias) is high enough, there arises the already mentioned population inversion and the p-n junction starts to function as an optical amplifier. The basic p-n junction is not used in practice. Usually, a thin semiconductor serving as an active region of the amplifier is inserted into it [1].

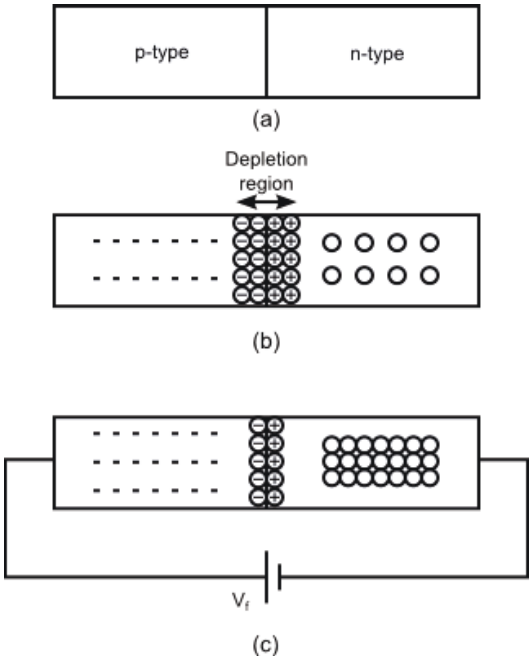

Figure 4.3: A forward-biased pn-junction used as an amplifier: (a) pn-juction; (b) Minority carrier concentrations and depletion region with no bias voltage applied; (c) Minority carrier concentrations and depletion region with a forward-bias voltage V_f [1].

Although SOA is small in size, with possible integration of semiconductor lasers, modulators, etc., and is potentially cheaper than EDFA, its power is still not comparable to it. SOA has higher noise, lower gain, medium dependence on polarization, and high nonlinearity with high transition time that causes crosstalks. Since this nonlinearity represents the most serious problem for optical communications, SOA is more suitable for treatment of optical signal in devices such as complete optical switches, etc. [1]

4.2 Raman scattering amplifier

Another type of amplifier used in optoelectronics is the amplifier that uses Raman scattering. We know from the previous chapter which deals with nonlinear effects that Raman scattering is a nonlinear phenomenon during which photons with different frequency shifts are emitted when the molecule descends into lower vibrational state of a given material. And it is the type of material what affects the resulting amplification curve shape. Fig. 4.4 shows various amplification curve shapes for different types of fibers [19].

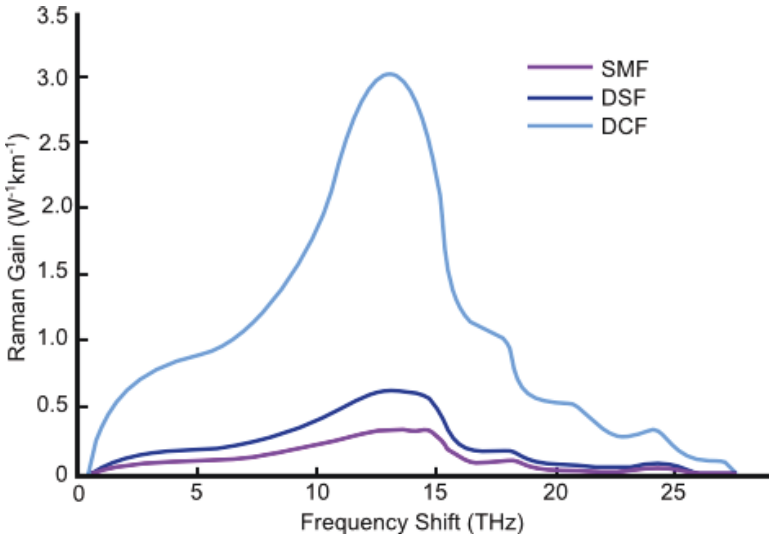

Figure 4.4: Raman gain profiles of a 1510-nm pump in three different fiber types. SMF – standard single mode fiber, DSF – dispersion shifted fiber, DCF – dispersion compensating fiber [19].

Frequency difference between the pump and the signal photon (v_p–v_s) is called the Stokes shift. When using standard Ge-doped fibers, its peak is about 13.2 THz.

Main advantages of using the stimulated Raman scattering is the speed of the amplification process, the possibility to choose any fiber, and the possibility to use a large range of amplified wavelengths depending on the wavelength of the laser pump source. Because of these three characteristics, the amplifier using the Raman scattering may seem as an ideal choice for application in optical systems. Nevertheless, it has negative properties as well, namely e.g. uneven amplification of the entire spectrum or the length of a fiber. That is why, the Raman amplifier is often used in combination with EDFA and it is mainly deployed as an in-line amplifier. Fig. 4.5 shows the classic connection of the Raman amplifier.

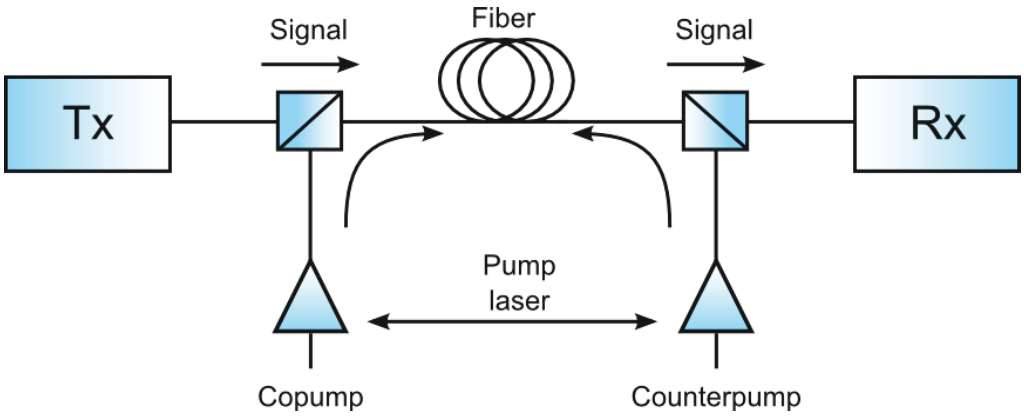

Figure 4.5: Schematic diagram of an optical communication system employing Raman amplification [19]

4.3 Brillouin scattering amplifiers

Stimulated Brillouin scattering is a nonlinear effect arising in silica fibers when exceeding certain signal intensity limit (usually in mW). This phenomenon was described in detail in Chapter 3.3.1. As a result of generating a frequency-shifted signal (mainly Stokes components), we achieve the required amplification of weak optical signals. Even though the spectral width of the amplified spectrum is very small, it is possible to use it in selecting only few channels or in their amplification. Therefore, such amplifying element can be utilized mainly in channel selection in WDM systems [15].

5 Erbium-doped fiber amplifier

A proposal of an EDFA, i.e. Erbium-Doped Fiber Amplifier, was developed by J. E. Geusic and H. E. D. Scovil. Although the project was first published already in 1962, its potential was not used in telecommunications until the 1990s because of economically demanding pump lasers. The principle of EDFA amplifier resides in the fact that it enables a transmission path to increase its capacity by increasing the number of wavelengths, not by increasing the bit rate.

In the previous chapters, we have focused on the most widely known and commonly used amplifiers, except one – the most important one – the already mentioned Erbium-Doped Fiber Amplifier. Since this work is primarily focused on this type of amplifier, we have decided to dedicate a whole chapter to it where we can pay attention to details. As evident from its name, it is an amplifier that uses rear-earth doped fibers.

As for an overview of the following chapters, at first we will take a close look at level systems, and at the basic circuit of optical amplifiers with its possible modifications. Another chapter will be dedicated to pump lasers, in particular to the question of what types of lasers are commonly used and what demands are placed on them. We will also minutely examine doped fibers and will go through a list of the rare earths which are used as dopants. The last part of the EDFA section will be dedicated to other components which are necessary for constructing EDFA amplifiers.

5.1 Level system of gain media

Level systems in a gain medium represent an essential issue. It is important to realize that what laser needs in order to function properly is a population inversion which is possible only in at least three-level systems. If we want to express a population inversion using Einstein coefficients, we can follow these formulas [20]:

For two-level system:

$$\Delta N = \frac{N}{1 + 2I / I_{sat}}, \tag{5.1}$$

For three-level system:

$$\Delta N = N \frac{1 - I / I_{sat}}{1 + I / I_{sat}}, \tag{5.2}$$

For four-level system:

$$\Delta N = -N \frac{I / I_{sat}}{1 + I / I_{sat}}, \tag{5.3}$$

where ΔN is the quotient of the number of absorptions and the number of emissions; N, on the other hand, is sum of these numbers; and $I_{sat} = A / B$ is the saturation intensity, where A and B are Einstein coefficients [20].

Formula 5.1 clearly expresses that ΔN is always positive regardless of the value of I. It follows that it is not possible to achieve a population inversion when using a two-level system. In the second case, the ΔN is already negative, and in the third case, it is always negative. So it is the four-level system where the inversion is achieved most easily and with less energy than in the three-level system. Fig. 5.1 shows that the four-level system, compared to the three-level one, has also second non-radiative crossing. Since the difference between energies is very small in the fast crossing, it is possible to achieve the population inversion even more easily. In the case of the three-level system, the stimulated emission takes place between the metastable and the ground state; as for the four-level system, it occurs between the metastable state and the low level. There is also a special case represented by the quasi-three-level system which is a combination of the three and the four-level system. The low level is so close to the ground state that certain part of the population remains in thermal equilibrium. Consequently, the unused power is repeatedly absorbed on the wavelength corresponding to the type of the medium [21].

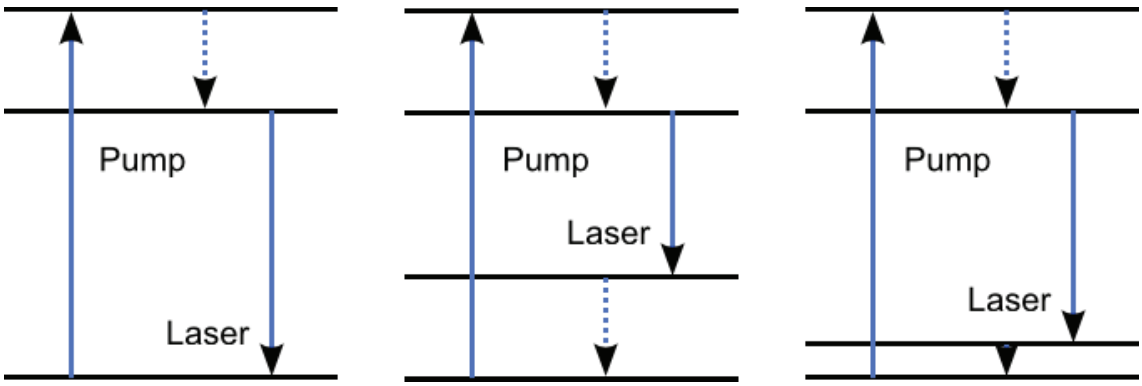

Figure 5.1: Energy level diagrams of different laser systems. A three-level system (left), a four-level system (middle), a quasi-three-level system (right) [21]

5.2 Basic circuit of EDFA

One of the most important components in EDFA amplifiers is the doped fiber itself because this is where the amplification takes place. According to type of the dopants, all the amplifiers are divided into several categories, such as e.g. EDFA, PDFA, TDFA or YDFA. Character of a doped fiber has a great influence on the spectral range of the amplifier and,

thanks to various dopants, we are not limited to the C or the L band only, we can also move in the O or in the S band.

Another important part of an amplifier is its laser which is used as a power supply for the doped fiber. This kind of laser is called the pump and, using its spectral and power characteristics, it influences the effect of fibers.

Both of these components will be discussed in the following subchapters which will be directly focused on them. In the subchapter dedicated to fibers, we will present different types of dopants and the related number of levels in these systems, and also the influence of fiber length on the amplification. Subchapter 5.3 will focus on the already mentioned pump lasers and their characteristics, we will demonstrate their possible connection configurations and their influence on the amplifier [22].

Fig. 5.2 shows the standard connection of the EDFA amplifier.

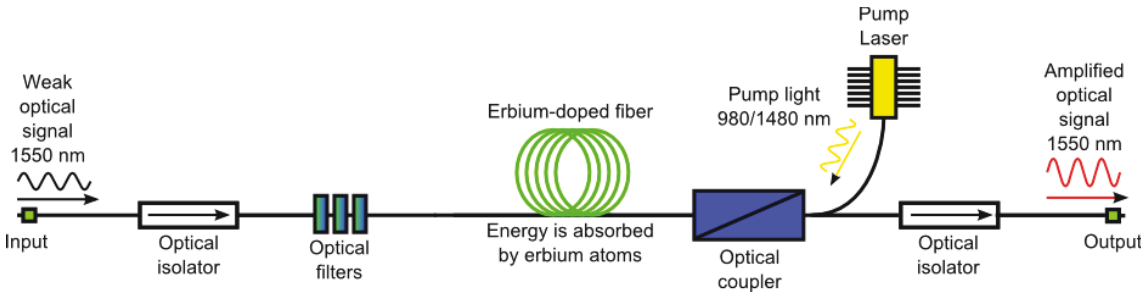

Figure 5.2: Erbium-doped fiber amplifier [23]

A weak optical signal is brought to the input of the amplifier. The signal passes through the optical isolator which prevents the light beam from going back to the radiation source which could cause its untuning. The signal then goes through a system of filters in order to prevent further passing of the light beam of the 980 nm or the 1480 wavelength from the pump. After passing through all the input section of the amplifier, the weak signal gets to the EDF (erbium doped fiber) where its energy is absorbed by Er^{3+} ions. The energy they absorb is provided by the pump on the 980 nm or 1480 nm wavelength. The process of absorption has already been described in Chapter 2.1. What follows is the stimulated emission of the wavelength of around 1550 nm. At this moment, ASE parameter (see Chapter 3.4.3) appears. The pump light is then transferred from the pump using a WDM coupler. After the amplification, the original signal passes again through the optical isolator that blocks the pump wavelength, and is emitted at the output of the amplifier [22], [24].

In the following subchapters, we will focus on erbium as a dopant, and on pump lasers. After this, we will go through theoretical foundations of WDM couplers and isolators as important components for proper function of the amplifier.

5.3 Pump lasers

5.3.1 Introduction

As already suggested, the pump laser represents a very important part of the EDFA amplifier. It takes care of the supply of optical energy to the doped fiber, contributing thus directly to its amplification. That is why, there are great demands placed on them. Since doped fibers absorb energy only at certain wavelength depending on the dopant they are doped with, the laser must be well thermally stabilized so as to avoid untuning of the wavelength as well as power fluctuation. Of course, these parameters are influenced also by the manufacturing process, that is why, the laser is so economically demanding. There are not only diodes that excite the laser, there is also a possibility to use other mechanisms such as discharge tube, discharge in gas, collision or recombination excitation, chemical processes or semiconductors.

Wavelengths used for pumping not only in EDFA but also in TDFA and other amplifiers are dependent on the dopants used in the doped fiber. In the case of erbium, there are the wavelengths of 980 and 1480 nm. This fact will be discussed in the next chapter where we will point at the main differences of these two wavelengths. The subsequent subchapter will explore various pump circuit configurations and the influence of the pump on the amplifier. The last section of this chapter will be dedicated to determining absorption intensity of the light pumped to the doped fiber, and to a certain extent, to pump process efficiency.

5.3.2 Pump types

As already mentioned several times, two fundamental wavelengths used for EDFA amplifiers are 980 nm and 1480 nm. In the past, there were experiments with shorter wavelengths performed, with 514.5 nm, 670 nm, 532 nm and 800 nm in particular. However, their properties were not sufficient and, because of that, they were abandoned.

The pumping source of the 1480 nm wavelength is used primarily for its favourable price and reliability. Its negative aspects, on the other hand, are gradual wear and aging causing deterioration of performance, i.e. untuning of the central wavelength and power losses. This fact, in the case of pumping the erbium-doped fiber, represents a serious problem. Nevertheless, their reliability helped them to create a permanent position in ground and especially in submarine paths were demands on the reliability of fiber amplifiers are extremely high. Depending on power, gradual wearing of the pump can be compensated. This compensation can be set so that the pump creates sufficient power at desired degree of reliability.

At the beginning, the pumping source with the 980 wavelength did not reach such high degrees of reliability as was the case with the pumping source with the wavelength of 1480 nm. There were frequent failures and surface reactivity, because of which they were susceptible to optical damages. However, thanks to technological development, pumps with much higher reliability have been developed, and these could be deployed to ground as well as to submarine paths. The following table shows a direct comparison of properties of both pump types [25].

Table 5.1: Comparing pumps with 980 nm wavelength and 1480 nm wavelength [26]

Parameter	980-nm Laser	1480-nm laser
Minimum noise figure	<4dB	<5.5dB
Fiber coupled power	300 mW (standard)	250 mW (standard)
	>500 mW (high power)	310mW(high power)
Spectral width	5 nm @250 mW	8 nm @ 250 mW

The most important parameter shown in Table 5.1 is the minimum noise figure. We know from Chapter 3.4.3 that the ASE noise represents one of the most critical parameters in EDFA amplifiers, so its reduction at different wavelengths is essential. Another parameter is the fiber coupled power and, as we can see, the 980-nm laser has the possibility to use more power, which proves to be useful particularly in remote pumping.

The picture 5.3 shows that, because of different pumping, the electrons are excited to different energy levels. Absorption of erbium at various wavelengths will be explained more specifically in Chapter 5.4.2 [26].

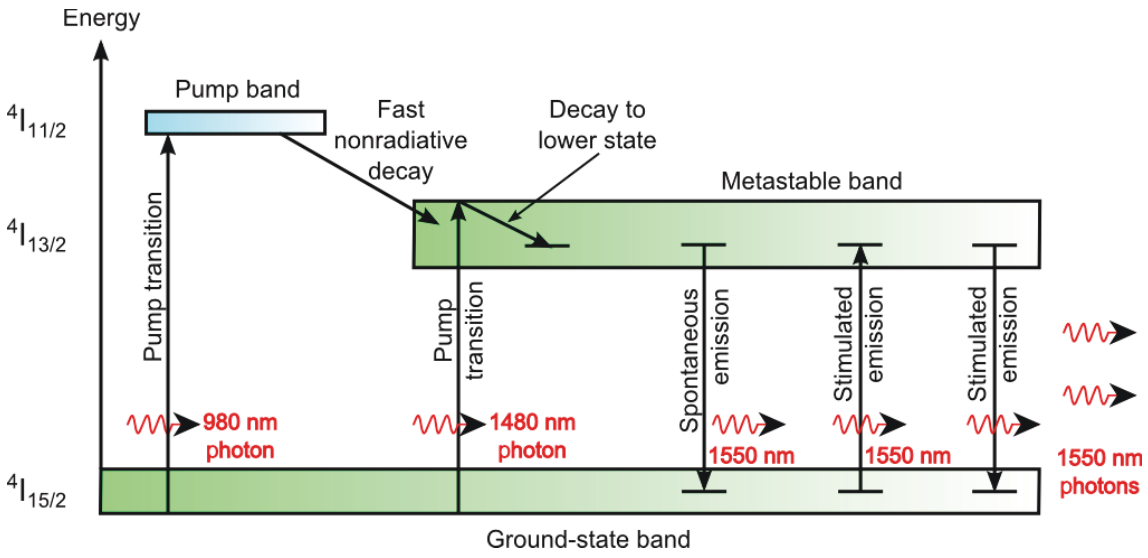

Figure 5.3: Comparing pumps with 980 nm and 1480 nm wavelength [26]

5.3.3 Main types of pump circuit

When pumping the active environment, we have three basic pump connection options. The first one is the so-called co-directional pumping consisting in pumping the doping light in the same direction as is the direction of the signal. The second possibility, the so-called counter-directional pumping, resides in pumping the light in the opposite direction as is the direction of the signal. And finally the third one, the so-called dual pumping, represents a combination of the first two. Fig. 5.4 shows all three of them [26].

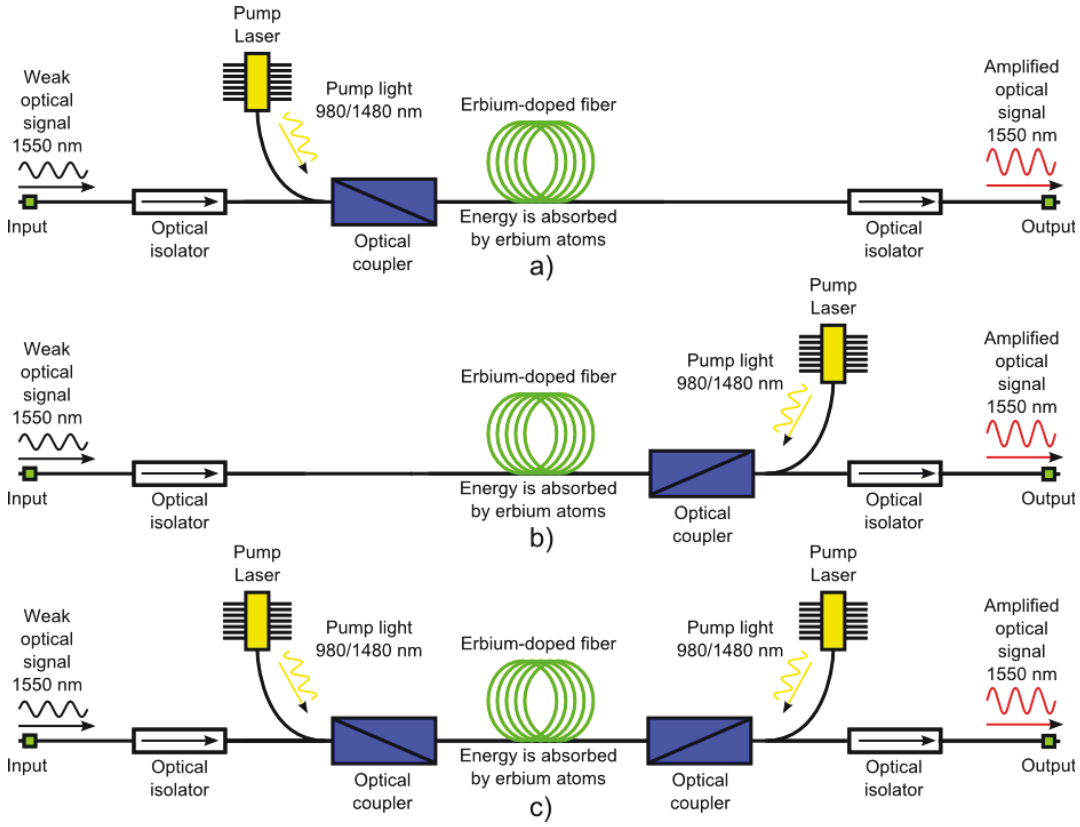

Figure 5.4: Configuration of EDFA and possible pumping methods. (a) Co-directional pumping; (b) counter-directional pumping; (c) dual pumping [26]

Counter-directional pumping is suitable for use as a booster circuit because, although it has higher noise, we can use higher power for pumping and thus get better overall power of the amplifier. On the other hand, co-directional pumping has better noise characteristics and lower power, therefore it is more suitable to use it as a preamplifier. Connection of the pump is also dependent on the wavelength used. Thus, if we use dual pumping where there are two pumps facing each other, there arises an opportunity to use different wavelengths. Another circuit variant is represented by multilevel connection, as indicated by Fig. 5.5.

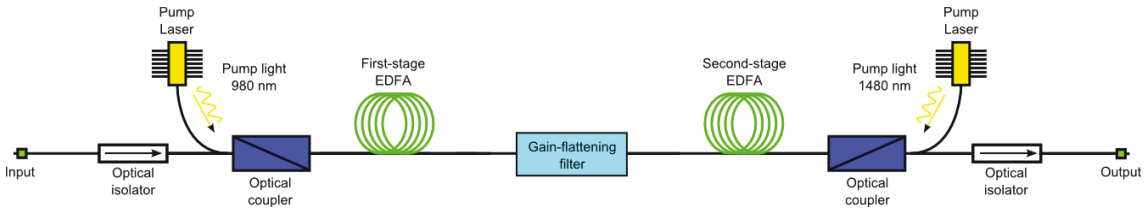

Figure 5.5: Multiple-stage EDFA plus gain-flattening filter with both co-directional and counter-directional pumping [26]

5.3.4 Light dropping

The active region of an amplifier may be affected not only by the direction of pumping but also by the angle at which the light is supplied to the active region. One possibility is the so-called end pumping, the other one the so-called side pumping. The former has better beam quality, the latter, on the other hand, can achieve higher power. As we can see, each solution has its pros and cons.

The end pumping is usually used for lasers with power up to 50 mW. What is a critical factor in using this circuit is the power limit which is caused by the fact the diameter of the active region frontend (crystal frontend in the case of the laser) is only a few millimetres wide. Intensity formed on such a small area does not have to be absorbed, which may result in overheating and therefore in a change in the refractive index of the material itself. In the case of side pumping, this problem is eliminated because the laser intensity is spread over a larger area. As shown in Fig. 5.6, in the end pumping, the doping light is delivered to the active region using a reflecting mirror [27].

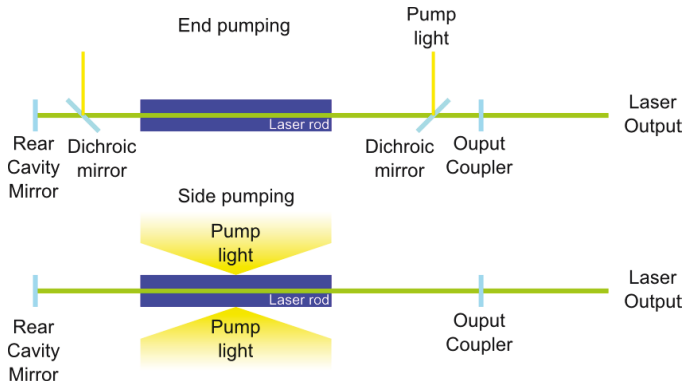

Figure 5.6: Diode pumping from side or end [27]

Another possibility to excite the laser is to use a thin disk. The optical beam falling on the disk of the surface S causes emission of the radiation which is perpendicular to the surface. An advantage of the thin disk is the possibility of sufficient cooling and hence the possibility to achieve high power. The disk excitation is shown in Fig. 5.7 [20].

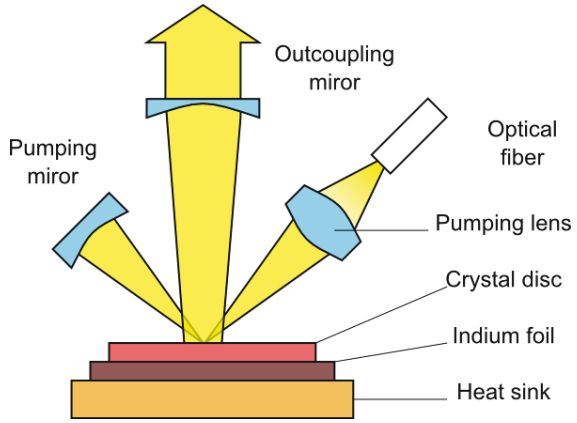

Figure 5.7: Exciting the laser by the thin disk [20]

5.3.5 **Remote pumping**

Remote pumping gains in importance in long-distance-paths where there is difficult to install electrical equipment (e.g. laser), or in paths where electrical energy supply is impossible. In these very cases, we can fully exploit properties of the EDFA. Since the only active element is the pump laser, there is the possibility to push it into places with electrical energy supply, giving thus rise to remote pumping. Remote pumping of doped fibers is used e.g. in amplifying submarine optical paths. Fig. 5.8 shows gradual development of remote pumping [24].

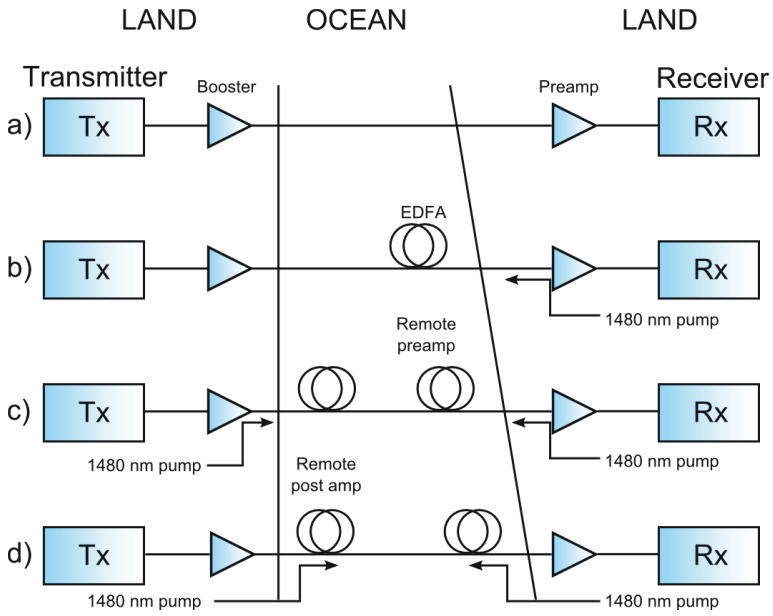

Figure 5.8: Progression of repeaterless systems from a simple preamplifier and a power amplifier to remote pumping [24]

The A part of Fig. 5.8 represents the original connection without the amplifier on the path. In this case, the amplifier was used only at the beginning and at the end of the path. At the beginning of the path, it amplified the power to the maximum possible level that could be coupled into the fiber. At the end of the path, it was amplified to a level that is necessary for proper functioning of the detector. This solution, however, contained limitations not only in transmission capacity but also in accessible distances.

The first connection of erbium-doped amplifier with remote pumping (Fig. 5.8.b) was implemented by overcoming the loss of 19.7 dB out of the total 62 dB at 310 km long path and 1.855 $Gb \times s^{-1}$ bit rate. In this experiment, the pumping was carried out using the pump on the receiver side at the distance of 34.6 km from the doped fiber. The amplifier was constructed using a 15 m long fiber and 9.9 dB gain. The pumping power was 192 mW at the 1480 nm wavelength.

In the following case (Fig. 5.8.c), there was pumping from both ends of the optical path. This kind of pumping (just as the A version) uses for supplying pump signal a low-loss fiber which is separated from the fiber that transmits the signal.

In the last connection (Fig. 5.8.d), there are pumps connected directly to remote EDFs. In each remote pumping, there is high power used and, that is why, negative phenomena occur to a large extent. We talk e.g. about nonlinear effects, Brillouin scattering and dispersion, mentioned already in Chapter 3 [24].

5.3.6 **Pump absorption**

Absorption of the pump light is an important factor for every fiber optic amplifier. In the light absorption we want the energy transfer from the pump laser to be as efficient as possible.

The rate of absorption is dependent on wavelength. Another parameter is the width of the absorption band of the doped medium or material. This width is related to the bandwidth of the pump laser. Therefore, we want these two bandwidths to overlap. Of course, the frequency stability can also be influenced by temperature. The rate of absorption is given by the following formula [28]:

$$A = 1^{-(-N_{dop}\sigma_{abs}L)}[-], \tag{5.4}$$

where N_{dop} is the doping concentration, L is the length of the doped medium, and σ_{abs} is the absorption cross section at the pump wavelength.

Another factor which may affect the rate of absorption is polarization of the pumping source or of the doped medium. This problem is usually solved by proper configuration of both polarizations in relation to each other. However, this difficulty tends to grow in significance when using a fiber-coupled diode laser which is dependent on temperature and movement of the

fiber, and is not entirely linear. These sources are often less stable. This phenomenon occurs especially in anisotropic laser crystals [28].

5.3.7 Saturation of pump absorption

A significant degree of saturation can be observed especially in quasi-three-level medium lasers. However, the resulting absorption can be saturated only to the extent allowing the depletion of ions from the ground state. The extension of saturated absorption is dependent mainly on the power supplied by the pump laser. But once we get over certain laser threshold, the absorption rate will no longer increase.

The saturation intensity for low power amplifier can be calculated from the following formula [28]:

$$I_{sat} = \frac{hv}{(\sigma_{em} + \sigma_{abs})\tau}\left[W \times cm^{-2}\right], \tag{5.5}$$

and the power can be derived from [28]:

$$P_{sat} = AI_{sat} = \frac{Ahv}{(\sigma_{em} + \sigma_{abs})\tau}\left[mW\right], \tag{5.6}$$

where *hv* is the photon energy at the signal wavelength, σ_{em} and σ_{abs} are the emission and absorption cross sections at the emission wavelength, τ is the upper-state lifetime, and A is the mode area.

5.4 Doped fibers

In this chapter, we will focus on physical and chemical properties of individual dopants. We will acquaint ourselves with the most commonly used ones, and will present advantages and disadvantages of their employment. Then, we will look at their application in three or four-level systems, and their reduction from the three to the two-level system. Finally, we will explain the issue of the doped fiber length and its influence on the parameters of the amplifier.

5.4.1 Material used as matrices

If we want to understand the composition of doped fibers, it is important to focus not only on rare earth ions used as dopants, but also on matrices. A matrix is the material to which a

dopant is added. Let us start with type of glass. In the case of erbium-doped fibers, the silica glass is used. However, there are also other options such as oxide glass, halide glass, chalcogenide glass, etc. [29]

Another important fiber components are admixtures that are added to the SiO_2 in order to improve its characteristics. We can e.g. increase the refractive index using GeO_2, TiO_2, Al_2O_3 or P_2O_5. On the other hand, decrease in the refractive index can be achieved by using B_2O_3 or F. Dependence of the refractive index on the used dopant is described by the following figure:

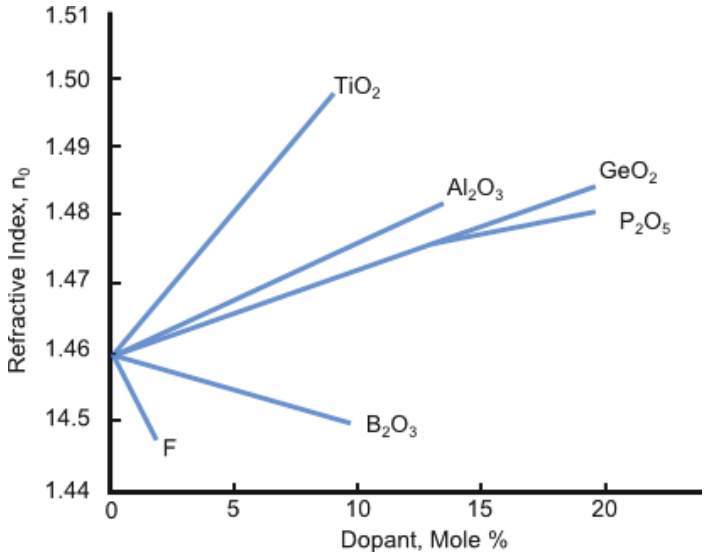

Figure 5.9: Refractive index of common dopants for silica [29]

5.4.2 Types of dopants

Since we have already looked at materials used as matrices, we can now focus on the dopants themselves, and primarily on erbium because this chemical element represents the main substance of EDFA amplifiers. Of course, we will mention some other elements as well, namely neodymium, ytterbium, thulium, holmium, praseodymium and cerium.

Erbium

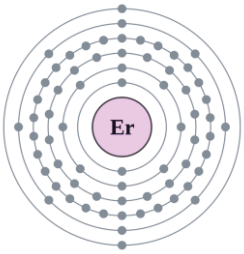

Figure 5.10: Electron configuration of erbium

Erbium is a transition metal element of silvery white colour ranking among lanthanides. Its electron configuration is 2, 8, 18, 30, 8 and 2. If we want to create the erbium ion Er^{3+}, we need the following ionization energies:

Table 5.2: Ionization energies of erbium

Ionization energies	1st: 589,3 kJ.mol-1
	2nd: 1150 kJ.mol-1
	3rd: 2194 kJ.mol-1

The Er^{3+} ions are pink and they are used in optoelectronics because of their property of fluorescence. Thanks to the fluorescence at the wavelengths from 1530 to 1570 nm, they are perfectly suitable for the use in telecommunications. This phenomenon is described in Fig. 5.11.

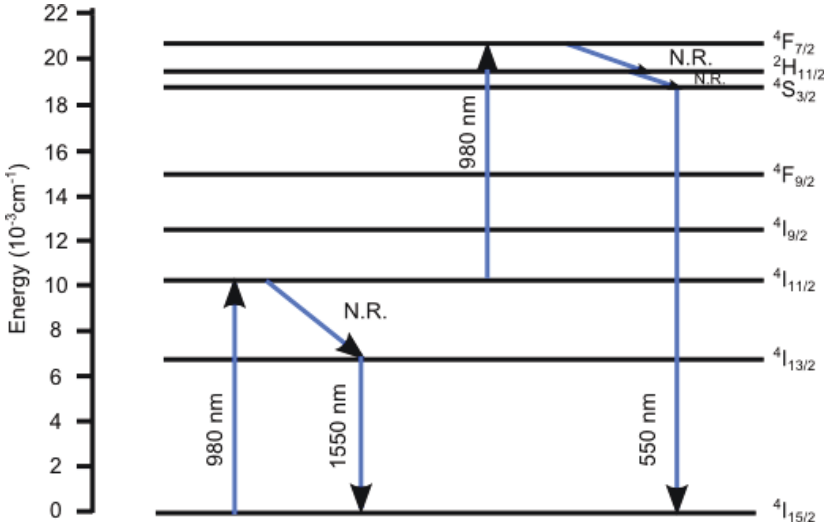

Figure 5.11: Energy level diagram for Er^{3+} [29]

When using a pump at the 980 nm wavelength, the Er^{3+} ion is excited from the $^4I_{15/2}$ to the $^4I_{11/2}$ level. This transition is immediately followed by the transition to the $^4I_{13/2}$ level which functions as a metastable level. The $^4I_{11/2}$ to $^4I_{13/2}$ level transition is very fast and non-radiative. In the case of the reverse transition from the metastable to the lowest level, a photon with approximately 1530 nm bandwidth is generated. Ions remain in the metastable level for about 10 ms. We should take into consideration that emission of the 1530 nm photon is a result of stimulated emission. Of course, there is also the already mentioned spontaneous emission which results in noises. Another option is transferring energy among the individual ions [29].

Although the dominant fluorescence in erbium occurs between the levels $^4I_{13/2}$ and $^4I_{15/2}$, it is also possible that the population inversion will partly take place in the transition between the levels $^4I_{11/2}$ and $^4I_{15/2}$ [29].

Fig. 5.11 shows that energy of the $^4F_{7/2}$ level corresponds to energy of two photons. And if the excited ion receives the energy of these two photons, it will get to this very level. It is the so-called ESA, or the excited-state absorption. Then, the ion can descend to levels $^4I_{9/2}$, $^4I_{11/2}$, $^4I_{13/2}$, $^4I_{15/2}$ with the emission of light of the 1720 nm, 1220 nm, 850 nm or 550 nm wavelength respectively. Table 5.3 shows possibilities of erbium [29].

Table 5.3: Characteristics of Representative CW Er-Doped Silica Fiber Lasers [22]

Laser wavelength	Pump wavelength	Erbium concentration	Fiber length	Other features	Threshold	Slope efficiency	Output power / max. pump power
1.566 µm	514.5 nm	35 ppm Er ion	13 m	Ar-ion laser pump	44 mW	10 %	56 mW / 0.6 mW
~1.56 µm	532 nm	150 ppm Er_2O_3	1 m	Ring laser	10 mW	5.1 %	1.8 mW / 45 mW
1.535 µm	532 nm	100 ppm Er	15 m	Doubled Nd:YAG	NA	28 %	1 W / 3.6 W
1.56 µm	806 nm	500 ppm Er	3.7 m	LD array pump	10 mW	16 %	8 mW / 56 mW
1.62 µm	808 nm	300 ppm Er	1.5 m	LD pump	3 mW	3.3 %	0.13 mW / 7 mW
1.56 µm	980 nm	0.08 wr% Er	0.9 m	Dye laser	2.5 mW	58 %	4.7 mW / 11.3 mW
~1.54 µm	980 nm	1100 ppm Er	9.5 m	Ti:sapphire / Tuneable	>10 mW	>49 %	260 mW / 540 mW
1.552 µm	~1.46 µm	1370 ppm Er ion	5 m	Two LD pumps	37 mW	14 %	8 mW / 93 mW
1.552 µm	1.47 µm	1370 ppm Er ion	7 m	LD pump	44 mW	6.3 %	~1mW / 60 mW
1.555 µm	1.48 µm	~45ppm Er	60m	LD pump / Ring laser	6.5 mW	38.8 %	3.3 mW / 15 mW
~1.56 µm	1.48 µm	110 ppm Er_2O_3	42.6m	LD pump	4.8 mW	58.6 %	14.2 mW / 29 mW

Other important parameters of doped fibers are absorption $\sigma_a(\lambda_s)$ and emission cross-section. While measuring absorption belongs among simple operations, measuring emission is much more difficult. The relationship between these two values is described with the McCumber theory. Using experimental measurements, it has been found out that the ratio of particular types of matrices is different. Calculating the emission coefficient is then simple. Coefficients for 3 fiber types are given in the following table [29]:

Table 5.4: Absorption and emission cross-sections for different types of erbium doped silica fibers [29]

Fiber type	σ_e (x 10^{-25} m)	σ_a (x 10^{-25} m)
GeO_2-SiO_2	6.7 ± 0.3	7.9 ± 0.2
Al_2O_3-SiO_2	4.4 ± 0.6	5.1 ± 0.6
GeO_2-Al_2O_3-SiO_2	4.4 ± 1.0	4.7 ± 0.8

Another dopants

Erbium is not the only chemical element used as a dopant. There are also other rare earths belonging among lanthanides such as e.g. ytterbium, thulium, neodymium or praseodymium. Each of these earths is excited using a light of different wavelength. Subsequently, they emit light of another wavelength. A list of the most important wavelengths together with common host media for rare earths is presented in Table 5.5:

Table 5.5: Parameters of another dopants [30]

Ion	Common host media	Important emission wavelengths (μm)
Neodymium (Nd^{3+})	YAG, YVO_4, YLF, silica	1.03–1.1, 0.9–0.95, 1.32–1.35
Ytterbium (Yb^{3+})	YAG, tungstates, silica	1.0–1.1
Erbium (Er^{3+})	YAG, silica, tellurite, chalcogenide glass	1.5–1.6, 2.7, 0.55
Thulium (Tm^{3+})	YAG, silica, fluoride glasses	1.7–2.1, 1.45–1.53, 0.48, 0.8
Holmium (Ho^{3+})	YAG, YLF, silica	2.1, 2.8–2.9
Praseodymium (Pr^{3+})	silica, fluoride glasses	1.3, 0.635, 0.6, 0.52, 0.49
Cerium (Ce^{3+})	YLF, LiCAF, LiLuF, LiSAF, and similar fluorides	0.28–0.33

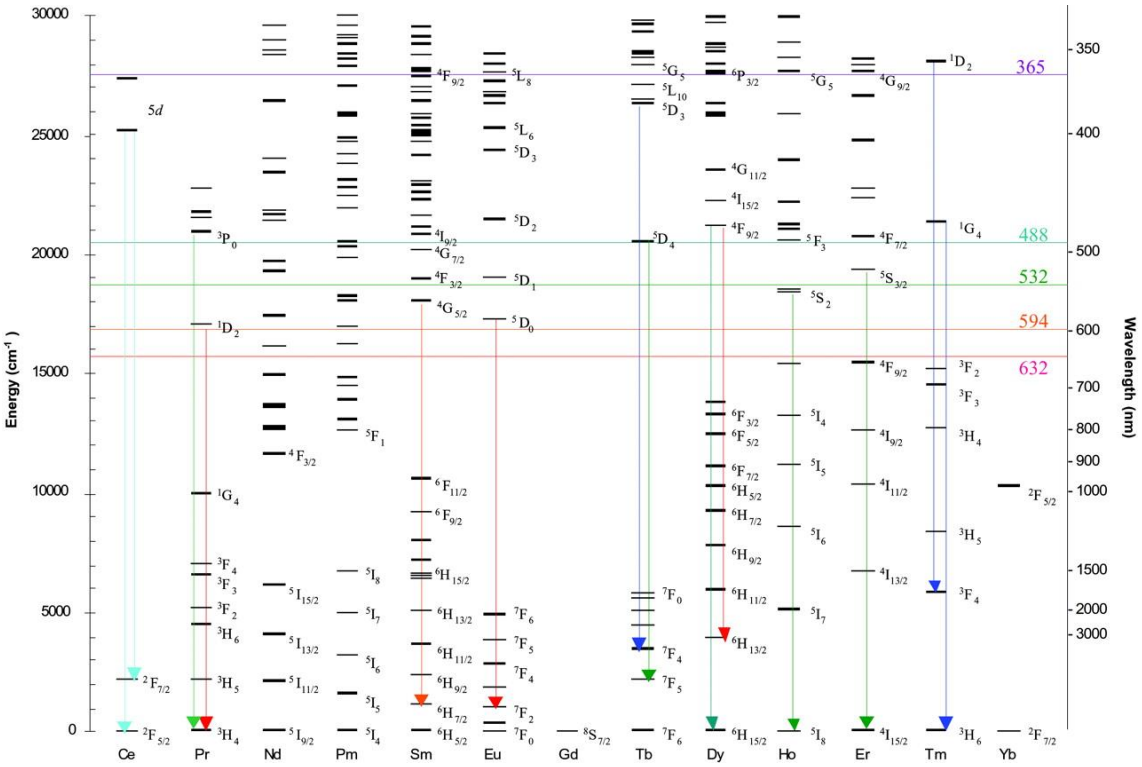

Figure 5.12: Energy levels of another dopants [31]

5.4.3 Length of fiber

An optimum fiber length is one of the key parameters during the amplifying process of EDFA. The amplifying fiber length is dependent primarily on the quantity of a rare earth the fiber core is subsidized with. This is also related to intensity of absorption of one meter of the fiber, which is usually indicated for individual wavelengths by the manufacturer in the fiber data sheet. As for erbium at the 980 nm wavelength, the absorption ranges from 3.5 to 27 $dB \times m^{-1}$ for fibers produced by Fibercore IsoGain. [Appendix A]

Fig. 5.13 shows a curve of gradual fiber saturation up to the saturation point in which the fiber stops amplifying and begins to lose its gain. This allows us to find the optimal EDF length, and the point is where the fiber is cut. As for longer doped fibers which are used e.g. in GS-EDFA (EDFA with a long fiber), we must keep in mind an uneven distribution of the pumping power along the whole length of fiber [24].

Fiber amplifiers manufacturers try to find other options then just using several-metre-long erbium-doped fibers, e.g. fibers doped with ytterbium which achieve the absorption of ~1700 dB/m (Fibercore DF1100). [Appendix A]

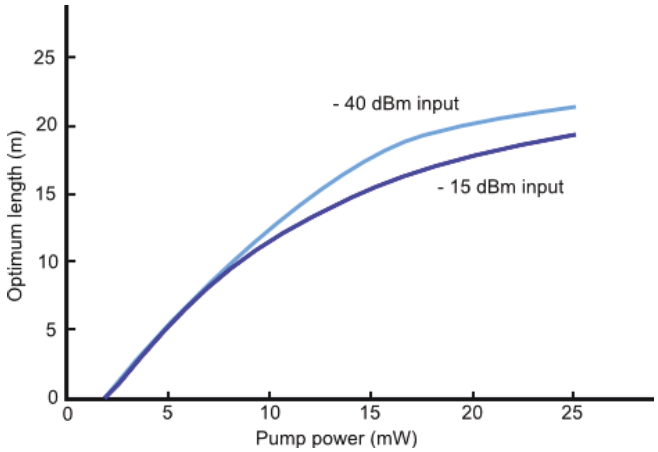

Figure 5.13: Optimal fiber length (in m) for gain at 1530 nm, pumped at 980 nm [24]

5.5 Another components used in EDFA

5.5.1 Wavelength selective coupler

A WDM coupler represents a very important part for the structure of EDFA. Its primary task is to merge the original beam with a beam of the pump into the doped fiber. The most important parameters of the coupler are the insertion loss for both branches, separation ratio and isolation ratio. These parameters are polarization dependent [31].

A coupler design is usually based on two basic principles which constitute two kinds of couplers: fused fiber couplers or miniaturized interference filter reflectors, as indicated in Fig. 5.14.

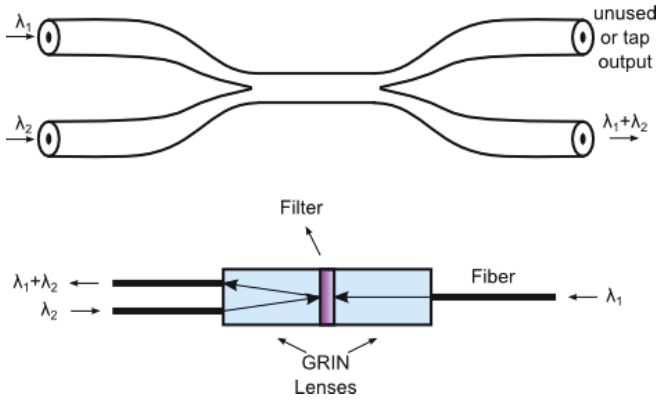

Figure 5.14: WDM designs to combine signal and pump (upper: fused fiber type; lower: miniaturized filter type) [31]

The advantage of fused fiber couplers is their low cost. The interference-based filters, on the other hand, are less dependent on polarization and also have greater width of passband. These two methods are compared in detail in the following tables:

Table 5.6: Comparison of fused fiber and interference filter WDMs when combining 1480 nm and 1550 nm signals [31]

Parameter	Fused Fiber	Interference Filter
Isolation (dB)	≥10	12 (1480) 30 (1550)
Max. insertion Loss (dB)	0.5	0.4
Back-reflection (db)	-55	-68
Polarization-dependent loss	≤0.1	0.015
Thermals stability ($dB \times °C^{-1}$)	≤0.002	≤0.005
Passband (nm)	10	33 (1480) 35 (1550)

Table 5.7: Comparison of fused fiber and interference filter WDMs when combining 980 nm and 1550 nm signals [31]

Parameter	Fused Fiber	Interference Filter
Isolation (dB)	20	60 pump
Max. insertion Loss (dB)	0.4	0.4
Back-reflection (db)	-55	-68
Polarization-dependent loss	≤0.1	0.015
Thermals stability ($dB \times °C^{-1}$)	≤0.002	≤0.005
Passband (nm)	20	30 (980) 60 (1550)

There is a method to achieve better properties of fused fiber couplers that resides in curling fibers in coupling region together, and in their cladding with low-index polymer. Because of this, the insertion loss is ≤ 1.2 dB and the dependence on polarization is ≤ 0.1 dB [31].

5.5.2 Isolators

Fresnel reflections caused by connectors or by Rayleigh scattering on a long fiber can have a negative effect on light sources connected e.g. to the amplifier input. There are not only power fluctuations but also spectral untuning. That is why, isolators are being connected to the circuit. These may prevent e.g. back reflection of the ASE noise on the amplifier input, and thus improve the signal-to-noise ratio. Fig. 5.15 illustrates the typical structure of polarization-independent isolator in forward as well as in backward direction [31].

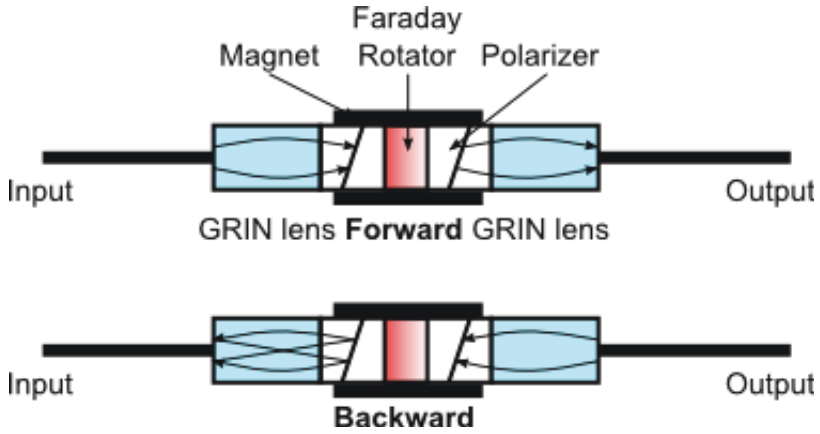

Figure 5.15: Forward and backward connection of isolator [31]

When the beam passes through the isolator in the forward direction, it is first divided into two beams using GRIN Lens which are followed by a doubly refracting prism (TiO_2). Then there is the Faraday rotator composed of $Y_3Fe_5O_{12}$ crystal surrounded by a permanent magnet which causes a 45 degree rotation of the two beams. Thus rotated beams are then merged together again while passing through another doubly refracting prism, so they can eventually pass through the isolator.

On the other hand, when the beam passes in the backward direction, there is a 90 degree rotation of the beams, so they cannot get to the output of the isolator. In order to achieve better properties, in individual transitions antireflective-coatings are used. Isolators are always used at specific wavelengths corresponding to the material used. Fig. 5.16 shows the dependence of the isolator on the wavelength [31].

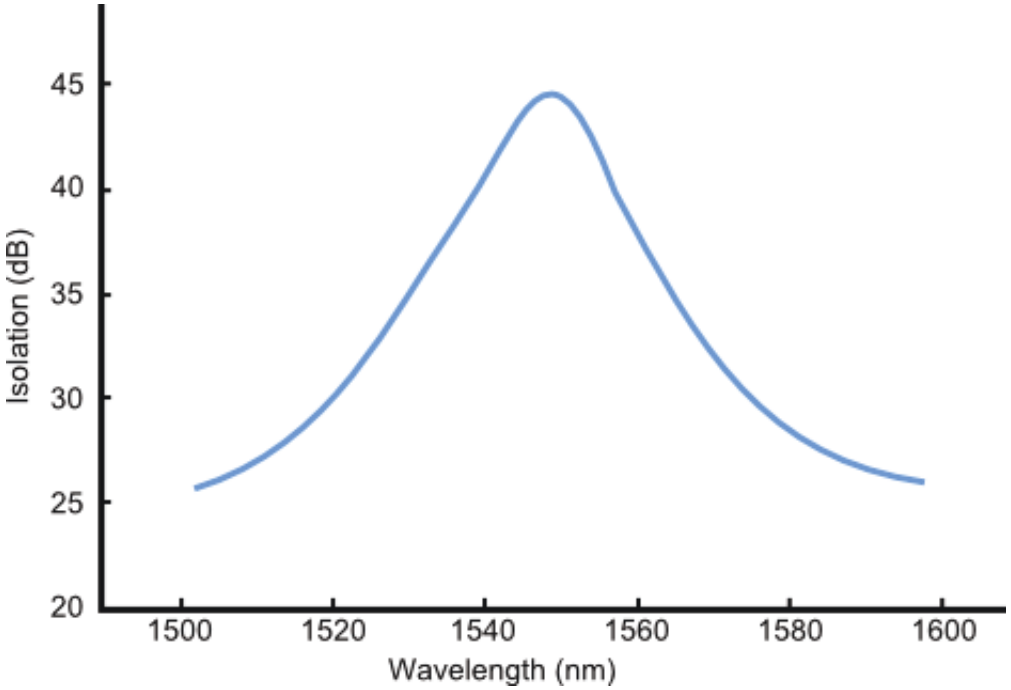

Figure 5.16: Isolation dependence on wavelength [31]

6 Measurements

In the previous chapters, we explained basic physical phenomena and properties of amplifiers. In this chapter and its particular subchapters, we will focus on the proposal of an amplifier and its measurements. First of all, we will look at the proposed circuit and the used components. In subsequent parts, we will successively test the stability of the pump laser depending on different temperatures, find the ideal length of the doped fiber at different temperatures, and measure the influence of the pumping source untuning on the gain and spectrum of the amplifier. The last section of the practical part of the thesis will be focused on connecting the amplifier to a real WDM-PON topology and on measuring its properties.

6.1 Used components and amplifier circuit

6.1.1 Used components

The first important component is the pumping laser. We used a butterfly-type laser together with the adapter by Thorlabs.

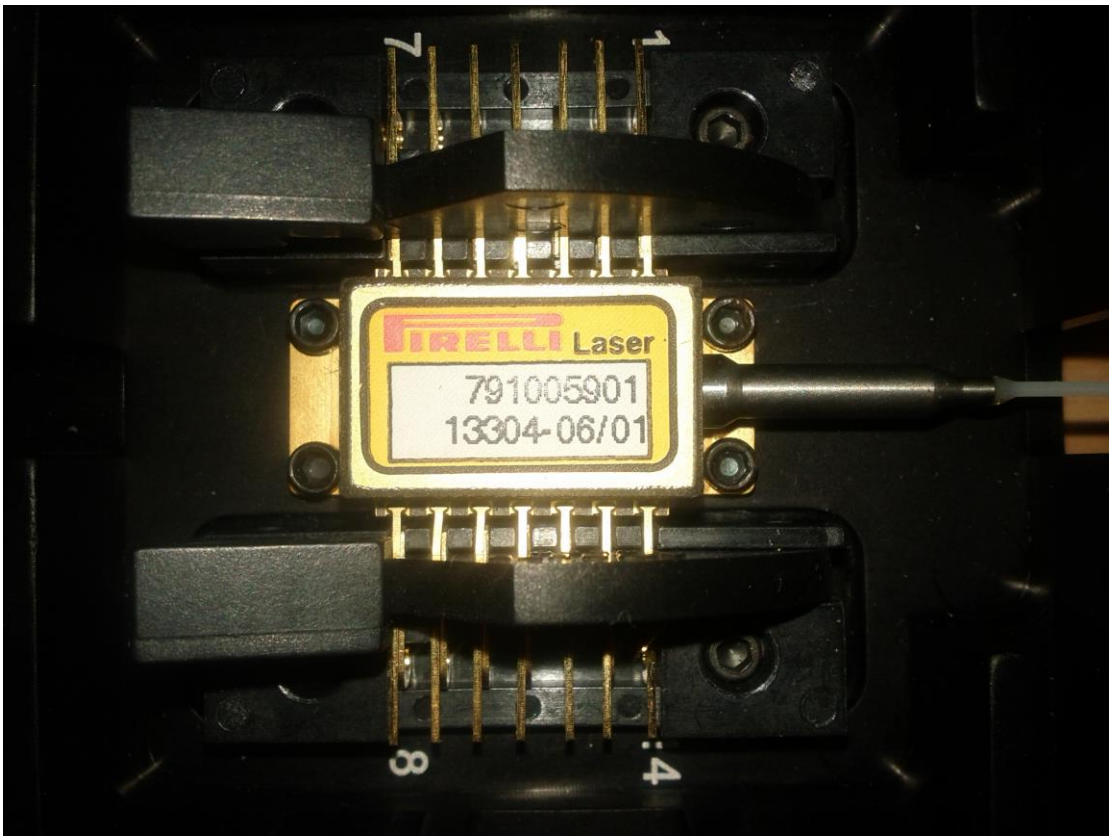

Figure 6.1: Pump laser placed in the butterfly laser diode mount Thorlabs LM14S2

For the circuit, we chose the source by Pirelli, the parameters of which at 25 °C are given in Table 6.1. Under the table, there is the pump laser $P \times I^{-1}$ characteristic and spectrum characteristics of the pump laser. Since the laser is nearly 13 years old, it was impossible to find out any other information. The datasheet regarding this laser can be found in Appendix A.

Table 6.1: Parameters of the pump laser

Parameter	Value
Rated power (mW)	125
Threshold Current (mA)	20,40
Forward Current (mA)	21,56
Kink current (mA)	258
Peak Wavelength (nm)	976.6

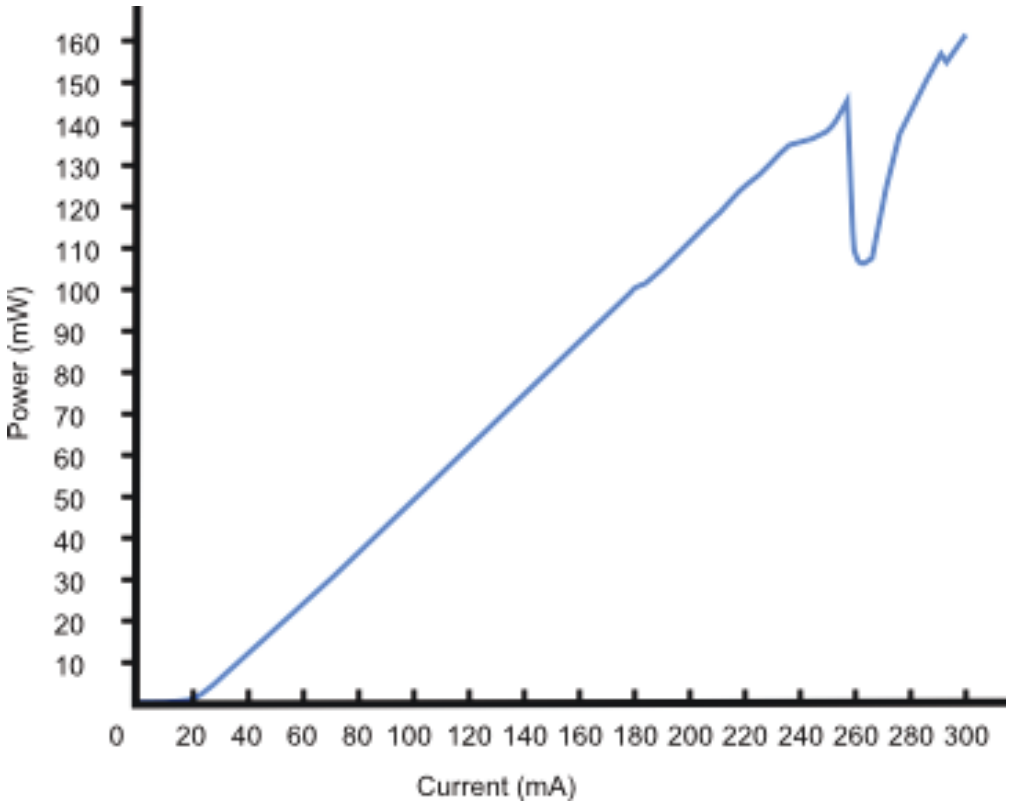

Figure 6.2: $P \times I^{-1}$ characteristics of the pump source

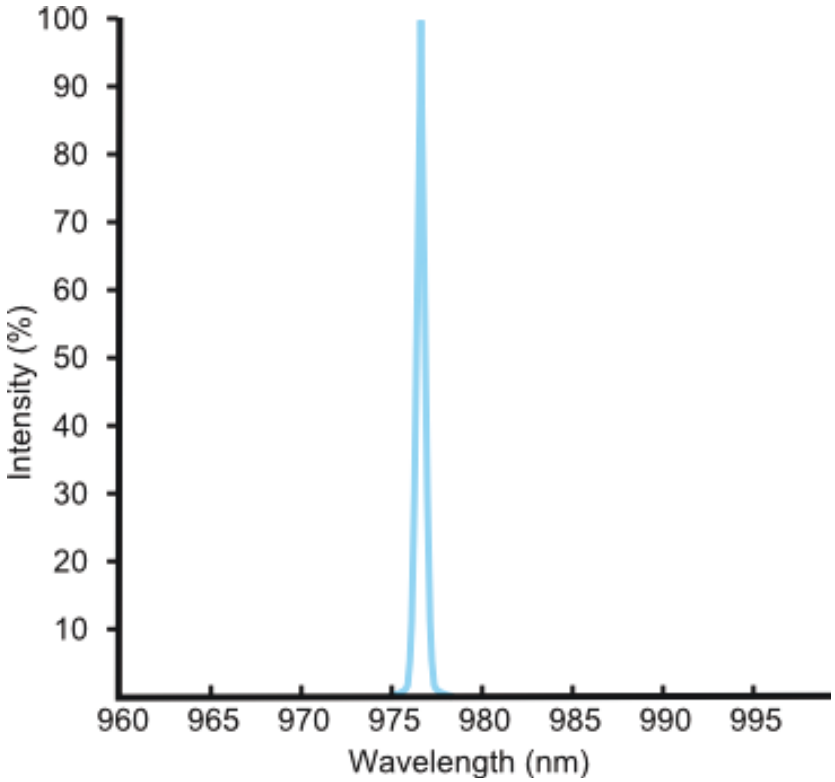

Figure 6.3: Spectral characteristics of the pump laser

Another important component is the erbium doped fiber. For our measurement, we used a fiber by Fibecore, and it was most suitable for our purposes to use a fiber of the IsoGain series, the IsoGain I-6 type in particular. Basic parameters of this type of fiber can be found in Table 6.2, and the whole datasheet in Appendix A. Given that FiberCore was very communicative and open, a detailed document about testing and measuring the IsoGain I-6 fiber can be found in the appendix section as well.

Table 6.2: Parameters of the erbium doped fiber IsoGain I-6

Parameter	**Value**
Cut-off wavelength (nm)	870-970
Numerical Aperture	0.22-0.24
MFD @ λ_{op} (µm) nominal	3.5 @ 980
Absorption at 980 nm (dB×m^{-1})	4.5-5.5
Attenuation at 1200 nm (dB×km^{-1})	≤ 10
PMD (ps×m^{-1})	≤ 0.005
Fiber diameter (µm)	125 ± 1
Core concentricity (µm)	≤ 0.3
Coating diameter (µm)	245 ± 5%
Coating type	Dual acrylate

Advantages of the IsoGain I-6 fiber lie primarily in the absorption intensity thanks to which it is possible to use shorter fiber length and thus lower power of the pumping source. As for this fiber, the information provided in the datasheet states that the ideal fiber length at the 115 mW power and the 977.1 nm wavelength is approximately 14 m.

Other components involved in the circuit were isolators and couplers. While the couplers met the exact needs for creating the amplifier, the isolators were not ideal. Instead of using isolators for the 980 nm wavelength, there were isolators with the 1550 nm design wavelength. This deficiency could cause different insertion loss than it is stated in the datasheet.

A concise list of the properties of these components can be found in Tables 6.3 and 6.4.

Table 6.3: Parameters of the WDM coupler

Parameter	Value
Operating Wavelength (nm)	980/1550
Insertion Loss at 980 nm (dB)	0.02
Insertion Loss at 980 (dB)	24.3
Insertion Loss at 1550 nm (dB)	0.06
Insertion Loss at 1550 (dB)	33.7
Directivity (dB)	>60
PDL (dB)	0.01
Fiber Type / Length (m)	OFS 980 Coupler Fiber / 1.0
Connector Type	FC/APC
Operating Temperature (°C)	-20~+70

Table 6.4: Parameters of the isolator

Parameter	Value
Fiber type	SMF-28
Operating Wavelength (nm)	1550
Insertion loss (dB)	0.26
Isolation (dB)	31.56
Polarization dependent loss (dB)	0.08
Polarization mode dispersion (ps)	<0.25 ps
Return loss, input / output (dB)	>60/55

A component which is essential for the amplifier but is missing in the list of the used components because of its high cost is the gain flattening filter. Its task is to equalize the spectrum of the amplifier. As we know from the previous chapters, the EDFA can amplify the entire band. Unfortunately, one of the ills of this kind of amplifiers is that they do not amplify the band evenly. That is why, gain flattening filters are used because they, as already mentioned, equalize and smooth the spectrum. Their downside is their high cost.

6.1.2 The amplifier circuit

As a model, we used a conventional erbium doped fiber circuit according to Fig. 5.2. This circuit was modified by adding another coupler in order to use the possibility of multi-directional pumping, which can be seen in Fig 6.4.

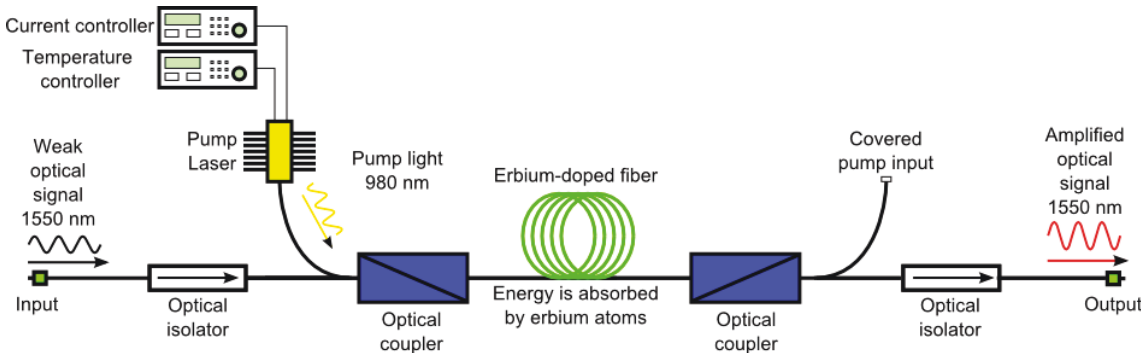

Figure 6.4: Circuit of the constructed amplifier

Instead of amplifiers which are available in WDM component shops, there were used much bigger components, so it was impossible to achieve at least partial integration. For that reason, the entire amplifier was placed on a mounting plate covered by a soft foam which acted as a protection of individual components and optical fibers.

Since it was expected from the beginning that it would be necessary to move the amplifier from one place to another, we built a two-storey construction that allowed us to manipulate it very easily, and at the same time it was "component-friendly". The very construction can be seen in Fig. 6.5 and 6.6.

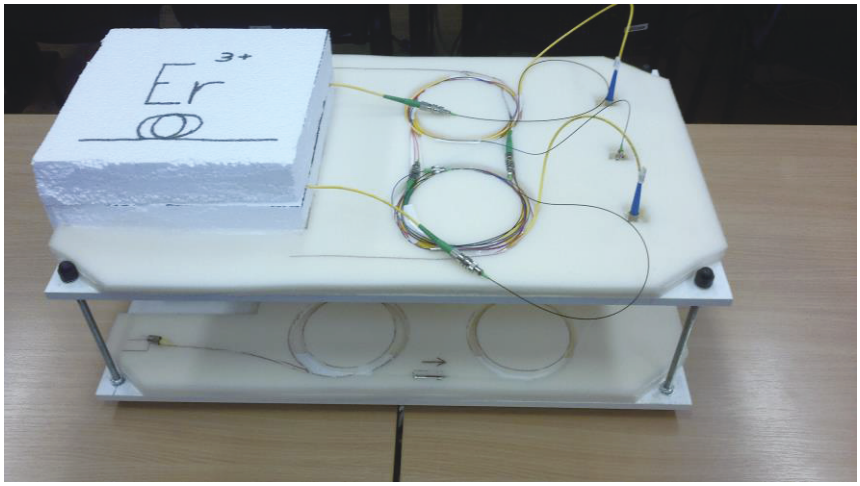

Figure 6.5: Construction of the erbium doped fiber amplifier

Figure 6.6: Construction of the erbium doped fiber amplifier

As far as laser drivers are concerned, we used appliances by Thorlabs, specifically Thorlabs LDC205 C for controlling electric current, and Thorlabs TED200C for temperature setting. Entering power values, we followed the $P \times I^{-1}$ characteristic from the datasheet.

For measuring the spectrum, we used the USB2000+ Ocean Optics spectrometer and the EXFO WA-7600 multiline optical channel analyser. Another appliance was the Digital optical power and energy meter Thorlabs PM100D with the photodiode power sensor S120C. In case of higher power, there was a tunable attenuator used.

6.2 Measuring stability of laser at different temperature conditions

One of the first significant measurements consisted of measuring the pumping laser stability at various temperatures. Within this measurement, we observed a change in the power level in time, and a shift of the wavelength. The circuit schema can be seen in Fig. 6.7.

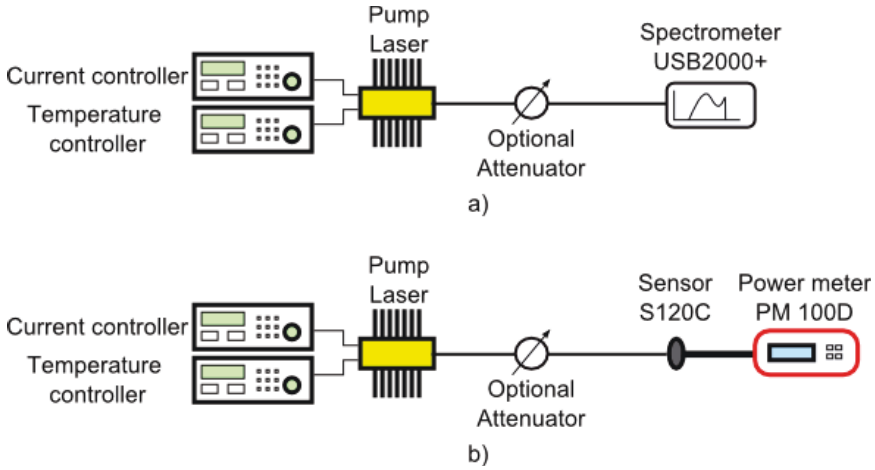

Figure 6.7: Measurement circuits for testing for spectral a) and power stability

Due to very high power at the input of the pumping source it was necessary to use a 3-dB attenuator for the power range from 50 mW to 80 mW, and a 6 dB attenuator for the power range from 90 mW to 125 mW.

As for measuring stability, we performed the total of 169 measurements with the 10 mW stepping from 10 mW to 125 mW, and with the 2.5°C temperature stepping from 10°C to 40°C.

Within a two-minute power measurement, we got a total of 1000 figures. This measurement is illustrated in the following charts.

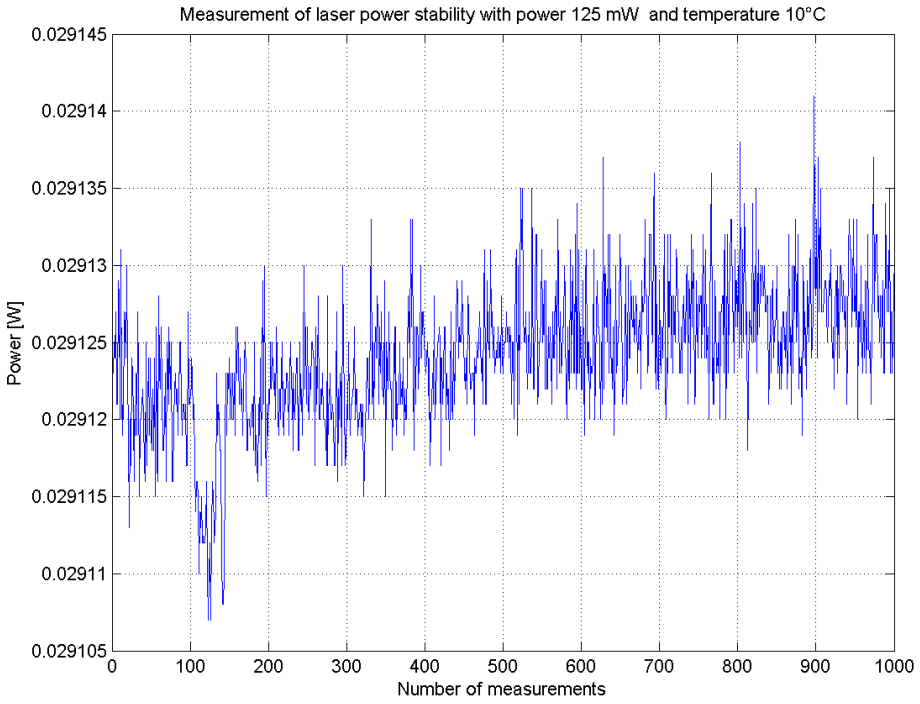

Figure 6.8: Measuring laser power stability at 125 mW power and 10°C temperature

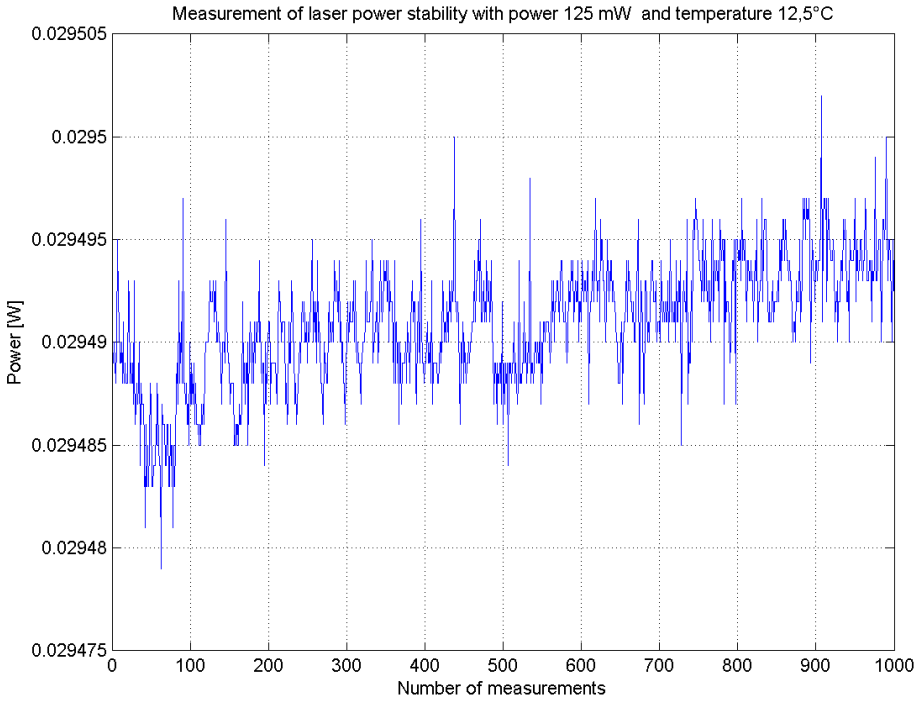

Figure 6.9: Measuring laser power stability at 125 mW power and 12.5°C temperature

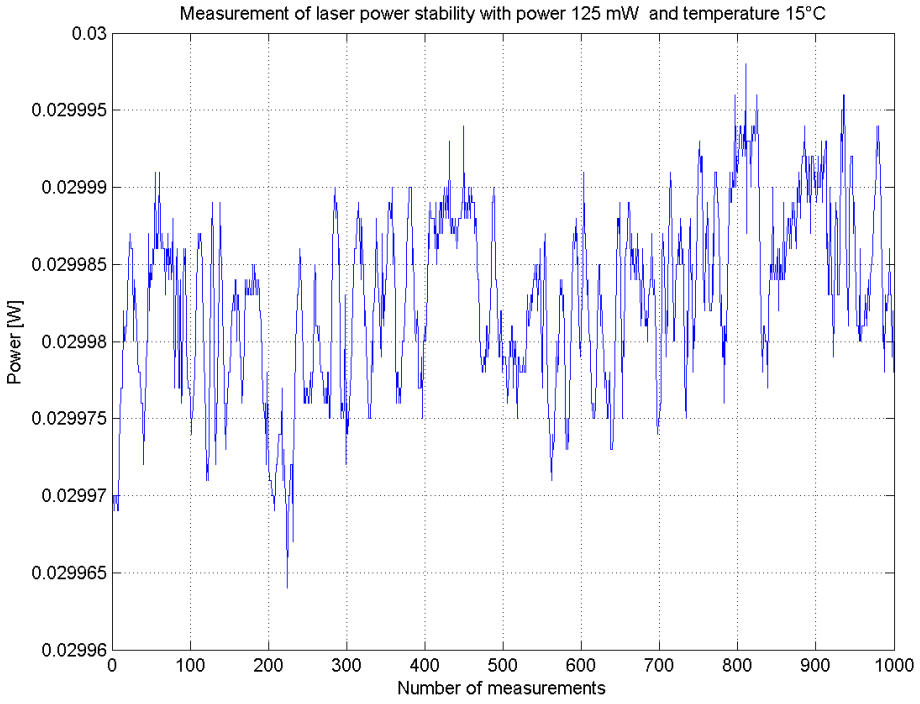

Figure 6.10: Measuring laser power stability at 125 mW power and 15°C temperature

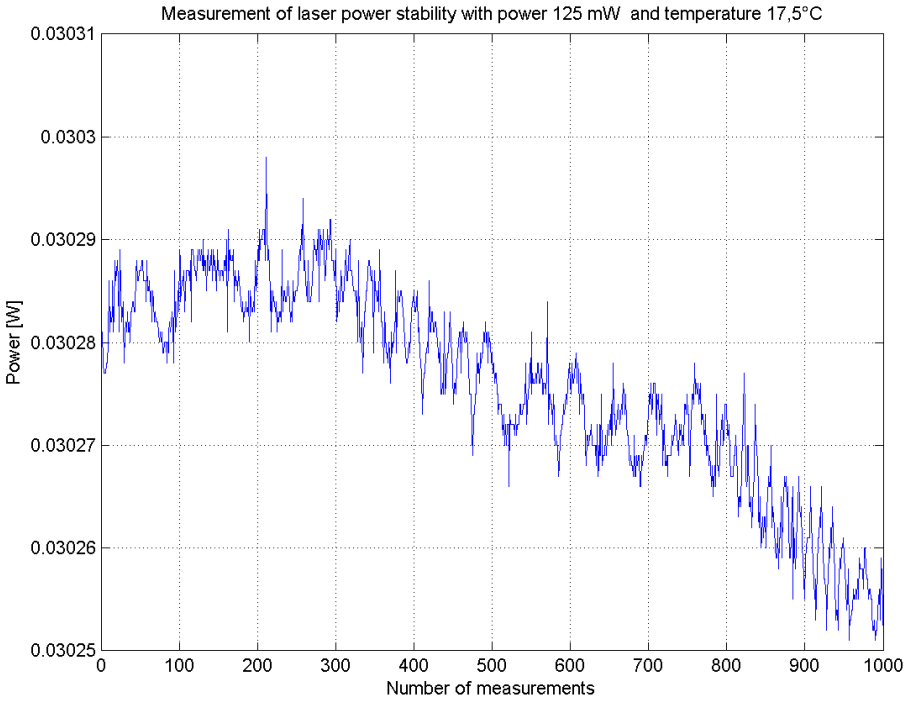

Figure 6.11: Measuring laser power stability at 125 mW power and 17.5°C temperature

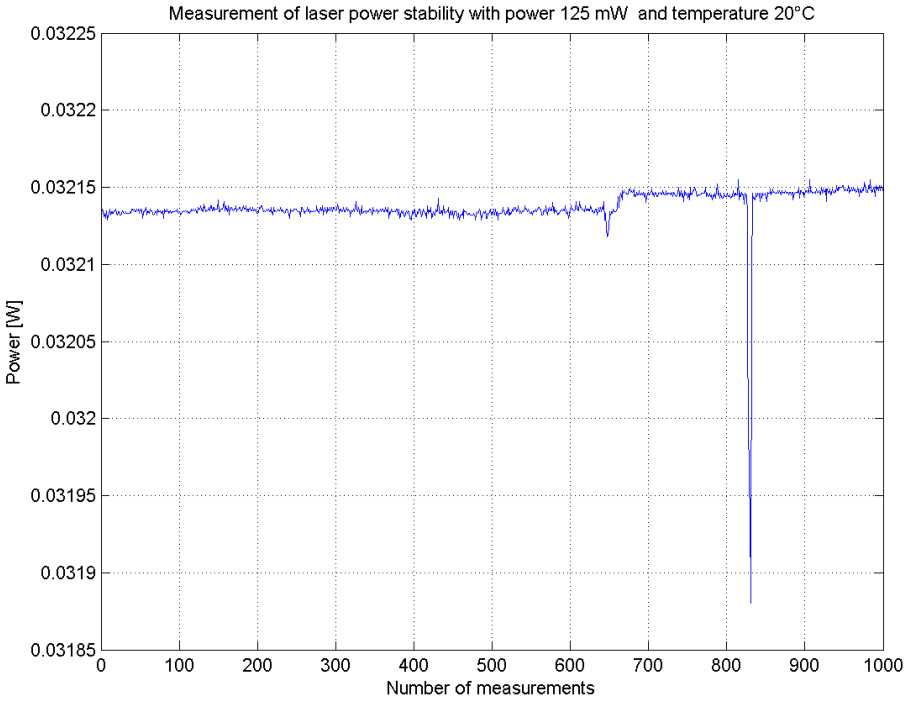

Figure 6.12: Measuring laser power stability at 125 mW power and 20°C temperature

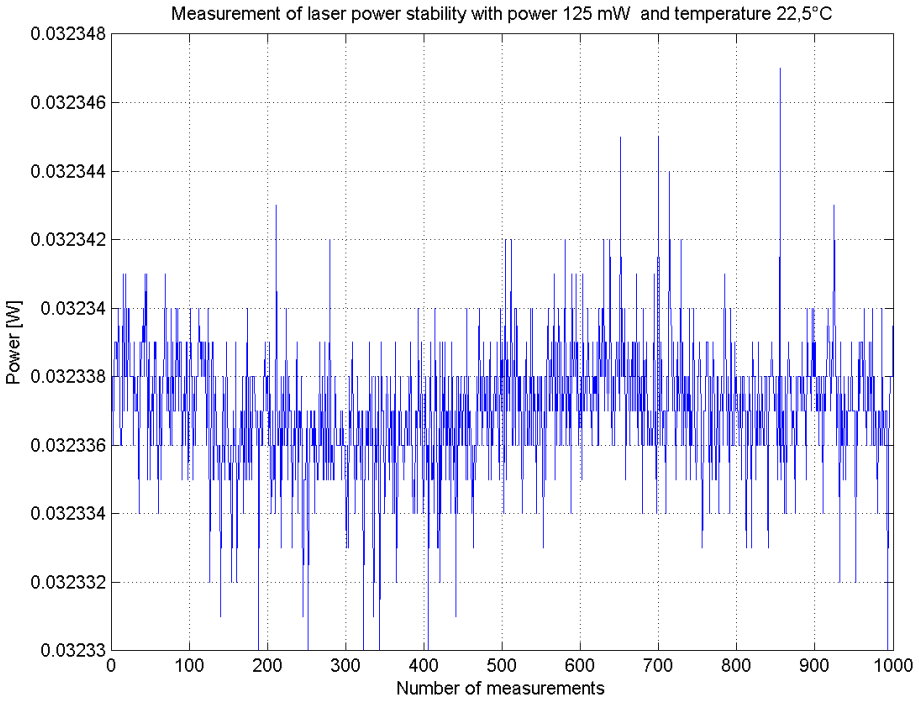

Figure 6.13: Measuring laser power stability at 125 mW power and 22.5°C temperature

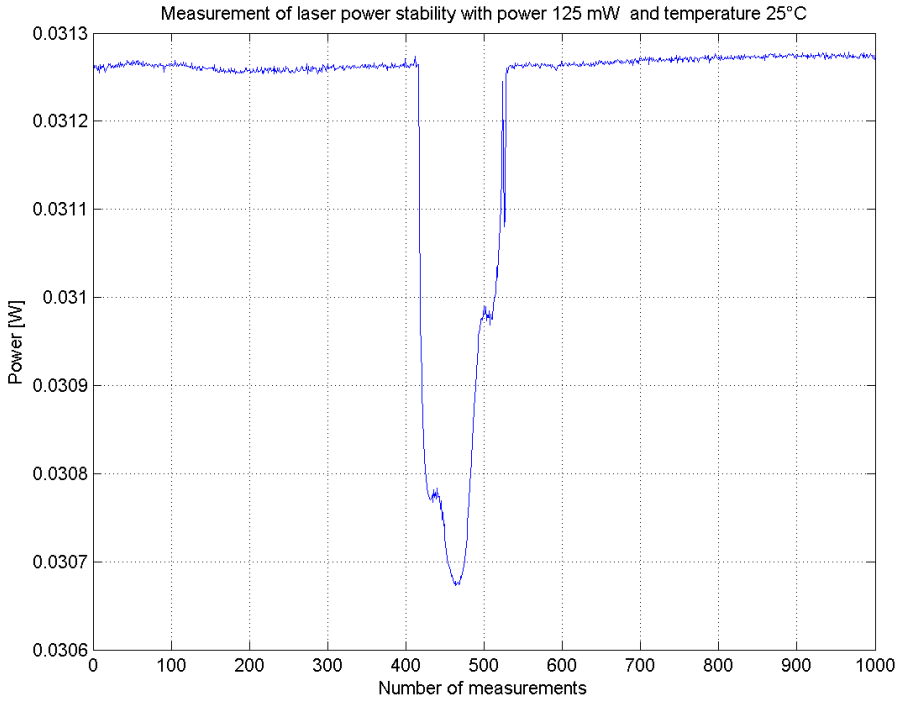

Figure 6.14: Measuring laser power stability at 125 mW power and 25°C temperature

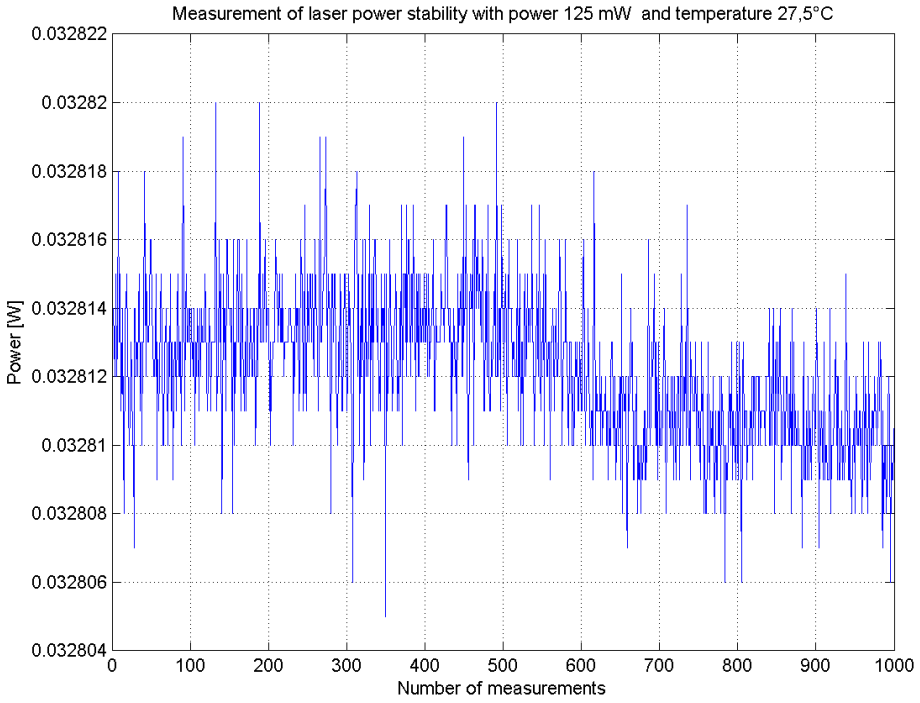

Figure 6.15: Measuring laser power stability at 125 mW power and 27.5°C temperature

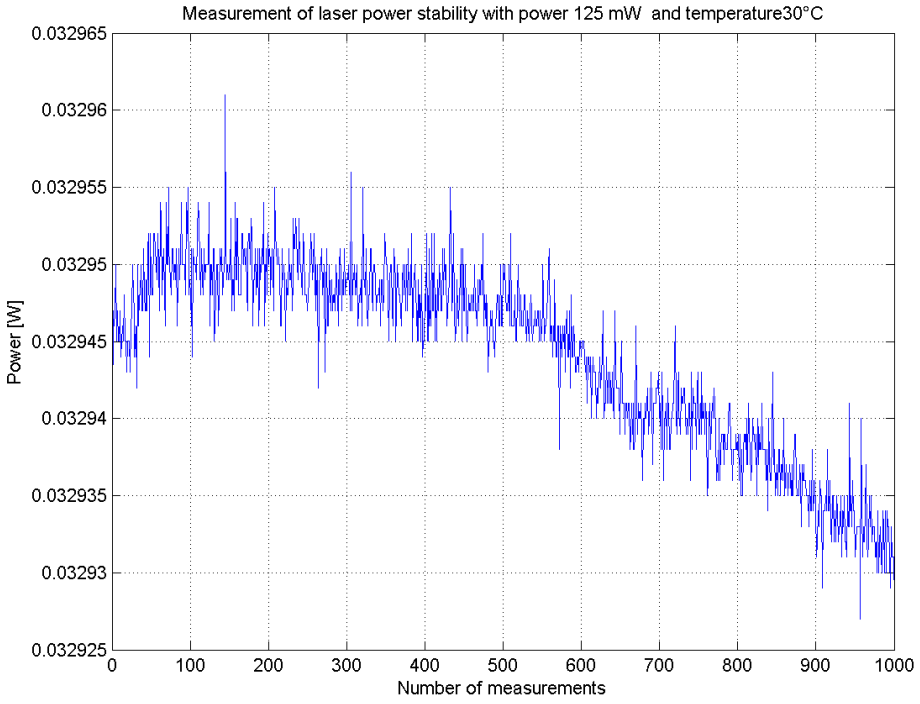

Figure 6.16: Measuring laser power stability at 125 mW power and 30°C temperature

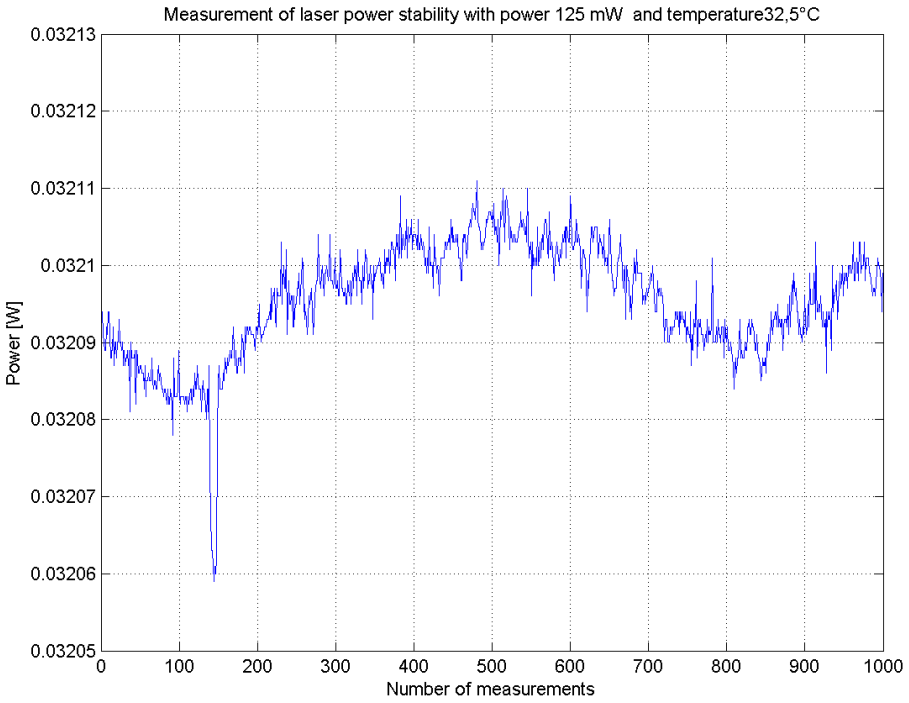

Figure 6.17: Measuring laser power stability at 125 mW power and 32.5°C temperature

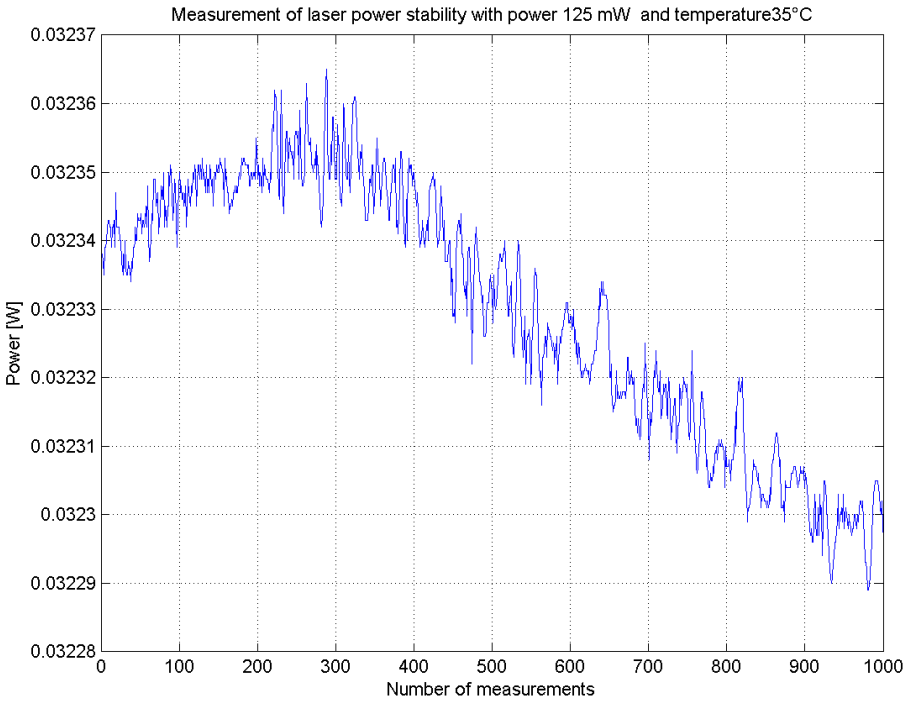

Figure 6.18: Measuring laser power stability at 125 mW power and 35°C temperature

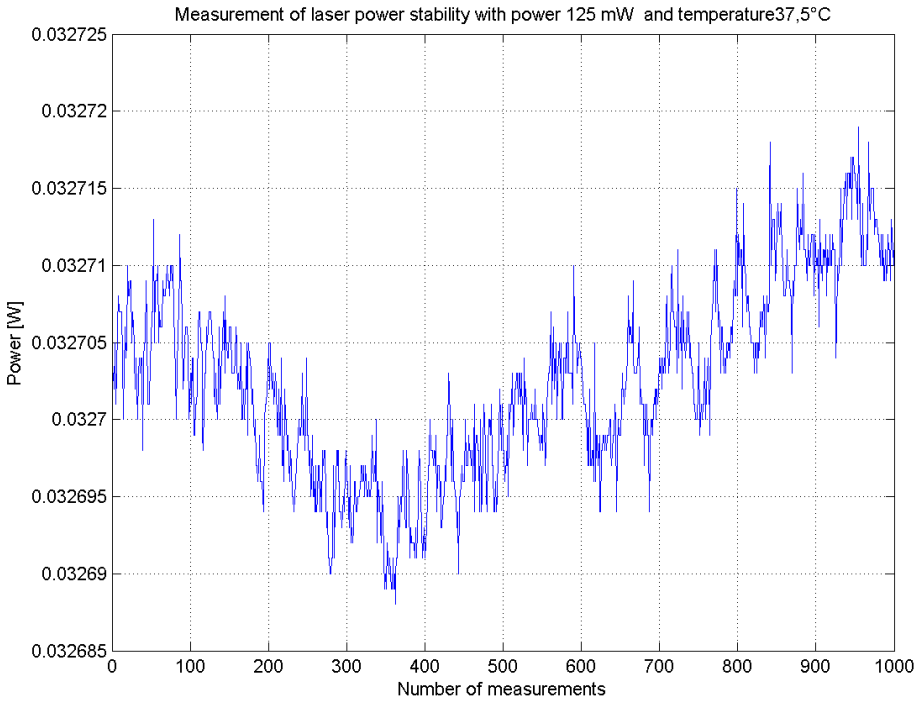

Figure 6.19: Measuring laser power stability at 125 mW power and 37.5°C temperature

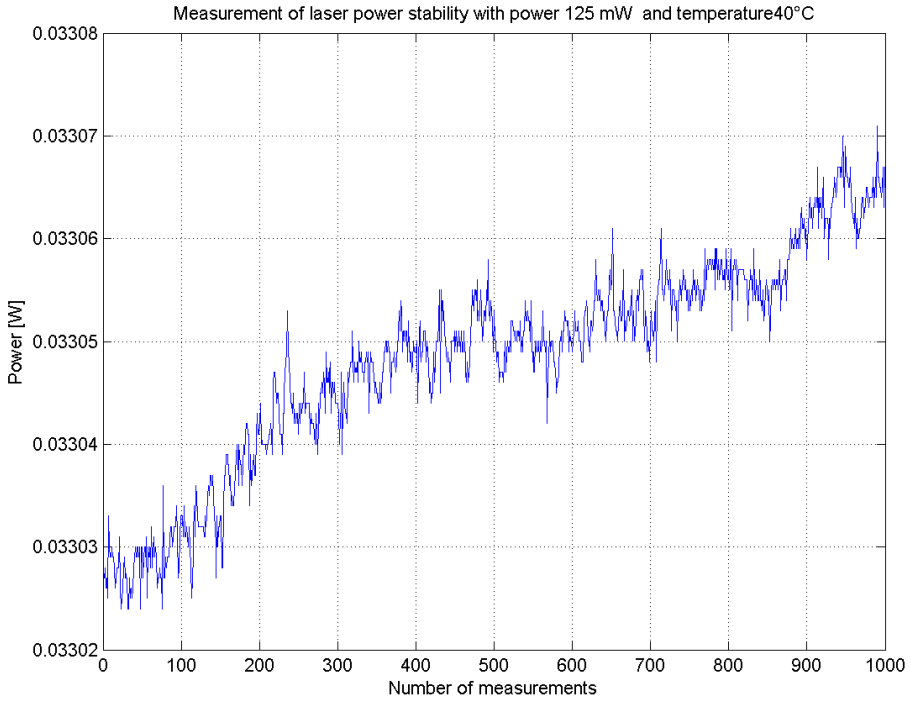

Figure 6.20: Measuring laser power stability at 125 mW power and 40°C temperature

For better clarity, charts for individual temperatures have been put together, as shown in Figures 6.21 to 6.33.

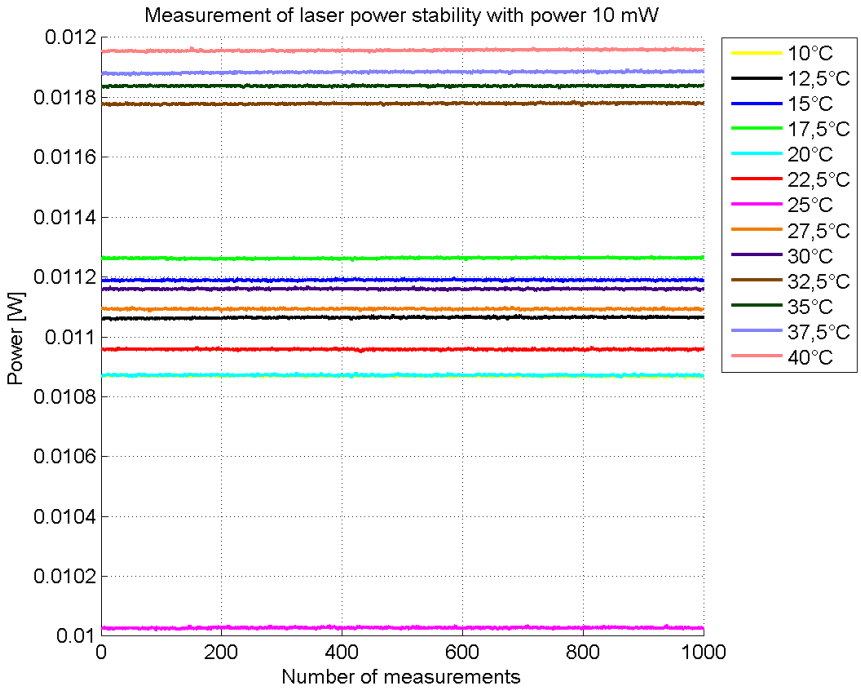

Figure 6.21: Measuring laser power stability at 10 mW power

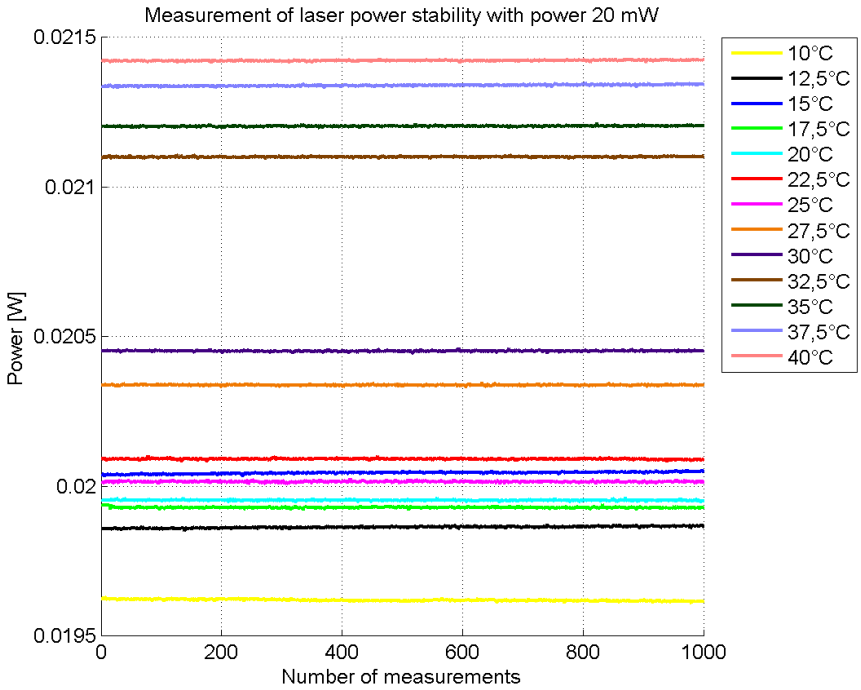

Figure 6.22: Measuring laser power stability at 20 mW power

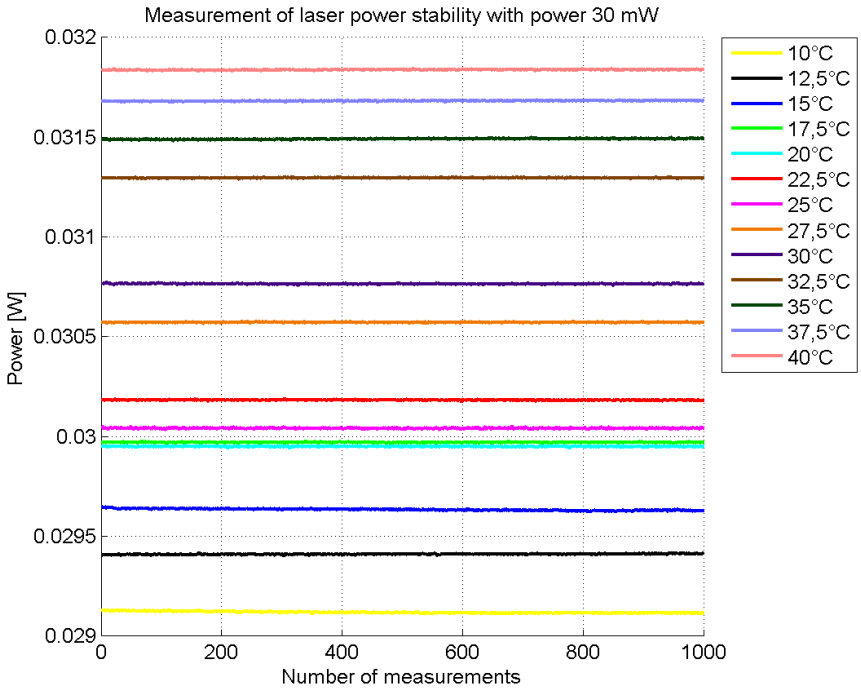

Figure 6.23: Measuring laser power stability at 30 mW power

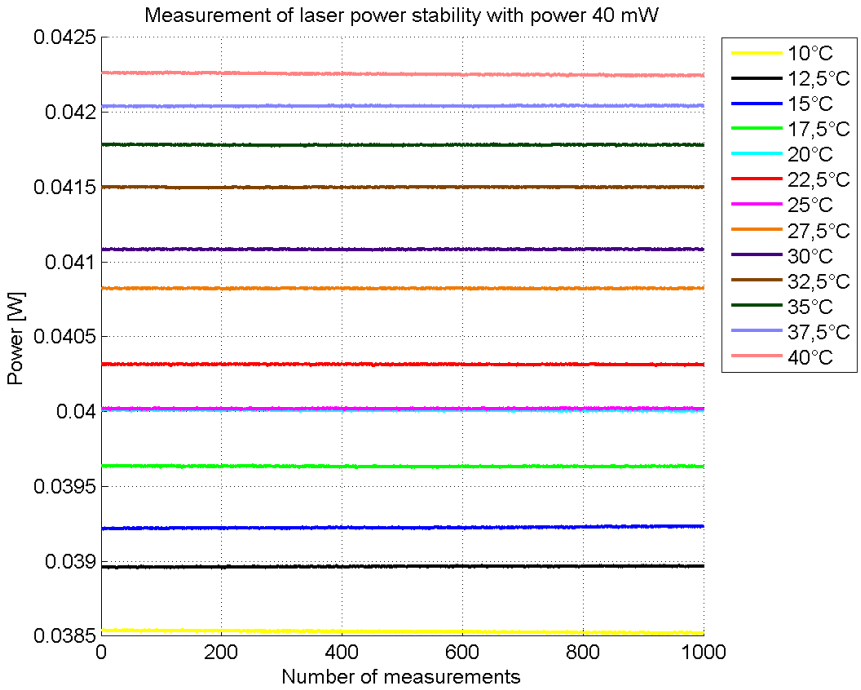

Figure 6.24: Measuring laser power stability at 40 mW power

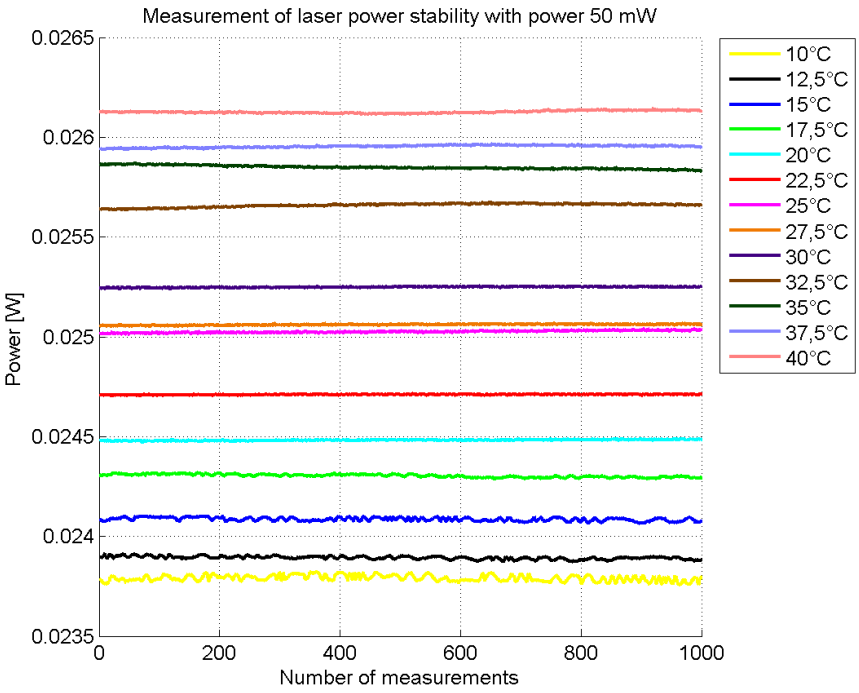

Figure 6.25: Measuring laser power stability at 50 mW power

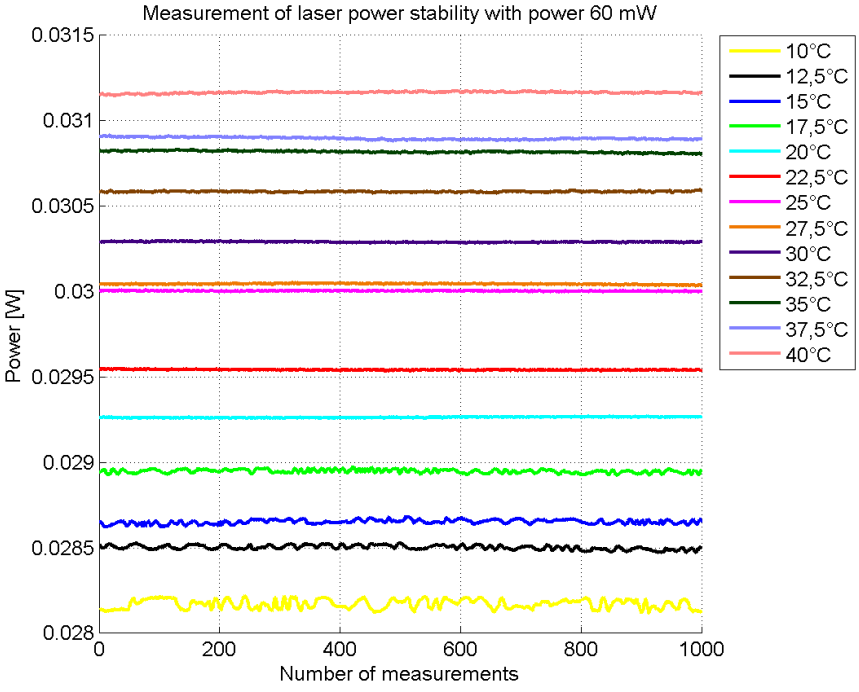

Figure 6.26: Measuring laser power stability at 60 mW power

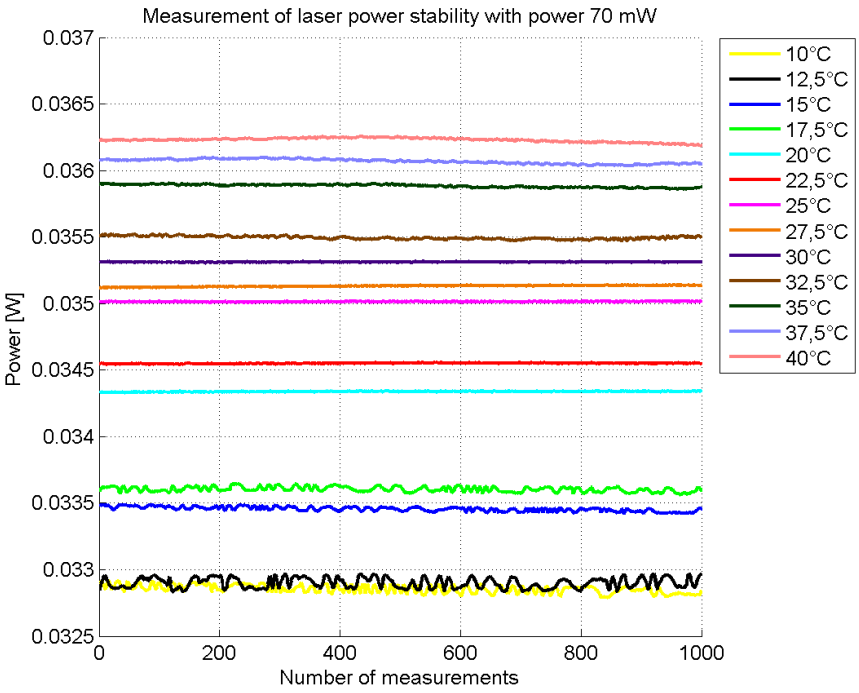

Figure 6.27: Measuring laser power stability at 70 mW power

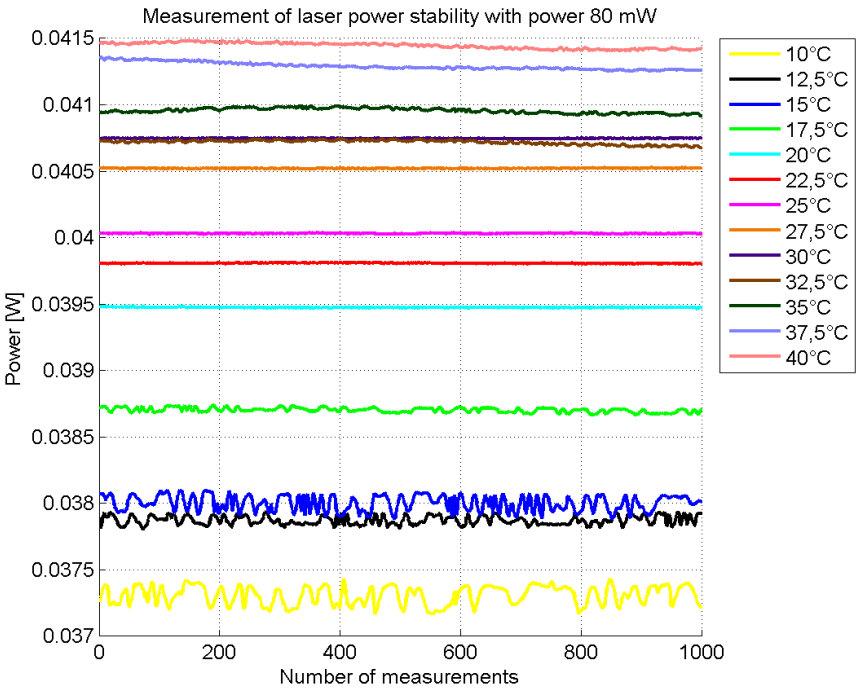

Figure 6.28: Measuring laser power stability at 80 mW power

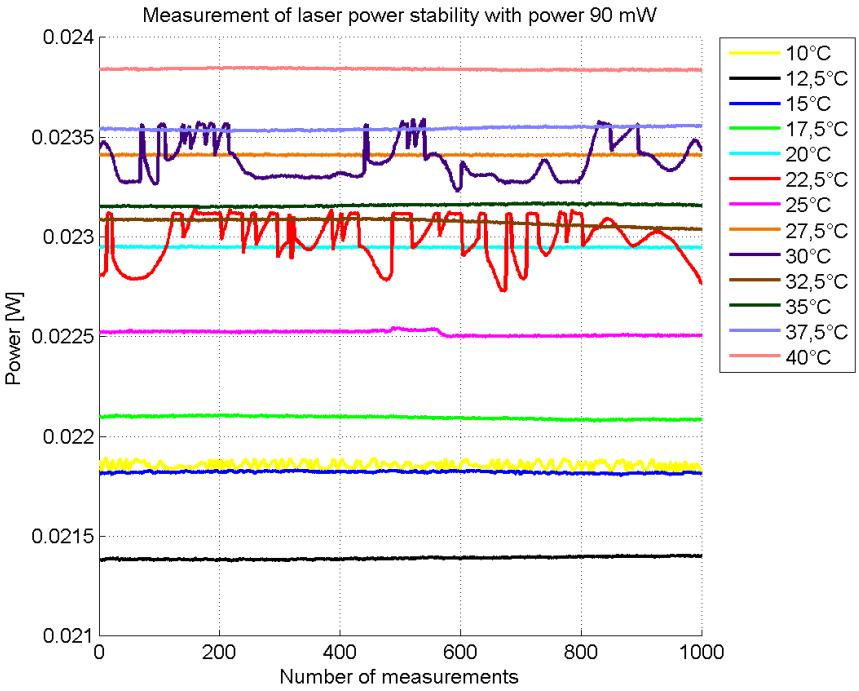

Figure 6.29: Measuring laser power stability at 90 mW power

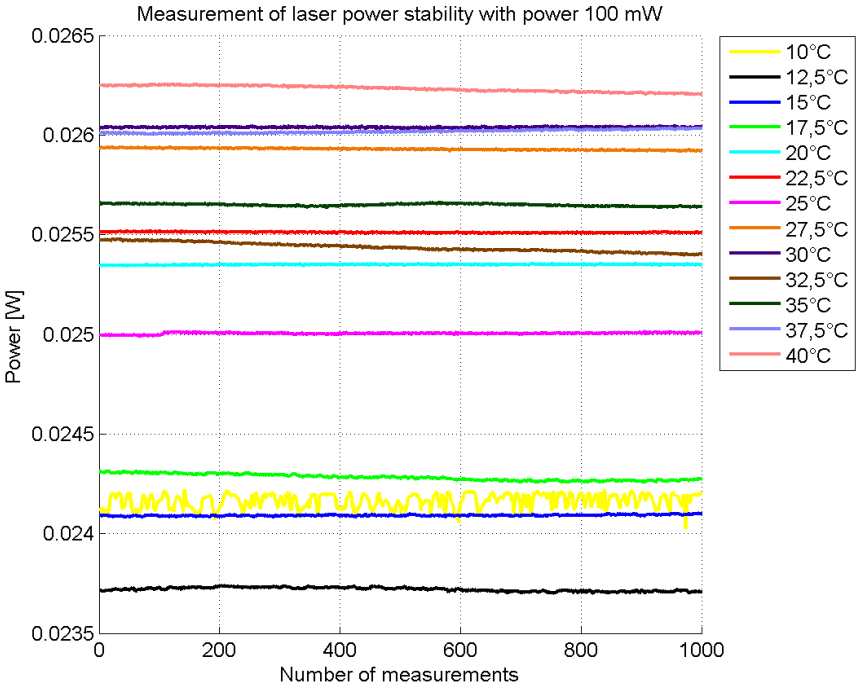

Figure 6.30: Measuring laser power stability at 100 mW power

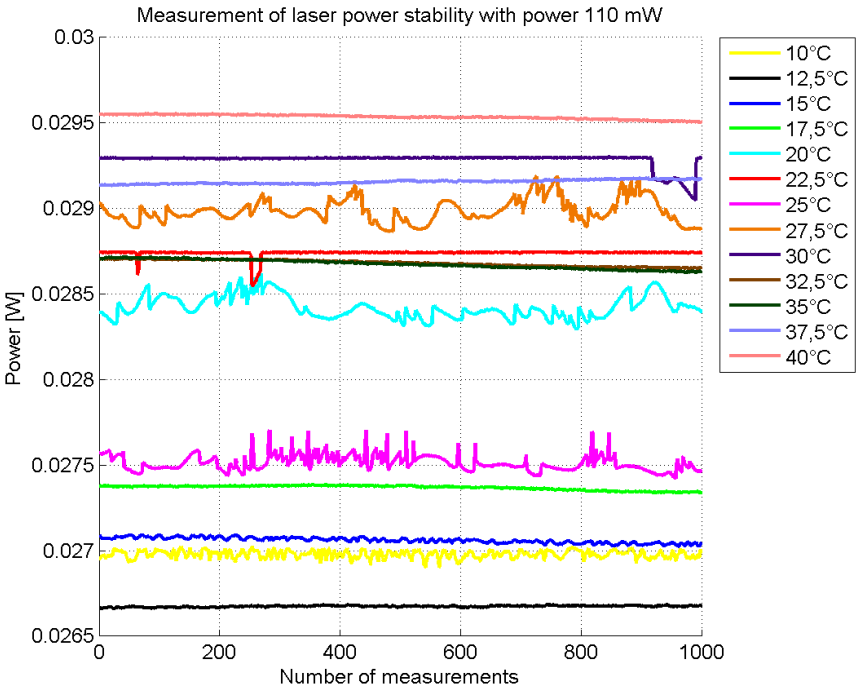

Figure 6.31: Measuring laser power stability at 110 mW power

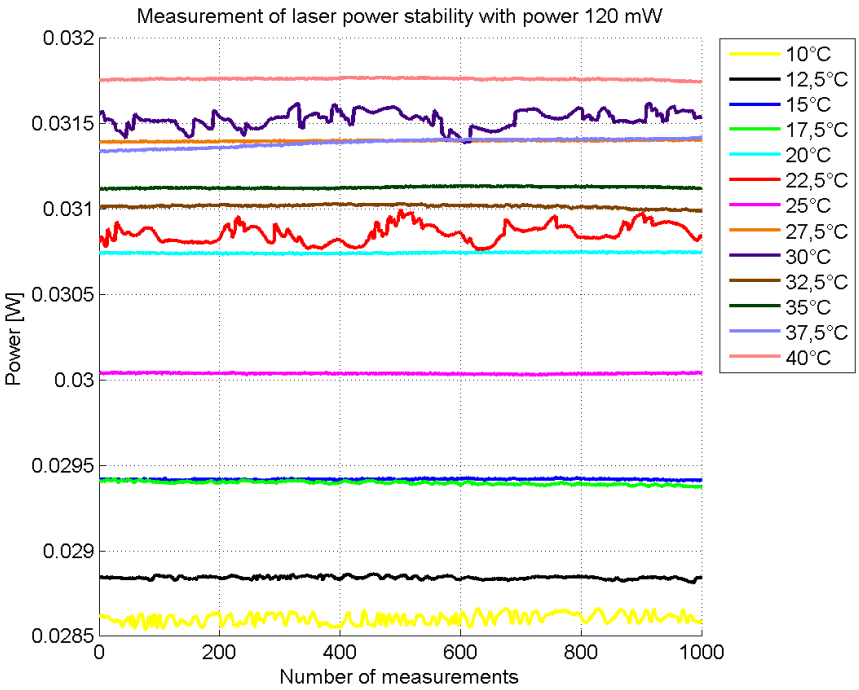

Figure 6.32: Measuring laser power stability at 120 mW power

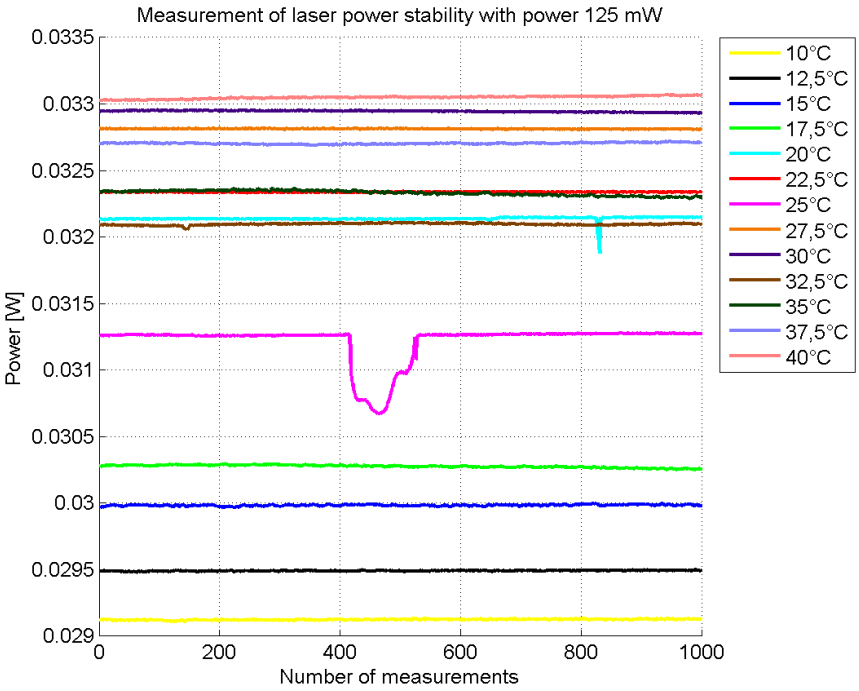

Figure 6.33: Measuring laser power stability at 125 mW power

As it is evident from Fig. 6.21 to 6.33, the power was stable up to 40 mW. At 50 mW power, the laser was less stable at lower temperatures, and this unstable behaviour continued up to 80 mW power. At 90 mW power, the laser is very unstable at temperatures from 22.5 to 30°C. At the lowest temperature, just a little instability could be observed. In the chart concerning 90 mW power and 25°C temperature, only a short-term drop in power could be seen. It was caused by a tremor of the measuring system and a manual attenuator in particular, because the attenuator is very sensitive to any kind of tremors. Similar behaviour of low as well as high instability could be observed also at powers of 100 mW, 110 mW and 120 mW. Since we have decided to use 125 mW power for our fiber, the last chart is the most important one. The laser was stable at all powers. The only instability appeared at 25°C temperature in one minute of the measurement. However, it was only a power fluctuation caused by incorrect handling of the attenuator. What can also be observed from Fig. 6.21 to 6.33 is the change of power at different wavelengths. It can be seen that power at the output of the pump increased together with the increase in temperature.

The last part of measuring the stability consisted in measuring spectral stability. It was almost the same in all the measurements. The spectrum fluctuated always in the first or in the second decimal place, so the instability was very low. Another finding from these measurements is the fact that the spectrum slowly shifted to higher wavelengths. This change became evident in gradual changes in power – from lower to higher. When measuring the spectrum stability, it was necessary to use a 60 dB attenuator due to very high sensitivity of the spectrometer. The spectra results can be found in Appendix C.

6.3 Measuring optimal length of the amplifying fiber in different working conditions of the amplifier

In this chapter, we will focus on measuring the ideal length of fiber in various temperature conditions. As already mentioned in Chapter 5.4.3, the length of fiber has a significant effect on the gain of the amplifier. Fig. 6.34 and 6.35 illustrate the circuit diagram that was designed for this measurement. In order to achieve high temperatures, we used the thermal bath Memert ONE 7 oil bath, and for cooling and achieving low temperatures, we made use of snow. For measuring at 25°C, the fiber was loosely placed on the table.

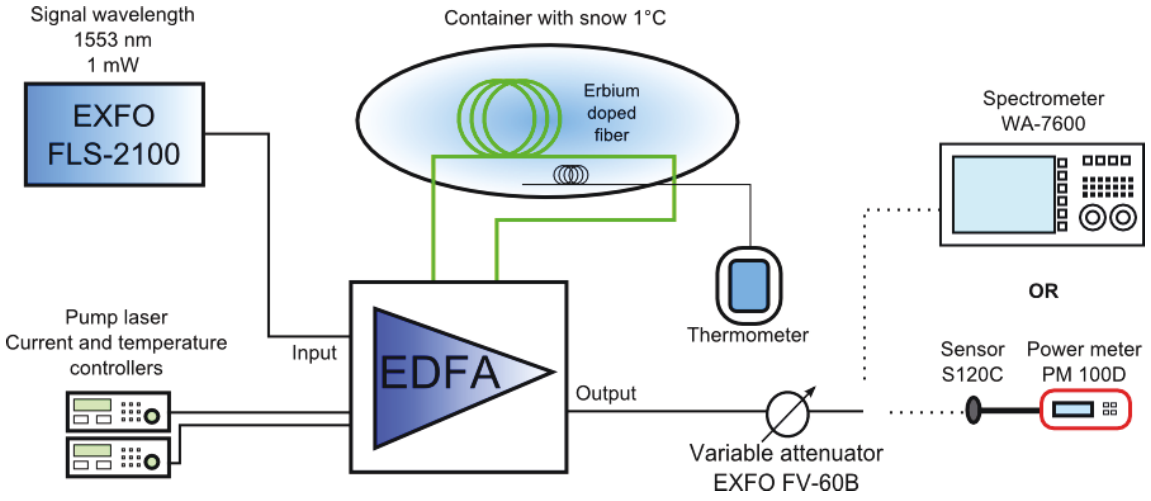

Figure 6.34: Measurement circuit for testing different lengths of EDF at 1°C temperature

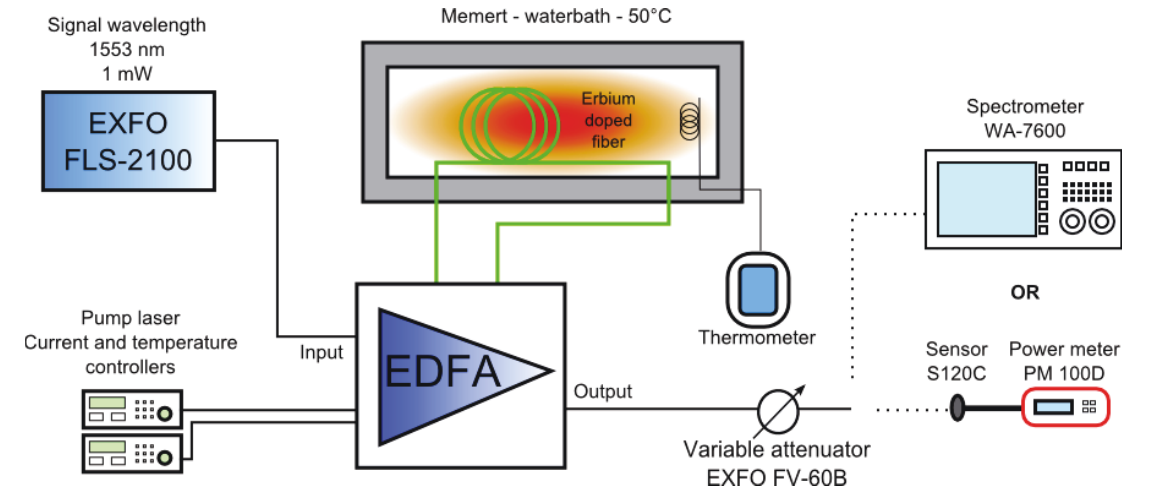

Figure 6.35: Measurement circuit for testing different lengths of EDF at 50°C temperature

We selected three basic temperature conditions for the fiber: 1°C, 25°C and 50 °C. A default fiber length was set to 20 m which was subsequently cut in 2 m parts. Another step consisted in welding pigtails to both ends of the fiber. Particular emphasis was placed on maximum precision so that each weld had the lowest possible attenuation. Thanks to this accuracy, the highest attenuation achieved was 0.01 dB. The welded fiber was then put in a plastic film and carefully sealed in order to prevent ingress of water to the fiber when it was placed in a temperature bath. Along with the fiber there was also a PalmSence FTC-PALM-ST. Fig. 6.36 illustrate storing the fiber in the thermal or in the snow bath. The disadvantage of this solution was condensing water inside the plastic film. That is why, the measurement had to be performed quickly.

Because of high output power of the amplifier, a variable digital attenuator EXFO FV-60b was placed between the very amplifier and the spectrometer. The attenuation of EXFO FV-60 b was set to 1.55 dB, and the internal attenuation of the digital attenuator was set to 2.5 dB.

Figure 6.36: Testing erbium doped fiber at different temperatures: 1°C (left) and 50°C (right)

The following tables and charts show the ideal fiber length at the pumping power of 10 mW, 50 mW and 125 mW. As for the amplified signal, we have chosen the signal with the 1553 nm wavelength and 1 mW power. It is obvious from the chart that the power for sufficient excitation of erbium ions is up to 125 mW. At lower powers, the fiber was attenuated or amplified only partially.

Table 6.5: Various EDF lengths at different temperatures and 10 mW pumping power

Fiber Length (m)	2	4	6	8	10	12	14	16	18	20
	Power (mW)									
Temperature 1°C	0.3025	0.573	0.5668	0.4313	0.312	0.2006	0.1326	0.0635	0.01688	0.00231
Temperature 25°C	0.326	0.567	0.5465	0.4915	0.304	0.1995	0.1178	0.0486	0.01538	0.00515
Temperature 50°C	0.27	0.564	0.5056	0.4245	0.241	0.1765	0.1129	0.044	0.01249	0.0036

Table 6.6: Various EDF lengths at different temperatures and 50 mW pumping power

Fiber Length (m)	2	4	6	8	10	12	14	16	18	20
	Power (mW)									
Temperature 1°C	0.4677	1.949	3.024	3.051	2.907	2.977	2.792	2.832	1.091	0.7
Temperature 25°C	0.5071	1.952	2.935	3.538	3.109	3.055	2.762	2.854	2.212	2.257
Temperature 50°C	0.43	1.959	2.757	3.146	3.134	3.062	3	2.874	2.231	2.257

Table 6.7: Various EDF lengths at different temperatures and 125 mW pumping power

Fiber Length (m)	2	4	6	8	10	12	14	16	18	20
	Power (mW)									
Temperature 1°C	0.5895	3.429	6.76	8.13	8.62	8.83	9.03	9.42	7.34	7.66
Temperature 25°C	0.5045	3.465	6.44	7.88	8.32	8.74	8.24	9.29	7.19	7.44
Temperature 50°C	0.5427	3.41	6.91	7.95	8.16	8.58	7.89	9.2	6.41	3.384

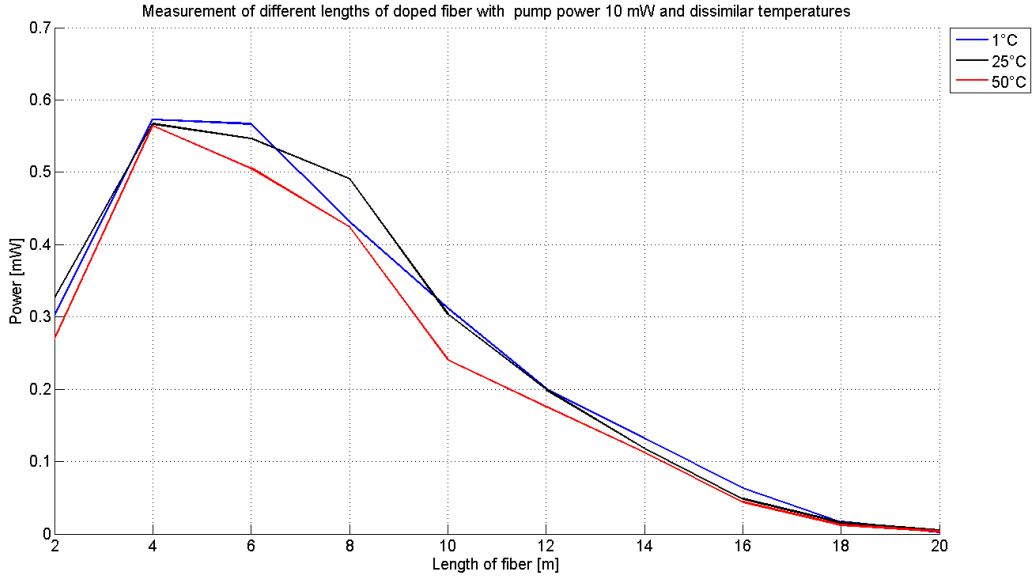

Figure 6.37: Measuring different lengths of doped fiber at 10 mW pump power and dissimilar temperatures

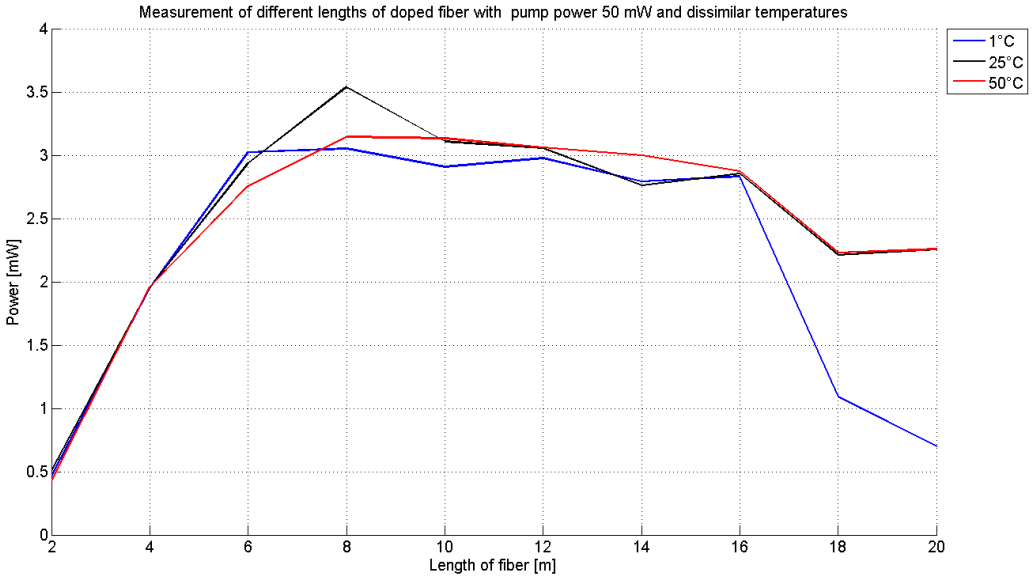

Figure 6.38: Measuring different lengths of doped fiber at 50 mW pump power and dissimilar temperatures

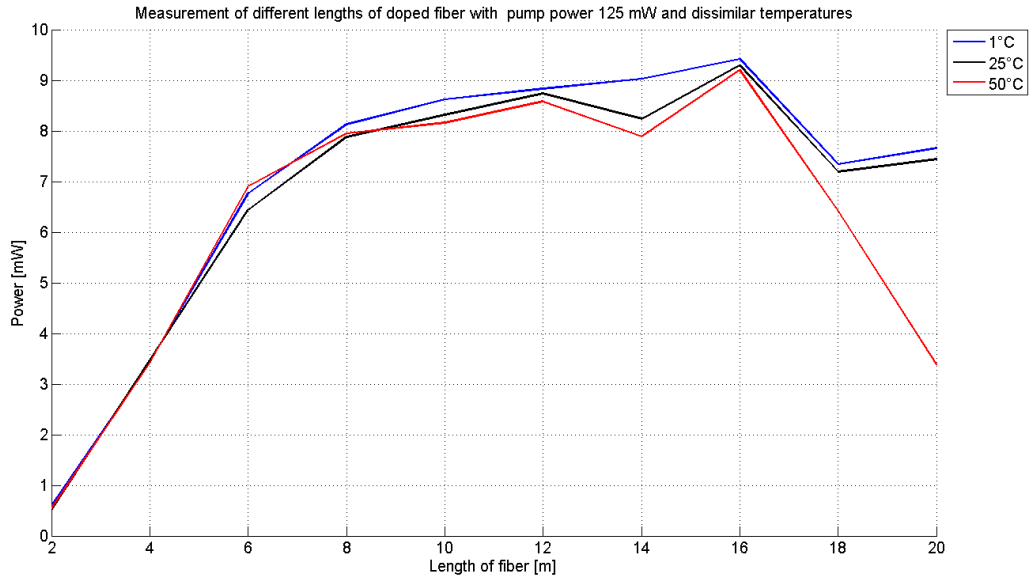

Figure 6.39: Measuring different lengths of doped fiber at 125 mW pump power and dissimilar temperatures

The ideal fiber length at all three temperatures was 16 m. However, a significant conclusion resulting from the measurements is that the change in temperature of the fiber did have an impact on the power of the amplifier. The lowest power could be observed at 50°C

temperature. This fact can be attributed to disruption of thermodynamic equilibrium of the level system in the erbium-doped fiber, due to which it is more difficult to achieve the population inversion. Fig. 6.40 to 6.48 show that temperature change did not influence the spectrum shift. Charts for other fiber lengths are included in Appendix D.

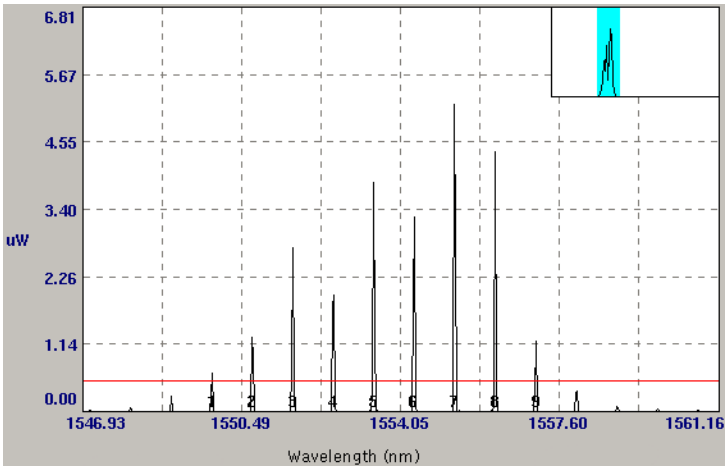

Figure 6.40: Spectrum of 16 m EDF at 10 mW pump power and 1 °C temperature

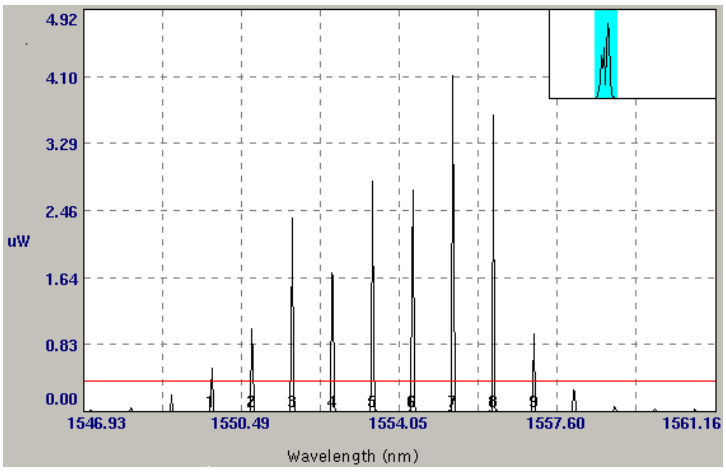

Figure 6.41: Spectrum of 16 m EDF at 10 mW pump power and 25 °C temperature

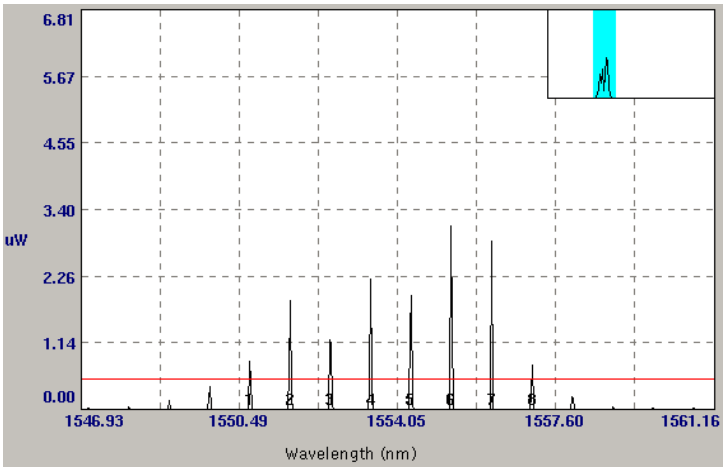

Figure 6.42: Spectrum of 16 m EDF at 10 mW pump power and 50 °C temperature

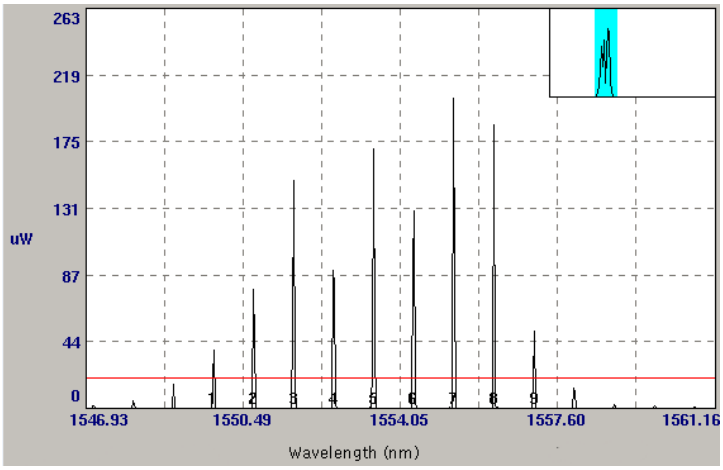

Figure 6.43: Spectrum of 16 m EDF at 50 mW pump power and 1 °C temperature

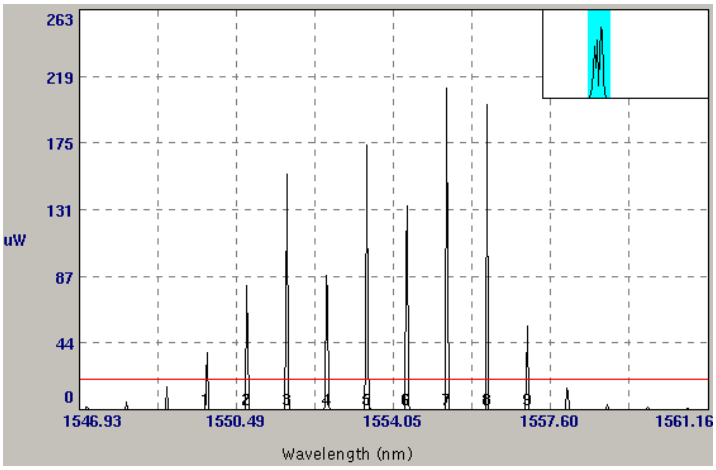

Figure 6.44: Spectrum of 16 m EDF at 50 mW pump power and 25 °C temperature

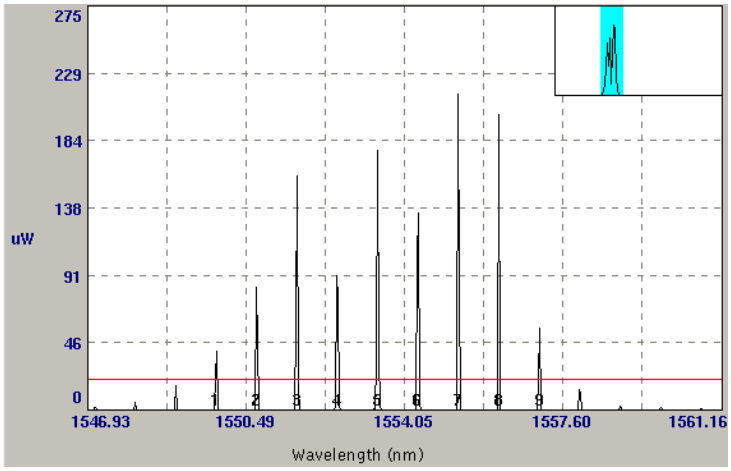

Figure 6.45: Spectrum of 16 m EDF at 50 mW pump power and 50 °C temperature

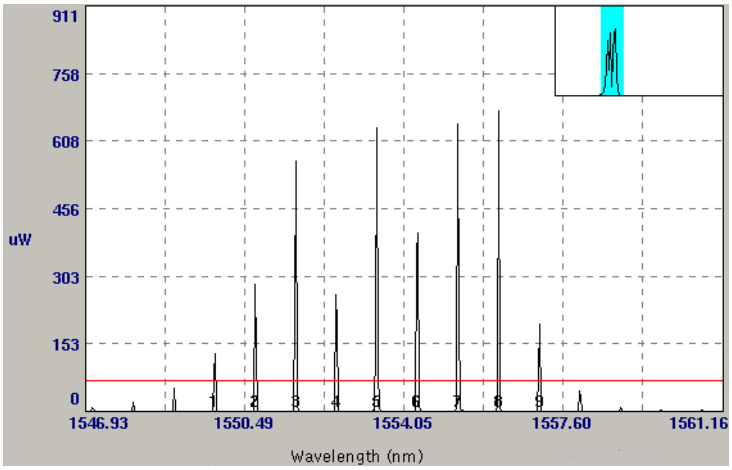

Figure 6.46: Spectrum of 16 m EDF at 125 mW pump power and 1 °C temperature

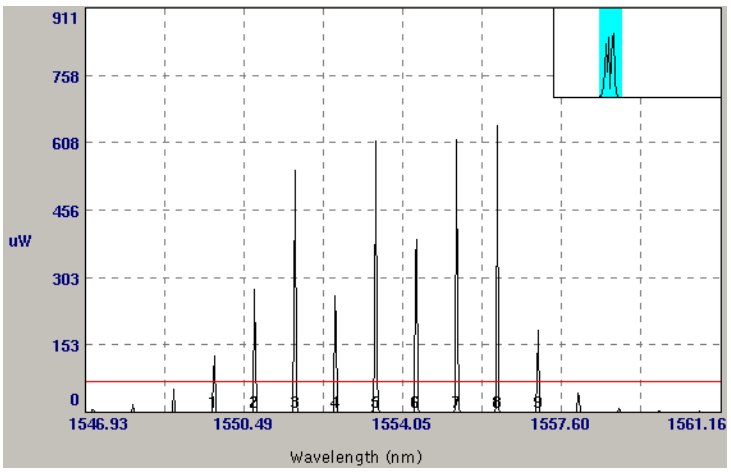

Figure 6.47: Spectrum of 16 m EDF at 125 mW pump power and 25 °C temperature

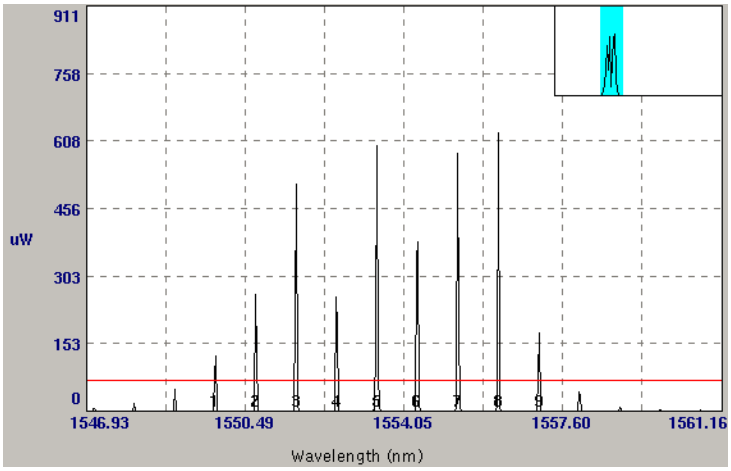

Figure 6.48: Spectrum of 16 m EDF at 125 mW pump power and 50 °C temperature

Another parameter measured within this point was also the ideal intensity of the input signal. The circuit used was the same as in the case of measuring the fiber length at 25°C. The only difference consisted in moving the digital attenuator to the input of the amplifier because of the regulation of attenuation of the amplified signal. A 3 dB attenuator was used in order to protect the spectrum analyser. The fiber length was 16 m.

Table 6.8: Effect of input signal level change on amplifier gain

Input power (W)	Output power (W)	Gain (dB)
1.17E-03	1.49E-02	11.049
5.54E-04	1.42E-02	14.091
2.81E-04	1.35E-02	16.817
1.44E-04	1.26E-02	19.400
6.69E-05	1.13E-02	22.288
3.41E-05	1.02E-02	24.773
1.74E-05	9.39E-03	27.328
8.95E-06	8.83E-03	29.941
4.73E-06	8.48E-03	32.539
2.62E-06	8.30E-03	35.014
1.56E-06	8.20E-03	37.206

A closer look at Table 6.8 tells us that the amplifier gain is highly dependent on the intensity of the input signal. While the gain of the input signal with the 1.17 mW power was only 11 dB, the gain of the signal with the 17.4 µW power was almost 28 dB.

6.4 Measuring influence of the change in wavelength of the pumping source on the function of the amplifier

The third part of the thesis consisted in measuring the influence of the change in wavelength of the pumping source on the properties of the amplifier. In order to change the wavelength of the pumping source it was necessary to change its temperature. As already stated in Chapter 6.2, the wavelength of the pumping source oscillated in the first or in the second decimal place at temperature changes from 10°C to 40°C. However, even such small changes manifested themselves in the output power of the amplifier.

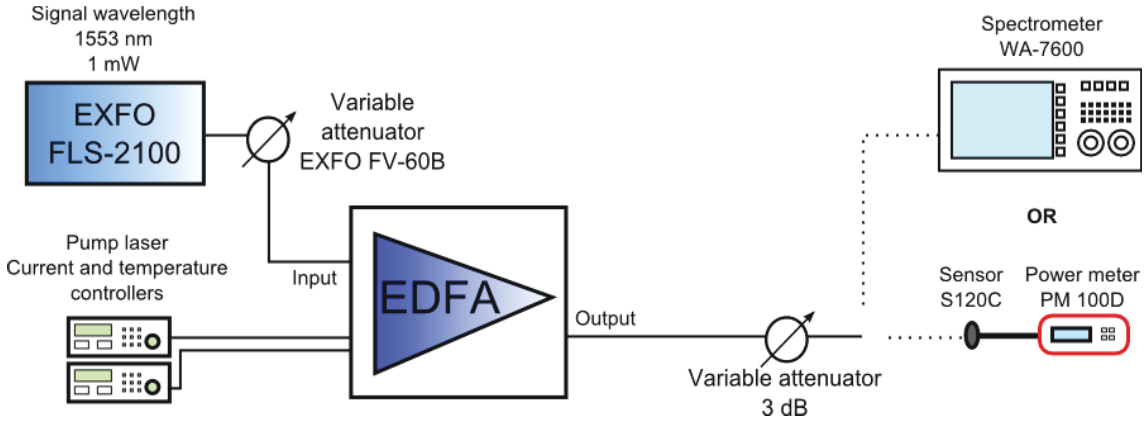

Figure 6.49: Measurement circuit for testing different wavelengths of the pump laser

The circuit was realized similarly to that we had already used in the previous chapter. Since we had already found the ideal amplifier fiber length (16 m), we could only cut the desired length from the spool and began measuring. We used two powers of the input signal, the first one of which was 1 mW and the second 100 µW. Again, the signal could be regulated using the variable digital attenuator which was connected at the input of the amplifier. In order to protect the spectrum analyser, there was also the 3 dB attenuator connected at the output of the amplifier. The pumping signal was 125 mW.

Table 6.9 shows us results of this measurement. We can observe that the increasing temperature goes hand in hand with the increasing output power of the amplifier. This fact can be attributed to the changing spectrum of the pumping source and thus to approaching to the ideal pumping wavelength. The datasheet of the very fiber states that the ideal wavelength for pumping sources is 977 nm. Our pumping source was emitting at the wavelength of 976.6 nm ± 0.1-0.2. Therefore it can be concluded that the pumping laser spectrum influenced the power of the amplifier because of slow approximation to the ideal wavelength at which the erbium doped fiber was absorbing. Characteristics of absorption of the fiber IsoGain I-6 can be found in Appendix A.

Table 6.9: Results of measuring EDFA's output power depending on input power and temperature level of the pump laser

Temperature (°C)	Output power for input signal 1 mW (mW)	Output power for input signal 0,1 mW (mW)
10	6.23	5.2
12.5	6.28	5.21
15	6.44	5.363
17.5	6.46	5.394
20	6.57	5.472
22.5	6.64	5.521
25	6.66	5.524
27.5	6.75	5.624
30	6.8	5.661
32.5	6.8	5.672
35	6.91	5.761
37.5	6.95	5.8
40	6.98	5.823

Again, the output spectrum of the amplifier did not change. What could be observed in the spectra was only the change in power depending on increasing temperature of the pump laser.

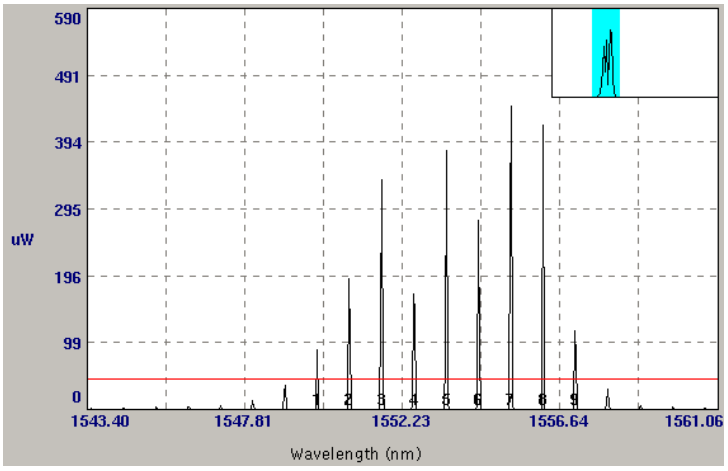

Figure 6.50: Spectrum of output signal: 1 mW input signal, 10 °C temperature

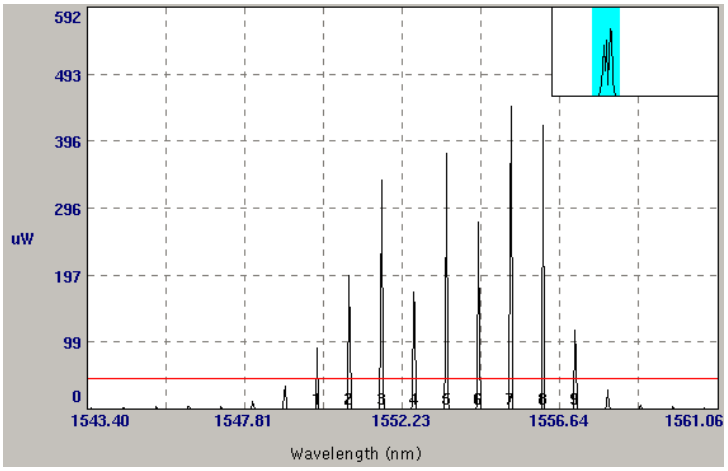

Figure 6.51: Spectrum of output signal: 1 mW input signal, 12.5 °C temperature

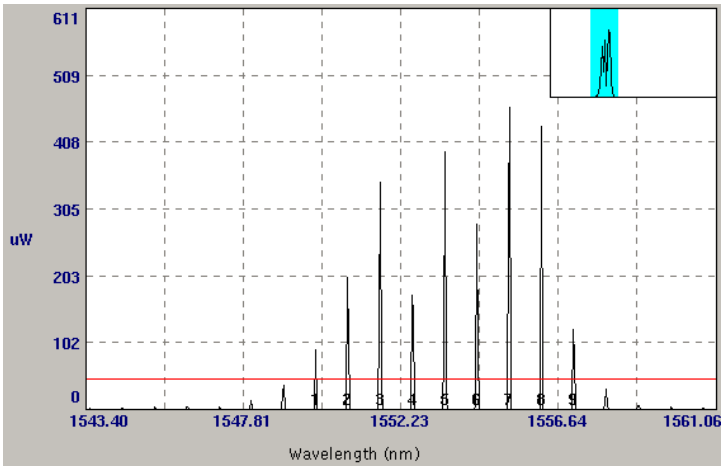

Figure 6.52: Spectrum of output signal: 1 mW input signal, 15 °C temperature

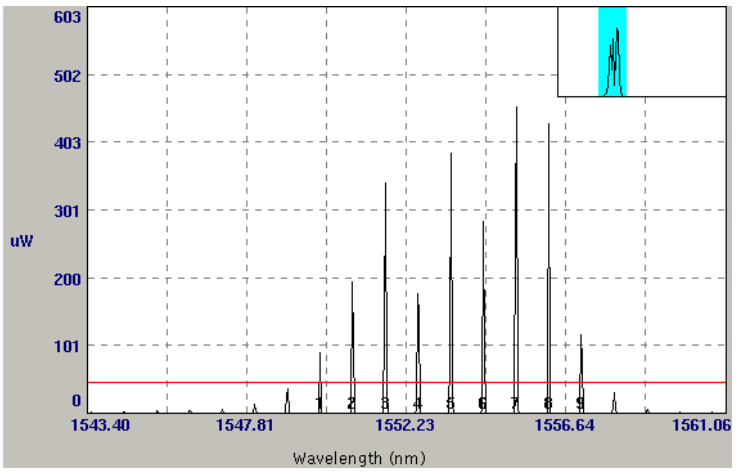

Figure 6.53: Spectrum of output signal: 1 mW input signal, 17.5 °C temperature

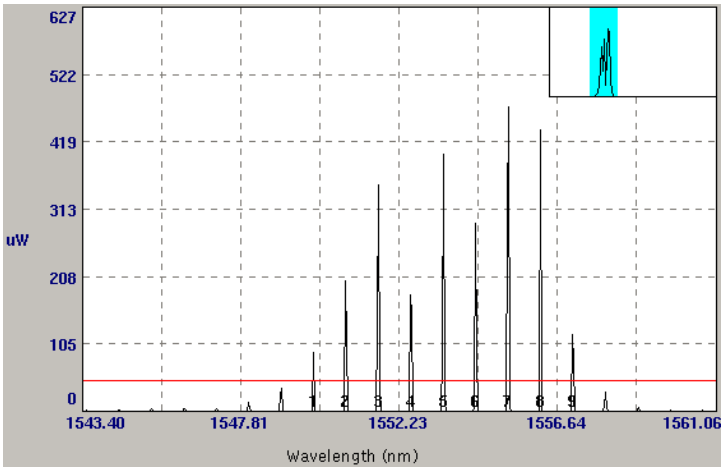

Figure 6.54: Spectrum of output signal: 1 mW input signal, 20 °C temperature

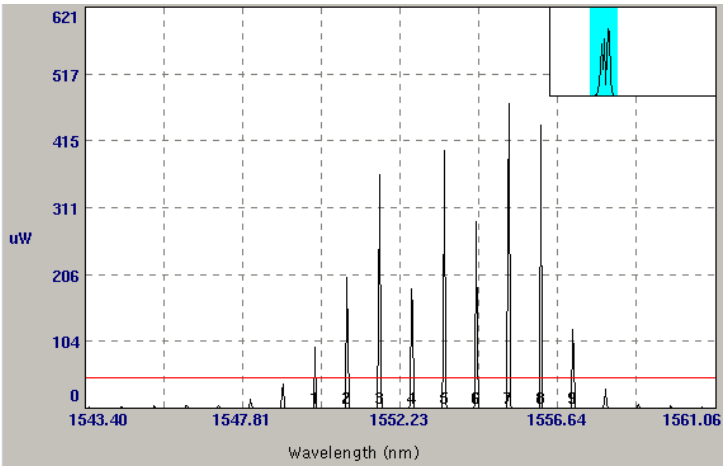

Figure 6.55: Spectrum of output signal: 1 mW input signal, 22.5 °C temperature

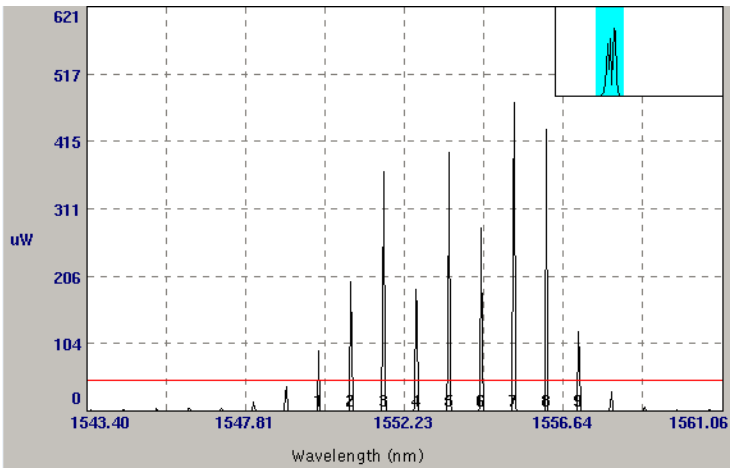

Figure 6.56: Spectrum of output signal: 1 mW input signal, 25 °C temperature

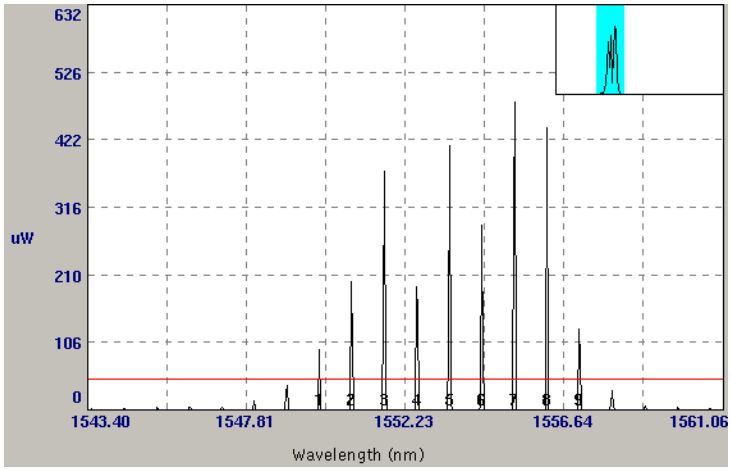

Figure 6.57: Spectrum of output signal: 1 mW input signal, 27.5 °C temperature

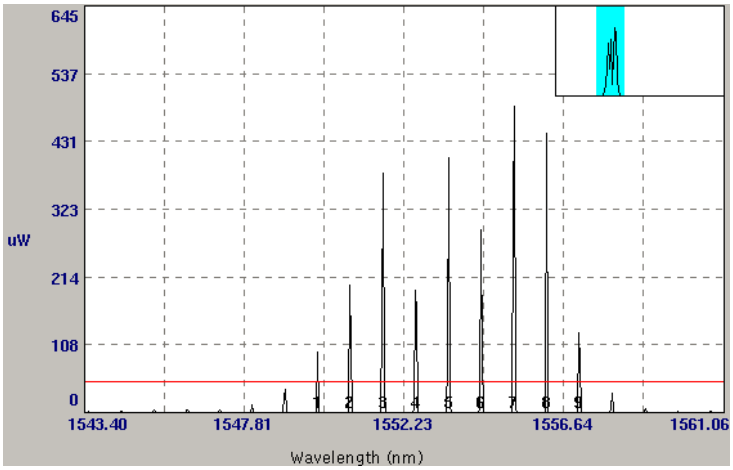

Figure 6.58: Spectrum of output signal: 1 mW input signal, 30 °C temperature

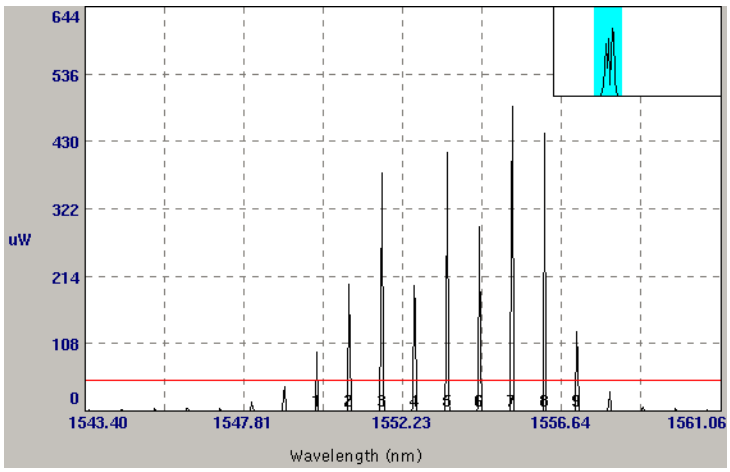

Figure 6.59: Spectrum of output signal: 1 mW input signal, 32.5 °C temperature

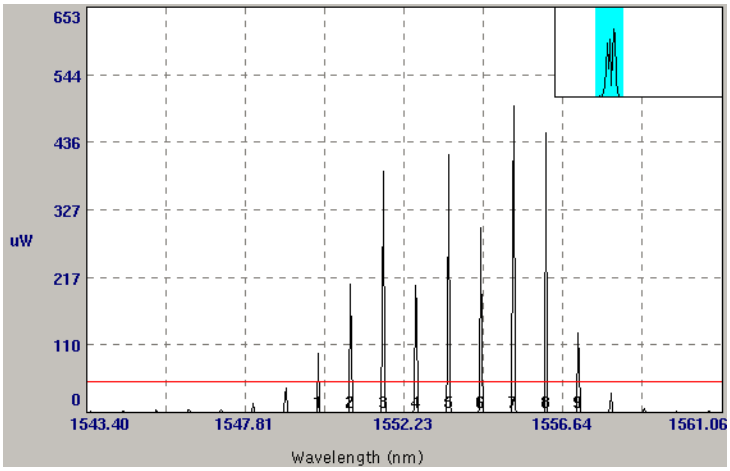

Figure 6.60: Spectrum of output signal: 1 mW input signal, 35 °C temperature

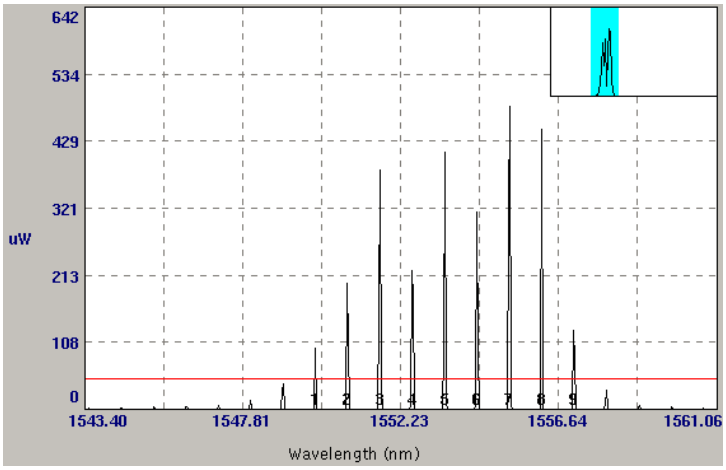

Figure 6.61: Spectrum of output signal: 1 mW input signal, 37.5°C temperature

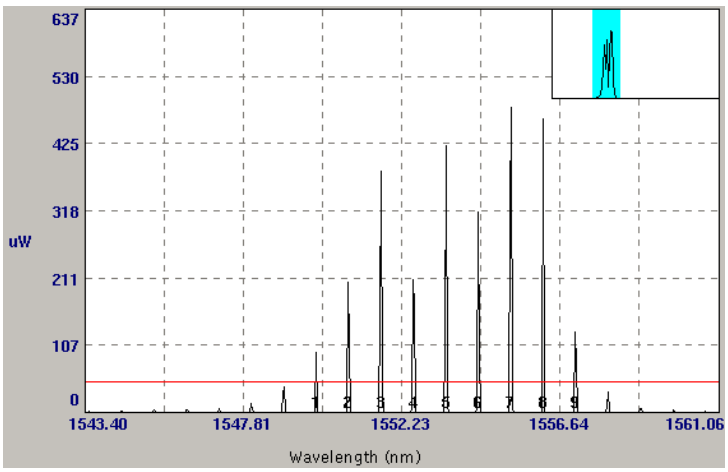

Figure 6.62: Spectrum of output signal: 1 mW input signal, 40 °C temperature

6.5 Measuring function of the amplifier in WDM-PON

The final part of the measurement consisted in connecting the amplifier into a real topology. Our designed solution amplified only the C-band, which had to be taken into account. The topology (OLT) we chose was LG-Nortel EAST 1100 with service card WDM-PON whose parameters can be found in Table 6.10. The ONU unit parameters are to be found in Table 6.11.

Table 6.10: LG-Nortel EAST 1100 – WDM-PON parameters

Parameter		**Specification**
PON interface	Wavelength band (nm)	1573-1600
	Mean launch power (dBm)	19
	Minimum sensitivity (dBm)	-29
	Channel interval (GHz)	100
	Transmission distance (km)	20
	Transmission speed (Mbps)	125
WPF	AWG insertion loss (dB)	5
Ethernet Access units	Wavelength band (nm)	1533 -1560
	Mean launch power (dBm)	-12 dBm
	Minimum sensitivity (dBm)	-36 dBm

Table 6.11: LG-ERICSSON EARU 1112 parameters

Parameter	**Specification**
Wavelength band	Colorless
Bands Tx @ Rx	C-band @ L-band
Input fiber type	SMF ITU-T G.652
Connector	SC/APC

Fig. 6.63 describes the whole diagram of connecting the amplifier into the WDM-PON. Using a circulator, the original signal had to be divided into two parts: the L-band for downstream and the C-band for upstream. Such circuit was needed because of the fact that the EDFA amplified only the C-band, and the L-band would not have passed through it. This could have resulted in non-functioning of the whole circuit because the ONU units would have not been tuned to the required wavelengths. Therefore, the L-band branch was just connected using an ordinary single-mode patch cord. In the opposite direction, there was the digital attenuator and the amplifier connected in a row.

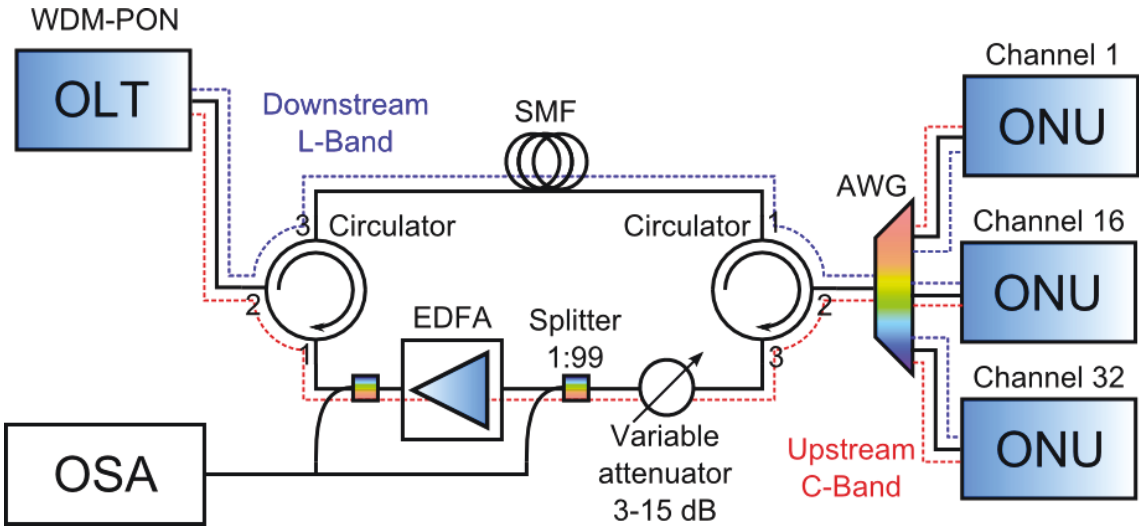

Figure 6.63: Diagram of connecting the amplifier into the WDM-PON

Other components were two splitters one of which was connected before the amplifier and the other behind it. The split ratio of these splitters was 1:99, where 99% of the power was connected before the amplifier, or behind it, as the case may be; and the remaining 1% of the power into the spectrometer which was necessary for measuring the spectrum that entered and subsequently left the amplifier. At the input/output of the circulator n. 2, AWG was connected, and it divided the individual signals for particular ONUs. The testing number of ONUs was set to 3 and they were tuned for 1-channel, 16-channel and 32-channel wavelength. Frequencies of all channel were based on ITU-T G.684.1 standards. As for the variable digital attenuator FVA-60B, we gradually set the attenuation to 3 up to 15 dB. The main deficiency of using the digital attenuator was the fact that it simulated only the attenuation of the path while the real path would show scattering and nonlinear effects which represent highly undesirable phenomena. Fig. 6.64 shows the real circuit in the laboratory.

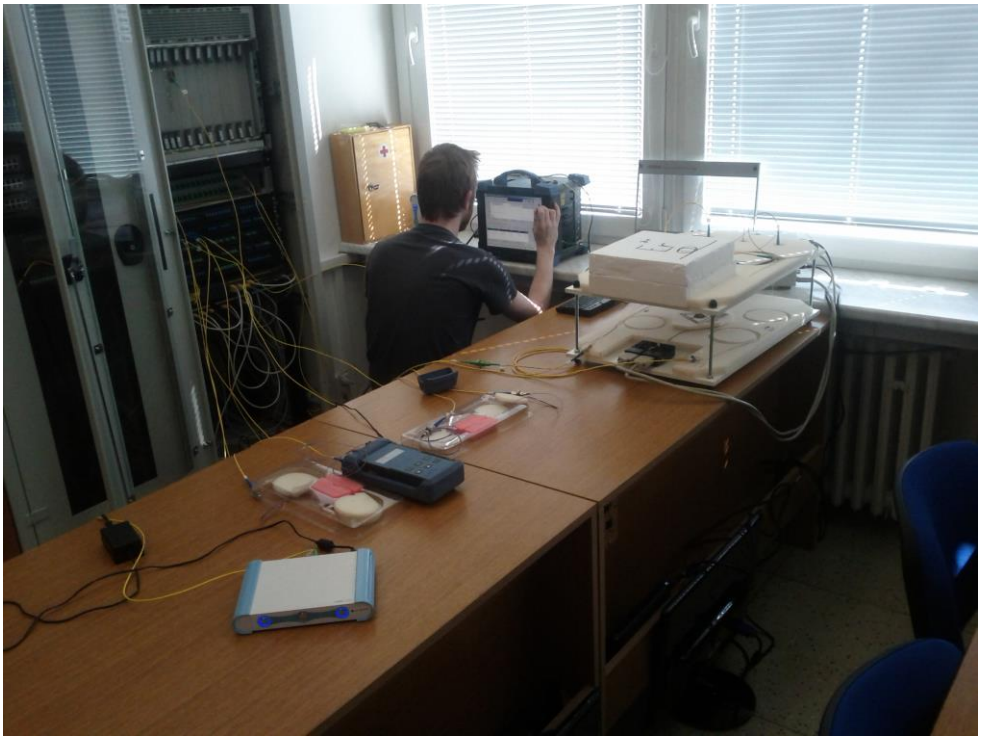

Figure 6.64: Circuit of connecting the amplifier into the WDM-PON in topology

The following charts illustrate measuring the spectrum at the input and the output of the amplifier. In the figures, there are always two lines: the black one is the input signal routed into the amplifier, while the red one is the output signal routed from the amplifier. The curve clearly shows that the apparatus amplified the whole C-band in which there were 3 channels. The disadvantage of our circuit resided in using the splitters 1:99 due to which a really low power got to the spectrometer. That is why there were no channels in higher power levels. Nevertheless, the individual channels are still recognizable from the particular charts.

At the 3 dB attenuation, the channel 1 had the power of -27.82 dBm, the channel 16 the power of -29.70 dBm, and the channel 32 the power of -25.89 dBm. We could recognize already from the first measurement that the amplifier does not amplify the whole spectrum evenly. As already mentioned, this problem could be solved using the gain flattening filter. It can be observed that when increasing the attenuation on the attenuator, the level of individual channels decreases. The ONU units stopped communicating with OLT after exceeding the value of 12 dB.

Another finding was noticeable untuning of OLT. This phenomenon was characterized by a random tuning of different channels in the OLT interface. A reason for this behaviour is wrong filtering of the pumping laser from the output of the amplifier, which is caused by inappropriately selected isolators. Another possible reason for this could be four-wave mixing which was mentioned in Chapter 3.3.3.

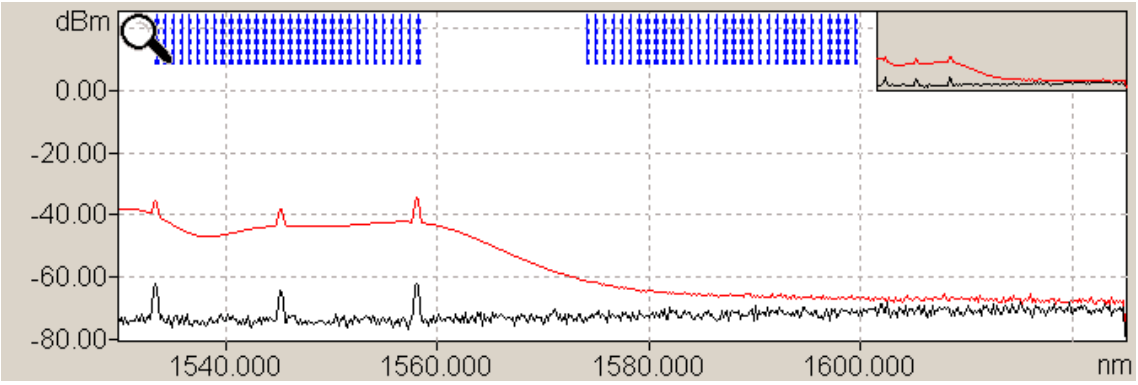

Figure 6.65: Signal at input (black) and output (red) of amplifier with attenuator set to 3 dB

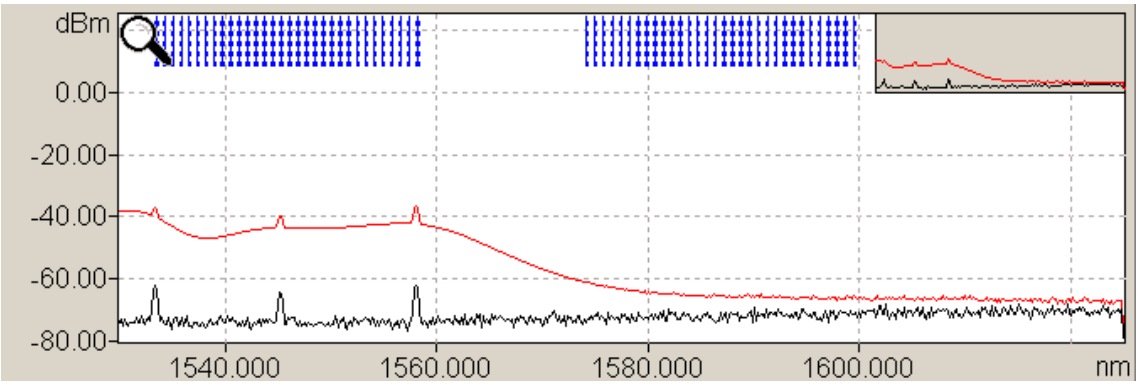

Figure 6.66: Signal at input (black) and output (red) of amplifier with attenuator set to 6 dB

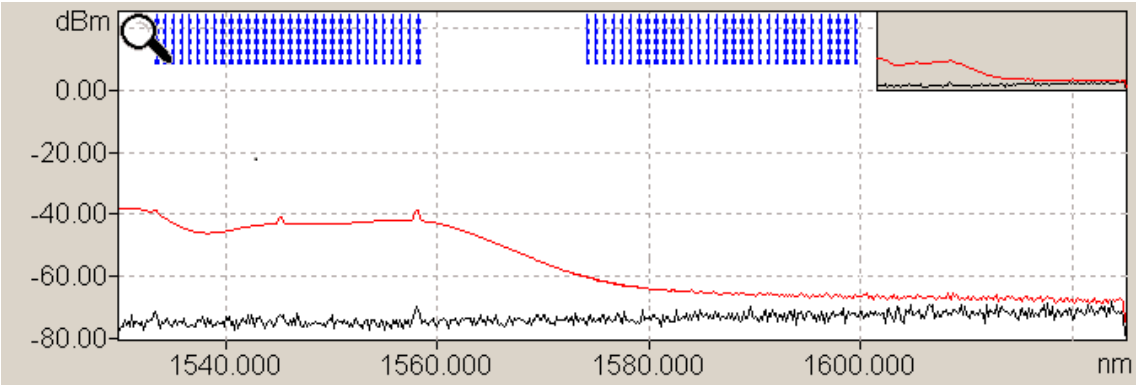

Figure 6.67: Signal at input (black) and output (red) of amplifier with attenuator set to 9 dB

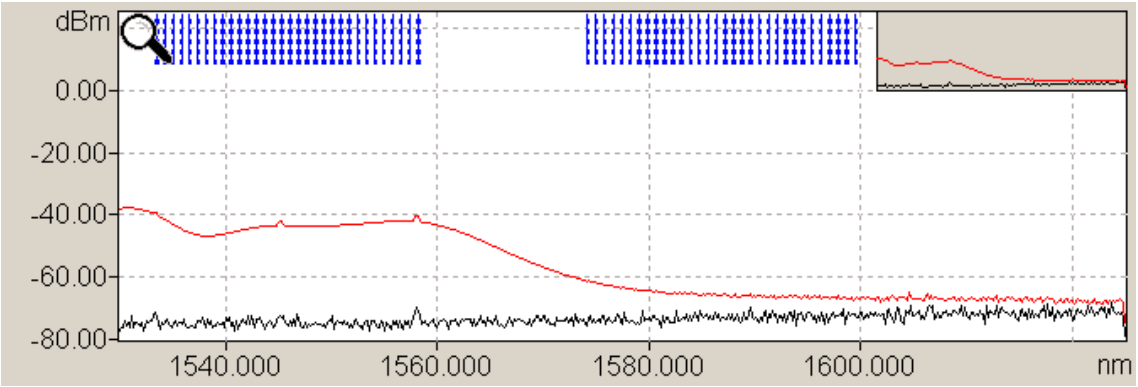

Figure 6.68: Signal at input (black) and output (red) of amplifier with attenuator set to 12 dB

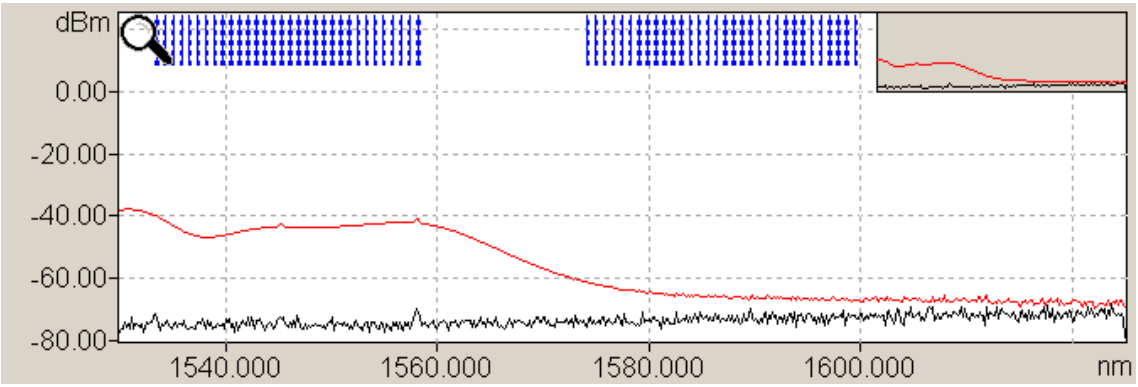

Figure 6.69: Signal at input (black) and output (red) of amplifier with attenuator set on 15 dB

Conclusions resulting from last part of our measurements are very satisfactory. The amplifier was successfully connected to the WDM-PON topology and, using it, it was possible to pass the path with the 12 dB attenuation. Assuming we use the optical fiber with the 0.25 $dB \times km^{-1}$ attenuation, we could span a distance of nearly 50 km.

7 Conclusion

The aim of this work was to highlight negative influences on erbium doped fiber amplifiers. Since the EDFA amplifiers represent the most important components used in optical WDM networks, it is necessary to keep improving them constantly.

The first part of this thesis was comprised of a theoretical basis necessary to understand the branch concerning optical amplifiers. We have explained in detail some basic physical principles and, gradually, we got to undesirable effects such as nonlinear effects which belong among highly monitored issues. Within the theoretical part, we have also looked into other areas, not just optoelectronics, especially into physics and chemistry. The chemistry was indispensable while examining various types of rear earths that are used in doped amplifying fibers. Since the whole of the thesis was interwoven with quite complex theory, it was necessary to draw upon a high number of sources written in English.

The second part of the thesis consisted in creating an EDFA amplifier from the components that were available at the department of the university. Even though some components were not ideal for constructing an amplifier, we have managed to do so and it even surpassed our initial expectations. Before the very testing of the amplifier properties, it was necessary to minutely examine the power as well the spectral stability of the pump that is one of the key components of an amplifier. These results were partially presented in the text, however, the majority of them is attached to the work in the form of CD appendices. After examining the pump stability, we could proceed to the actual testing of the amplifier.

The first thing to test was an ideal length of the fiber in different temperature conditions. This measurement has not confirmed that the temperature fluctuation has any significant effect on the ideal fiber length. However, the measured results clearly say that temperature influences on the output power of the amplifier which is directly dependent on the state of the pumping laser. What can be read from the charts is e.g. amplifying fiber characteristics in various power levels of the pumping source. The last chart concerning the 125 mW pumping power indicates the influence of temperature on the power of the amplifier depending on the amplifying fiber length. At all the testing temperatures, the optimum fiber length was 16 m, which corresponds to higher pumping powers and partly also to theoretical assumptions based on the datasheet provided by the fiber manufacturer.

Another point of the thesis was to test the spectral shift of the pumping source, and its influence on the characteristics of the fiber. As already mentioned in the chapter relating to this question, the spectral shift of the pumping source influence the amplifier very much. Thanks to this, the pumping source could approach or go away from the absorption wavelength. In our case, since our power was growing, we were approaching to the ideal wavelength.

The last part of the thesis was focused on connecting the EDFA amplifier to a real WDM-PON topology. Results of this measurement clearly show that our designed apparatus amplified all the C-band. Thanks to the gain of the amplifier, which was nearly 30 dB, we have managed to span the distance of 50 km approximately. If we take into consideration other

additional attenuations on the path caused by welds, connectors, patch cords and other components, this result is very satisfying.

Within a future research during the doctoral studies, we intent to improve the measurement methods used for testing doped fibers dependent on temperatures. We would like to make use of these results in order to upgrade the amplifiers or in order to prove their applicability in other spheres, e.g. in sensorics, not just in optoelectronics.

References

[1] RAMASWAMI, Rajiv; N SIVARAJAN, Kumar; H SASAKI, Galen. *Optical networks: a practical perspective.* 3rd ed. Amsterdam: Morgan Kaufmann, 2009, xxxiv, 893 p. Morgan Kaufmann series in networking. ISBN 978-0-12-374092-2.

[2] KEISER, Gerd. *Optical fiber communications.* 3rd ed. Boston, MA: McGraw-Hill, 2000, xxi, 602 p. ISBN 0-07-100785-7.

[3] BOHÁČ, Leoš. *Optické zesilovače v telekomunikační technice* [online]. 2009. 31 p. Přednáška. České vysoké učení technické v Praze. Available from WWW: <http://www.comtel.cz/files/download.php?id=4977 >.

[4] POTTER, B. G. *Attenuation in Optical Fibers.* 16 p. Available from WWW: <http://opti500.cian-erc.org/opti500/pdf/sm/Module3%20Optical%20Attenuation.pdf>.

[5] AGRAWAL, Govind P. *Fiber-Optic Communication Systems.* 3rd ed. New York: John Wiley, 546 p. ISBN 04-712-1571-6.

[6] BORN, Max; WOLF, Emil. *Principles of optics: electromagnetic theory of propagation, interference and diffraction of light.* 7th exp. ed. Cambridge: Cambridge University Press, 1999, xxxiii, 952 p. ISBN 05-216-4222-1.

[7] LÁTAL, Jan; KOUDELKA, Petr. *Měření v PON.* VSB-TUO: 2011, 90 p.

[8] YOSHIDA, Kazuaki; FURUI, Jasuro; SENTSUI, Shintaro; KUROHA, Toshiaki. "Loss factors in optical fibres". In: *Optical and Quantum Electronics.* January 1981, Vol. 13, Issue 1, pp. 85–89. ISSN 0306-8919.

[9] LÁTAL, Jan; KOUDELKA, Petr; HANÁČEK, František. "Využití distribuovaných optovláknových systémů při detekci průvanů v jeskynních systémech". In: *Electrorevue* [online]. 2010, Vol. 5, p. 7 [cit. 2013-04-22]. ISSN 1213–1539.

[10] DIPPEL, Bernd. "Raman scattering intensity". *Fundamentals, technologies, and applications of Raman spectroscopy* [online]. 2011 [cit. 2013-04-22]. Available from: <http://www.raman.de/htmlEN/basics/intensityEng.html>.

[11] FIBEROPTICAS FOR SALE CO. *What is Four-Wave Mixing (FWM) in Fiber Optic Communication Systems, Nonlinear Effects in High Power, High Bit Rate Fiber Optic Communication Systems* [online]. 2011 [cit. 2013-04-22]. Available from: http://www.fiberoptics4sale.com/wordpress/what-is-four-wave-mixing-fwm-in-fiber-optic-communication-systems/

[12] MALOMED, A., Boris. *SixtySec: Kerr Effect.* In: [online]. [cit. 2013-04-22]. Available from: www.exploregate.com

[13] "Kerr effect". In: *RP Photonics encyclopedia* [online]. 2013, 2013-03-22 [cit. 2013-04-22]. Available from: http://www.rp-photonics.com/kerr_effect.html

[14] RAMASWAMI, Rajiv; SIVARAJAN, N., Kumar and SASAKI, H., Galen. *Nonlinear photonics: nonlinearities in optics, optoelectronics and fiber communications*. 3rd ed. Berlin: Springer, 2002, 416 p. Morgan Kaufmann series in networking. ISBN 35-404-3123-3.LAUDE,

[15] PIERRE, Jean. *DWDM fundamentals, components, and applications*. Boston, Mass: Artech House, 2002. ISBN 15-805-3177-6.

[16] "Noise in photodetectors". In: *Optical technologies* [online]. 7.10.2008 [cit. 2013-04-22]. Available from: http://optical-technologies.info/noise-in-photodetectors/

[17] KASAP, S. *Optoelectronics and photonics: principles and practices*. 3rd Upper Saddle River: Prentice Hall, 2001, xi, 340 p. ISBN 02-016-1087-6.

[18] "Amplified Spontaneous Emission". In: *RP Photonics encyclopedia* [online]. 2013-04-10 [cit. 2013-04-22]. Available from: http://www.rp-photonics.com/amplified_spontaneous_emission.html

[19] HEADLEY Clifford; Govind P. *Raman amplification in fiber optical communication systems.* San Diego: Elsevier, 2005. ISBN 01-204-4506-9.

[20] SMRŽ, Martin. "Nové lasery pro průmysl a výzkum". In: *HILASE*. 2013.

[21] "Four-level and three-level gain media". In :*RP Photonics encyclopedia* [online]. 2013-04-10 [cit. 2013-04-22]. Available from: http://www.rp-photonics.com/four_level_and_three_level_gain_media.html

[22] DIGONNET, Michel J. *Rare-earth-doped fiber lasers and amplifiers*. 2nd ed., rev. and expanded. New York: Marcel Dekker, 2001, xii, 777 p. Optical Engineering (Marcel Dekker, Inc.), v. 71. ISBN 08-247-0458-4.

[23] "EDFA". In: *The free dictionary*.[online]. 2013 [cit. 2013-04-22]. Available from: http://encyclopedia2.thefreedictionary.com/EDFA

[24] BECKER, P; OLSSON, N and SIMPSON, J. *Erbium-doped fiber amplifiers: fundamentals and technology.* San Diego: Academic Press, c1999, xv, 460 p. ISBN 01-208-4590-3.

[25] "EDFA Pump Schemes." In: *Fiber* Optic Consulting [online]. 2011 [cit. 2013-04-22]. Available from: http://www.fiberoptic-networks.com/2011/12/edfa-pump-schemes/

[26] KEISER, Gerd. *Optical Communications Essentials*. McGraw-Hill Companies, July 03,2003. ISBN 0071737995.

[27] KEIRSTEAD, Mark. *Pump up the volume*. SPIE Newsroom [online]. s. - [cit. 2013-04-22]. ISSN 1818-2259. DOI: 10.1117/2.5200111.0008. Available from: http://www.spie.org/x26664.xml

[28] "Pump Absorption". In: *RP Photonics encyclopedia* [online]. 2013-04-10 [cit. 2013-04-22]. Available from: http://www.rp-photonics.com/pump_absorption.html

[29] HEWAK, Dan. *Properties, processing and applications of glass and rare earth-doped glasses for optical fibres*. London: INSPEC, 1998. ISBN 08-529-6952-X.

[30] "Rare-earth-doped gain media". In: *RP Photonics encyclopedia* [online]. 2013-04-10 [cit. 2013-04-22]. Available from: http://www.rp-photonics.com/rare_earth_doped_gain_media.html

[31] DEJNEKA, Matthew. PNAS. *Rare earth-doped glass microbarcodes* [online]. 2003 [cit. 2013-04-22]. Available from: http://www.pnas.org/content/100/2/389/F1.expansion.html

List of Abbreviations and Acronyms

APD	Avalanche Photodiode
ASE	Amplified Spontaneous Emission
AWG	Arrayed Waveguide Grating
BER	Bit Error Rate
C-Band	Conventional Band
CPM	Cross-Phase Modulation
dB	Decibel
DCF	Dispersion Compensating Fiber
DFB	Distributed Feedback Laser
DSF	Dispersion Shifted Fiber
DWDM	Dense Wavelength Division Multiplexing
EDF	Erbium Doped Fiber
EDFA	Erbium Doped Fiber Amplifier
ESA	Excited-State Absorption
FWM	Four-Wave Mixing
GHz	Giga Hertz
GS-EDFA	Gain Shifted Erbium-Doped Fiber Amplifier
ITU-T	Itu Telecommunication Standardization Sector
L-band	Long-Band
O-band	Original-And
OH	Hydroxide
OLT	Optical Line Termination
ONU	Optical Network Unit
PDFA	Praseodymium Fiber Amplifiers
PIN	Positive-Intrinsic-Negative
PMD	Polarization Mode Dispersion
PON	Passive Optical Network
Rx	Receiver
S-band	Short-Band
SMF	Single-Mode Optical Fiber
SOA	Semiconductor Optical Amplifier
SPM	Self-Phase Modulation
TDFA	Thulium-Doped Amplifier
TDM	Time Division Multiplex
Tx	Transmitter
WDM	Wavelength Division Multiplex
WPF	Wavelength Passive Filter
XPM	Cross-Phase Modulation
YDFA	Ytterbium Fiber Amplifiers

List of Figures

List of Tables

List of Appendices